NSWC TR 83-478

12

INVESTIGATION OF THE SAFETY RELATED CHEMISTRY OF THE LITHIUM SULFUR DIOXIDE (Li/SO_2) BATTERY

BY K. M. ABRAHAM L. PITTS (EIC LABORATORIES, INC.)

FOR NAVAL SURFACE WEAPONS CENTER
RESEARCH AND TECHNOLOGY DEPARTMENT

AUGUST 1983

NAVAL SURFACE WEAPONS CENTER

Dahlgren, Virginia 22448 • Silver Spring, Maryland 20910

REPORT DOCUMENTATION PAGE

READ INSTRUCTIONS BEFORE COMPLETING FORM

1. REPORT NUMBER: NSWC TR 83-478	2. GOVT ACCESSION NO.
3. RECIPIENT'S CATALOG NUMBER	
4. TITLE (and Subtitle): INVESTIGATION OF THE SAFETY RELATED CHEMISTRY OF THE LITHIUM SULFUR DIOXIDE (Li/SO_2) BATTERY	5. TYPE OF REPORT & PERIOD COVERED: 6 July 1982 - 5 July 1983
	6. PERFORMING ORG. REPORT NUMBER: C-721
7. AUTHOR(s): K. M. Abraham and L. Pitts	8. CONTRACT OR GRANT NUMBER(s): N60921-82-C-0178
9. PERFORMING ORGANIZATION NAME AND ADDRESS: EIC Laboratories, Inc. 111 Downey Street Norwood, Massachusetts 02062	10. PROGRAM ELEMENT, PROJECT, TASK AREA & WORK UNIT NUMBERS: 62765N; F65571; SF65571692; R33BE(C)
11. CONTROLLING OFFICE NAME AND ADDRESS: Naval Surface Weapons Center (Code R33) White Oak, Silver Spring, Maryland 20910	12. REPORT DATE: August 1983
	13. NUMBER OF PAGES: 100
14. MONITORING AGENCY NAME & ADDRESS (if different from Controlling Office)	15. SECURITY CLASS. (of this report): UNCLASSIFIED
	15a. DECLASSIFICATION/DOWNGRADING SCHEDULE

16. DISTRIBUTION STATEMENT (of this Report)

Approved for public release; distribution unlimited.

17. DISTRIBUTION STATEMENT (of the abstract entered in Block 20, if different from Report)

18. SUPPLEMENTARY NOTES

19. KEY WORDS (Continue on reverse side if necessary and identify by block number)

Li/SO_2 battery, safety hazards, discharge stoichiometry, $Li_2S_2O_4$, forced overdischarge, decomposition of $Li_2S_2O_4$, partially discharged cells, Li-polythionates.

20. ABSTRACT (Continue on reverse side if necessary and identify by block number)

The safety related chemistry of the Li/SO_2 battery has been further investigated. The normal discharge stoichiometry, $2Li + 2SO_2 \rightarrow Li_2S_2O_4$, has been confirmed for current densities up to 8 mA/cm^2 at room temperature, and for discharges at -25^{o}C. (Continued on reverse.)

Experiments have revealed that $Li_2S_2O_4$ in the carbon cathode decomposes at ~180°C producing one mole of SO_2 per three moles of $Li_2S_2O_4$. The other decomposition products are S, Li_2SO_3, and small amounts of CO_2, COS and CS_2. The decomposition of forced overdischarged cathodes containing $Li_2S_2O_4$ and Li appears to occur at an accelerated rate at ~180°C, producing larger quantities of COS, CO_2 and CS_2, along with SO_2. The higher exothermicity of the latter decomposition is believed to be due to the reduction of $Li_2S_2O_4$ by Li. The COS, CO_2 and CS_2 apparently result from direct reactions between C and SO_2, and C and S. Apparently, these reactions involving C are responsible for the formation of the same gases in cells which vent/explode during forced overdischarge. This has been confirmed by the identification of COS, CS_2 and CO_2 in the vented gases from an all-inorganic Li/SO_2 cell (Li/$Li_2B_{10}Cl_{10}$,SO_2/SO_2,C) which exploded during forced overdischarge at -15°C.

Our results indicate that direct reactions between C and SO_2, and C and S are integral parts of the mechanism of explosions/venting during forced overdischarge. Pressure build-up in such cells is also brought about by the Li-CH_3CN reaction producing CH_4, C_2H_4 and C_2H_2.

Our results suggest that practically the same mechanism is operating in both the room temperature and low temperature forced overdischarge explosions. The only apparent difference is that at low temperatures, the Li which plates onto the carbon cathode remains more active so that explosions are more prevalent at low temperatures. A scenario for the explosion hazard in forced overdischarged cells is presented.

A preliminary study of the chemistry in partially discharged and stored cells has been carried out. Li-polythionates along with $Li_2S_2O_4$ have been identified on the anodes of such cells. The implication of this chemistry to the safety of the system is not yet understood. The effects of parameters such as current density, depth of discharge, electrolyte composition, and storage time and temperature on the storage chemistry of the battery remain to be assessed.

FOREWORD

This report characterizes the chemistry and electrochemistry of forced over-discharge and storage of both commercial and specially constructed lithium-sulfur dioxide batteries. The results focus attention on lithium dithionite decomposition as the reaction most relevant to cell safety problems as opposed to the lithium-acetonitrile reaction formerly emphasized in literature. Recommendations are made on the cell construction to minimize hazards in this system.

The authors acknowledge the financial support of the Naval Sea Systems Command, Electrochemistry Technology Block Program and the valuable discussions with Dr. S. D. James, the Naval Surface Weapons Center's Contracting Officer's Technical Representative on this project.

Approved by:

J. R. Dixon

JACK R. DIXON, Head
Materials Division

CONTENTS

ILLUSTRATIONS

ILLUSTRATIONS (continued)

TABLES

CHAPTER 1

INTRODUCTION

The $Li/LiBr$, CH_3CN/SO_2 cell offers high energy density (up to 150 Whr/lb and 8.5 Whr/in^3) combined with excellent performance capability over a wide temperature range covering -54 to +71°C (1). It is the most advanced among the non-aqueous Li cells. Yet, concerns of safety have precluded it from being widely accepted.

In a recent study (2), involving a literature and user survey of the safety hazards of Li/SO_2 cells and batteries, we have identified three conditions under which the use of the battery may be hazardous.

(i) Forced overdischarge of Li/SO_2 cells. This situation, experienced by a weak cell in a series-connected battery, has been the most frequent cause of cell or battery venting or explosion.

(ii) Increased vulnerability of partially discharged and stored Li/SO_2 cells and batteries to subsequent harsh uses; e.g., shorts, high current pulses, overdischarge or incineration. This is a particularly hazardous condition in practical situations.

(iii) Low temperature discharge, particularly when a cell is driven into voltage reversal and subsequently warmed up to room temperature.

The purpose of this program was to carry out a systematic investigation of the causes of the aforementioned hazards and find solutions to them. The major emphasis in our studies has been on chemical analyses. In this respect, the large body of knowledge gained from analysis of two types of commercial C-size cells, performed in a previous Naval Surface Weapons Center (NSWC) program (3-5), served as the basis.

Our studies encompassed the following aspects:

1) Characterization of the chemistry and electrochemistry of forced overdischarge in well-specified EIC-built C-size cells. An objective was to reproduce in these cells the hazards observed in the commercial cells and to characterize the mechanism of forced overdischarge explosion hazards. The experiments were carried out at rooom temperature and at low temperatures (-10°C to -25°C).

2) Evaluation of the frequency of forced overdischarge hazards at low temperatures. This study, aimed at establishing the relationships among the extent

of overdischarge, the mass of dendritic Li plated onto the cathode and the hazardous events, was carried out with both commercial C-size and EIC-built cells.

3) Studies of the apparently increased vulnerability of partially discharged and stored cells to subsequent use under harsh conditions. This investigation was conducted using commercial cells.

Our results of these various studies are presented in the following chapters.

CHAPTER 2

EXPERIMENTAL PROCEDURES

GENERAL EXPERIMENTAL PROCEDURES

All experiments involving reagent handling and cell construction were carried out in the absence of air and moisture in an argon atmosphere using a Vacuum-Atmospheres Corporation drybox. Discharges and overdischarges of cells were carried out in the specially designed, hermetically sealed test chamber, described previously (3). This test vessel is designed to retain all materials released from cells which either vented during testing, or which were deliberately opened after electrochemical tests.

EIC-BUILT C-SIZE Li/SO_2 CELLS

C-size cells with spirally wound electrodes were constructed and specially instrumented for measuring individual electrode potentials and cell wall temperature. The major cell parameters are as follows:

Carbon Cathode

The cathodes were fabricated from a mixture of 90 w/o Shawinigan carbon black and 10 w/o Teflon, pressed onto an Al expanded metal (Delker 5AL7-077). The cathodes, typically measured, 2.5 cm x 25 cm x 0.08 cm with an area of 125 cm^2 (for both sides) and a carbon content of ~ 2 g/electrode. The tab connection to the electrode was made with an Al foil, 5 cm x 0.5 cm x 0.005 cm.

Li Anode

The anodes were fabricated from 15 mil thick Li foil and used no metal grids. Electrodes of two different dimensions were used: 3.7 cm x 25 cm with an area of 185 cm^2 and weighing ~ 1.8g (~ 7 A-hr); 2.7 cm x 25 cm with an area of 135 cm^2 and weighing 1.3g (~ 5 A-hr). The Li formed the outer electrode in the jelly-roll and connection to the nickel can was made by pressure-contact.

Li Reference Electrode

A Li reference electrode was incorporated in all cells. The reference electrode was made by pressing a small strip of Li onto a Ni wire and heat-sealing in a Celgard 2400 polypropylene separator. It was positioned at the core of the jelly-roll.

Separator

Celgard 2400(TM) polypropylene obtained from Celanese Corporacion was used. An IR spectrum of this separator film is shown in Figure 1.

Electrolyte

The preparation of the electrolyte was carried out by vacuum-techniques by condensing SO_2 into a solution of LiBr in CH_3CN. A 100g electrolyte typically contained 8.7g anhydrous LiBr (Alfa Ventron), 27.3g CH_3CN (Burdick and Jackson) and 64g SO_2 (Matheson Gas).

Assembly and Filling

The Li anode, the Celgard 2400 separator and the carbon cathode were wound into a tight roll such that the Li formed the outer layer of the roll. The Li reference electrode was positioned at the core of the jelly-roll, at the beginning of the rolling procedure.

The spirally wound electrode package is introduced into the C-cell can (nickel). The cell top consisted of a stainless steel plate with a silicone O-ring. The top was held tightly in place by four steel bolts leading to a bottom plate. The compression springs, being placed between the cover and the nuts, were adjusted such as to make it possible for the cell to vent at a pressure of ~ 450 psi. The positive lead and the reference electrode lead were taken through the Conax feed-through attached to the top of the steel plate cover. These electrical leads were fabricated from Al wire.

Temperature measurements were made with a copper-constantan thermocouple junction mechanically placed on the outer cell-wall and calibrated against an Omega ice-point reference.

A schematic representation of a fully assembled cell is shown in Figure 2.

The cell was filled with the electrolyte by vacuum technique.

Prior to the electrochemical tests, the filled cell was enclosed in the hermetically sealed test chamber. The threaded-rod which goes through the cover of the test chamber was modified by attaching a bent stainless steel piece at its end which fits over the valve of the cell. When desired, the cell could be manually vented by turning the threaded rod. Post-test analyses of the cells were carried out as described in our previous reports (3-5).

ANALYTICAL METHODS

Infrared spectra were recorded on a Beckman Acul3b 5 dual beam spectrometer. Solid samples were pulverized to ensure their homogeneity and then pressed into discs. Volatile species were analyzed with a Beckman Universal Gas cell with KBr windows. Table 1 lists the IR absorptions in the finger-print region of some of the sulfur-oxy compounds of interest (10).

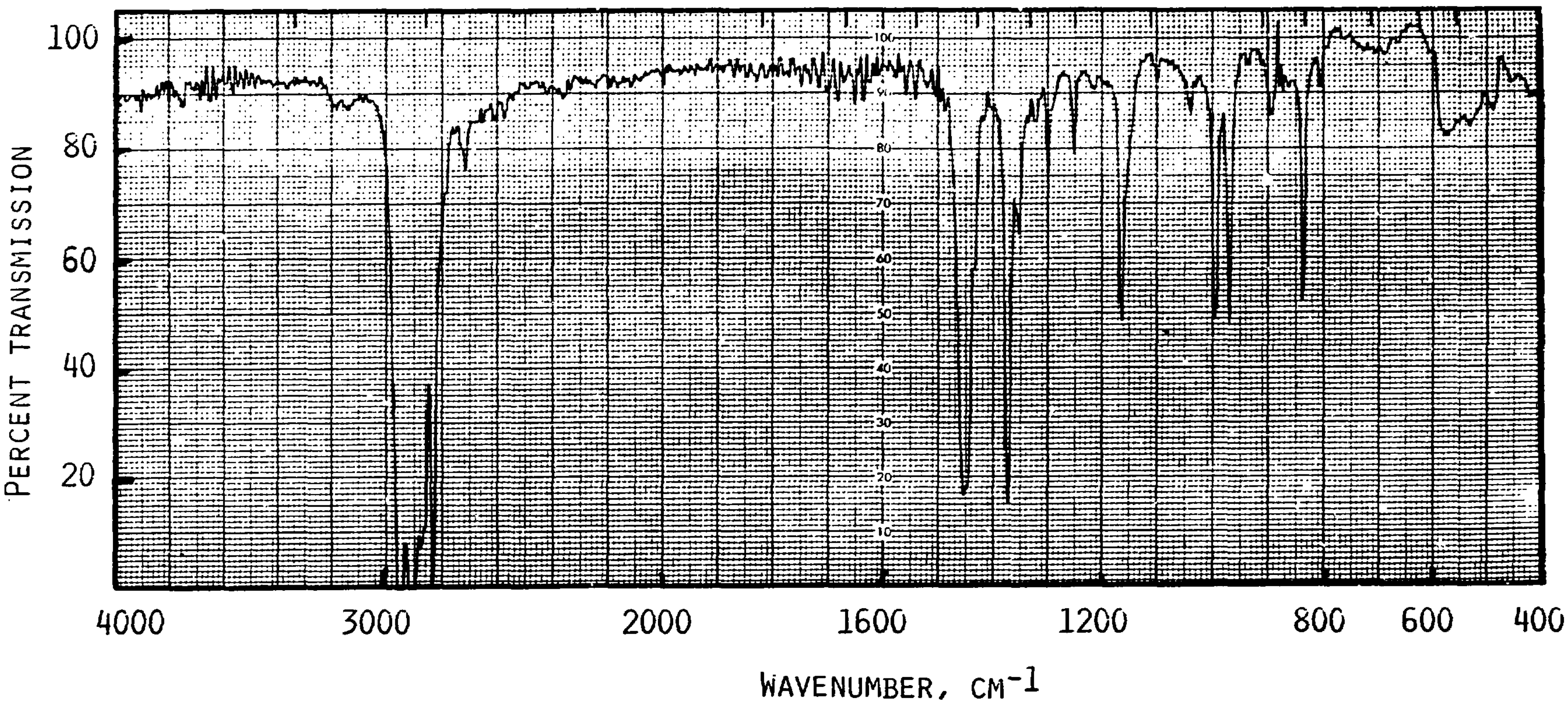

THE SPECTRUM AS OBTAINED BY PLACING THE FILM IN THE LIGHT BEAM PATH OF THE SPECTROMETER.

FIGURE 1. IR SPECTRUM OF POLYPROPYLENE CELGARD 2400

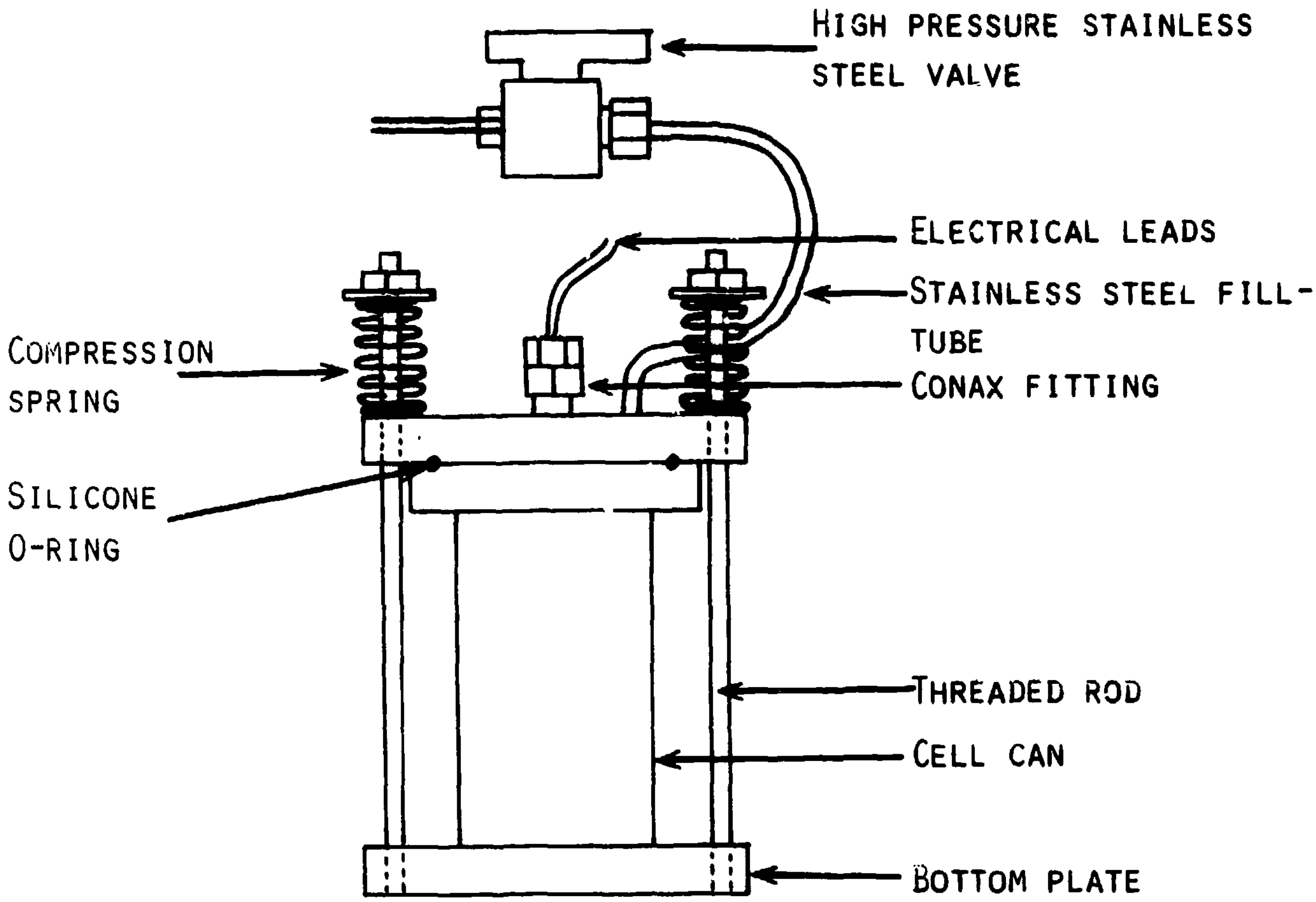

FIGURE 2. SCHEMATIC REPRESENTATION OF AN ASSEMBLED Li/SO_2 TEST CELL

TABLE 1. IR SPECTRAL ABSORPTION FREQUENCY RANGES IN THE FINGER-PRINT REGION OF SOME SULFUR-OXY COMPOUNDS

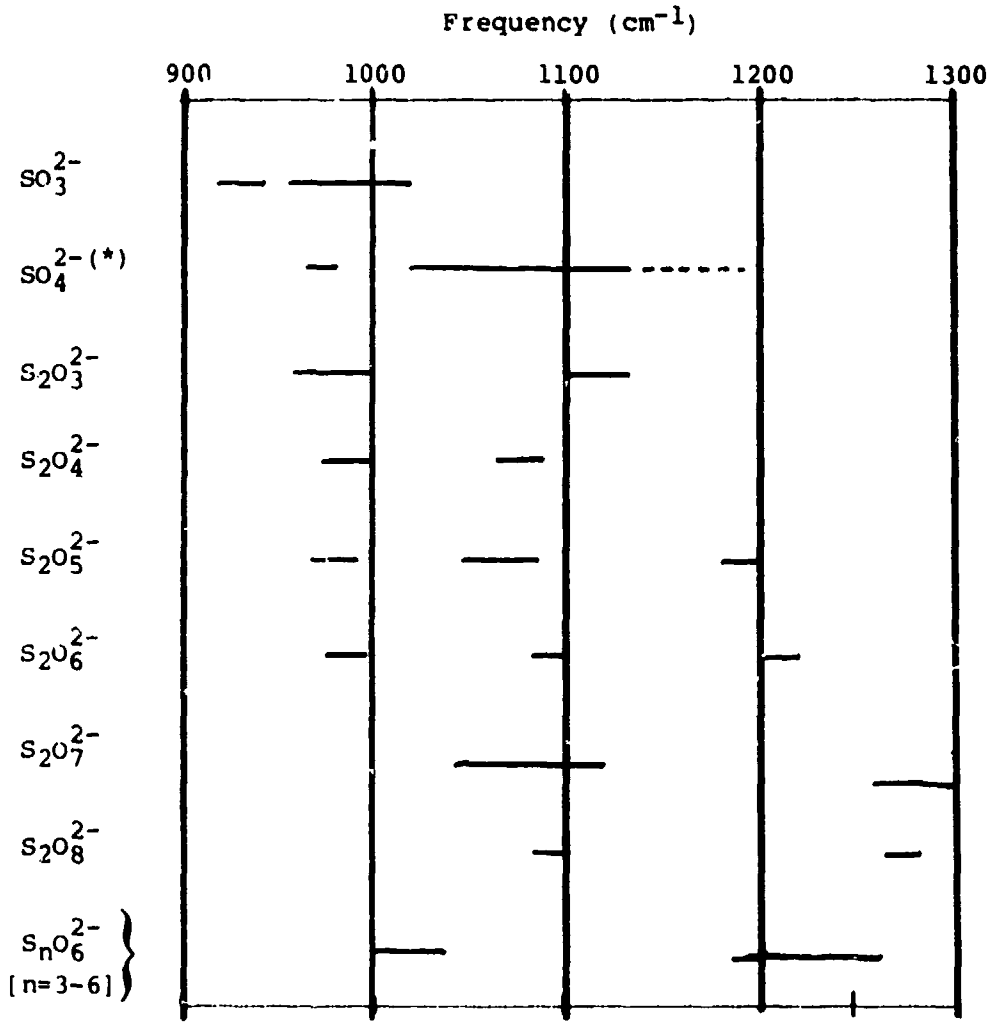

*The range for SO_4^{2-} is normally 1020-1150 cm^{-1}; relatively few compounds absorb at 1150-1200 cm^{-1}.

X-ray diffraction data were obtained by the Debye-Scherrer method using CuK_{α} radiation.

Mass spectra data were obtained with a Nuclide 1290G mass spectrometer at Biomeasure, Inc., Hopkinton, MA.

Gas chromotographic analyses were performed on a Varian 920 Gas Chromotograph equipped with a thermal conductivity detector and either a 4 ft Spherocarb (Analabs) or a 6 ft Chromosorb 104 (Analabs) resin in a stainless steel column at temperatures between 25-150°C. The assignment of peak identities was based on comparison to the retention times of standard samples. The relevant data for some of the species that could be separated on these columns are given in Table 2.

Quantitative analysis of the dithionite in discharged cathodes was carried out by the procedure we have developed and described elsewhere (3,5).

TABLE 2. GAS CHROMATOGRAPHIC DATA FOR SOME CHEMICALS OF INTEREST IN Li/SO_2 CELLS

	Experimental Conditions			Retention Times (min)				
Type of Column	He Flow Rate, ml/min	Column Temp., °C	Detector Temp., °C	H_2	CH_4	CO_2	H_2S	SO_2
6' x 1/8" SS Chromosorb 104	40	100	130		0.33	0.53	1.27	4.00
	20	50	110	0.50	0.68			
	20	35	60	0.52	0.72			
4' x 1/8" SS Spherocarb	50	200	200		0.42			2.83
	50	100	125		1.47			3.47

CHAPTER 3

DISCHARGE CHEMISTRY OF Li/SO_2 CELLS

In the prior program (3), we investigated the discharge chemistry of the Li/SO_2 cell corresponding to relatively low currents (< 300 mA in C-size cells) at room temperature. Under those conditions, the amount of $Li_2S_2O_4$ produced in the cell agreed very well with the stoichiometry shown in equation 1.

$$2Li + 2SO_2 \rightarrow Li_2S_2O_4 \qquad [1]$$

During the present program, we have extended this line of study to include high currents (1 ampere in C-size cells) and low temperatures (-25°C).

ROOM TEMPERATURE DISCHARGE AT HIGH CURRENTS

Cell E-1 was constructed with a Li anode having an area of 185 cm^2 and weighing 1.80g (6.95 A-hr). It contained 14.5g of electrolyte, composed of 9.3g (3.9 A-hr) SO_2, 3.9g CH_3CN and 1.3g LiBr. The cell was discharged at 1A, and the cell wall temperature and individual electrode potentials were measured.

The discharge of Cell E-1 is depicted in Figure 3. The discharge current of 1A corresponds to a current density of 8 mA/cm^2. Shown in the figure are the cell potential, the anode potential versus the Li reference, the cathode potential versus the Li reference and the cell wall temperature. The cell discharge is clearly limited by the carbon electrode. The capacity to 0.0 volt is 2.93 A-hr and the corresponding carbon utilization is ~1.40 Ah/gram. The cell was disassembled and analyzed. The following results have been obtained.

An infrared spectrum of the gases from the cell showed only SO_2 and CH_3CN. No absorptions indicative of a gaseous reaction product were observed. This conclusion was borne out by gas chromatographic analysis.

The cathode from the cell was analyzed for $Li_2S_2O_4$. An infrared spectrum was obtained on a KBr pellet, fabricated with a small portion of the cathode. The rest of the cathode was used for a quantitative analysis of $Li_2S_2O_4$ (5).

The infrared spectrum showed only those absorptions we previously characterized for $Li_2S_2O_4$: 1085 (s), 1020 (s), 900 (s), 550 (m) and 500 (m) cm^{-1}. We did not find any absorptions characteristic of either $Li_2S_2O_3$ or Li_2SO_3. (See Table 1.)

In performing the quantitative analysis, the cathode was cut into three portions of approximately equal lengths - inner 1/3, middle 1/3 and outer 1/3 and $Li_2S_2O_4$ in each portion was analyzed. This was done for an assessment of the product distribution profile in spirally wound cathodes when discharged at rela-

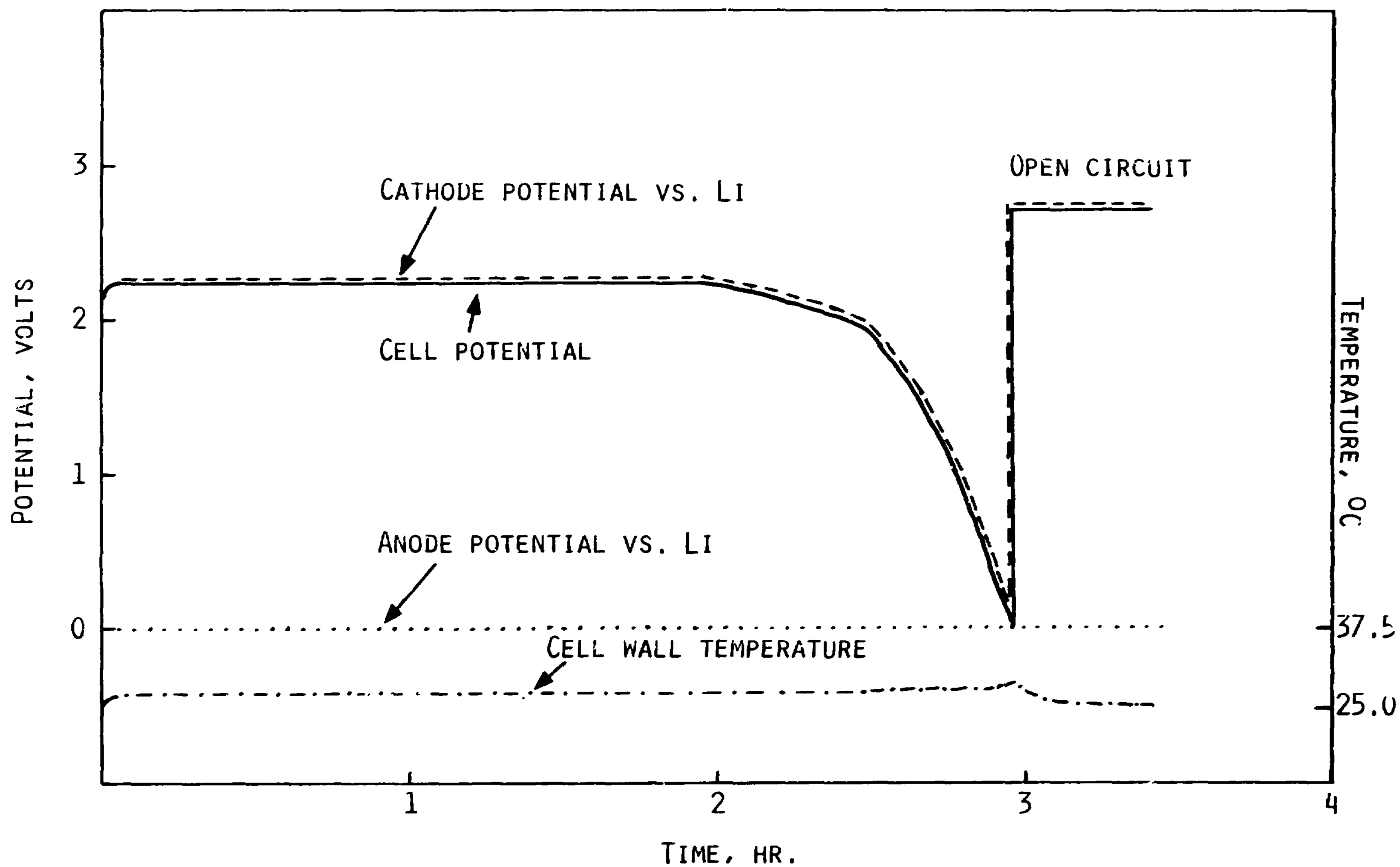

CURRENT, 1A; CURRENT DENSITY, 8 mA/cm^2

FIGURE 3. DISCHARGE DATA FOR Li/SO_2 CELL E-1

tively high currents. The result of the dithionite analysis is given in Table 3. The inner and middle fractions contain, within the experimental uncertainty, similar amounts of $Li_2S_2O_4$, while the outer fraction has a slightly lower amount. The total dithionite corresponds to ~ 95% of that calculated based on the total charge utilized in the discharge to zero volt.

TABLE 3. DITHIONITE ANALYSIS OF CELL E-1, DISCHARGED TO 0.0V

Capacity to 0.0V (mAhr)	$S_2O_4^{-2}$ (mAhr) Found in the Cathode Inner 1/3	Middle 1/3	Outer 1/3	Total $S_2O_4^{-2}$ Found, mAhr (% discharge)
2930	1046	956	777	2779 (95)

Although we quantitatively analyzed only one cell after a discharge at 1 ampere to 0.0V, it appears reasonable to conclude that the discharge reaction at the higher rate is not significantly different from that we characterized previously in cells discharged at relatively low rates. The principal discharge product in both cases is $Li_2S_2O_4$. Very little or no gaseous reaction products appear to be generated. We have found a rather uniform product distribution in the cathode; but this may be dependent on the type of carbon cathode and the method of cell construction.

DISCHARGE AT LOW TEMPERATURES

Cell E-16 was discharged at -25°C and then analyzed. This cell was constructed with 1.92g (7.4 A-hr) of Li and 9.6g (4.04 A-hr) of SO_2. It exhibited an OCV of 2.91V at -25°C.

The discharge curve at 300 mA is given in Figure 4. The cell capacity of 2.68 A-hr to 0.0V corresponds to a carbon cathode utilization of 1.2 A-hr/g.

An infrared spectrum of the cathode is shown in Figure 5. The spectrum is identical to those obtained from cathodes discharged at room temperature.

A quantitative analysis of the $Li_2S_2O_4$ in the cathode has given a total amount corresponding to 99% of the discharge capacity.

Infrared spectral data on cathodes discharged at high currents (1 ampere in C-cells) have been identical to those obtained from cathodes discharged at low currents. It appears that at both 25 and -25°C the Li/SO_2 cell exhibits an identical discharge chemistry.

The identical chemistry we have characterized for the 25 and -25°C discharges is in contrast to the results reported by others (6,7) for the discharge chemistry at elevated temperatures, i.e., 75°C. At the latter temperature, apparently a lithium polythionate is also formed.

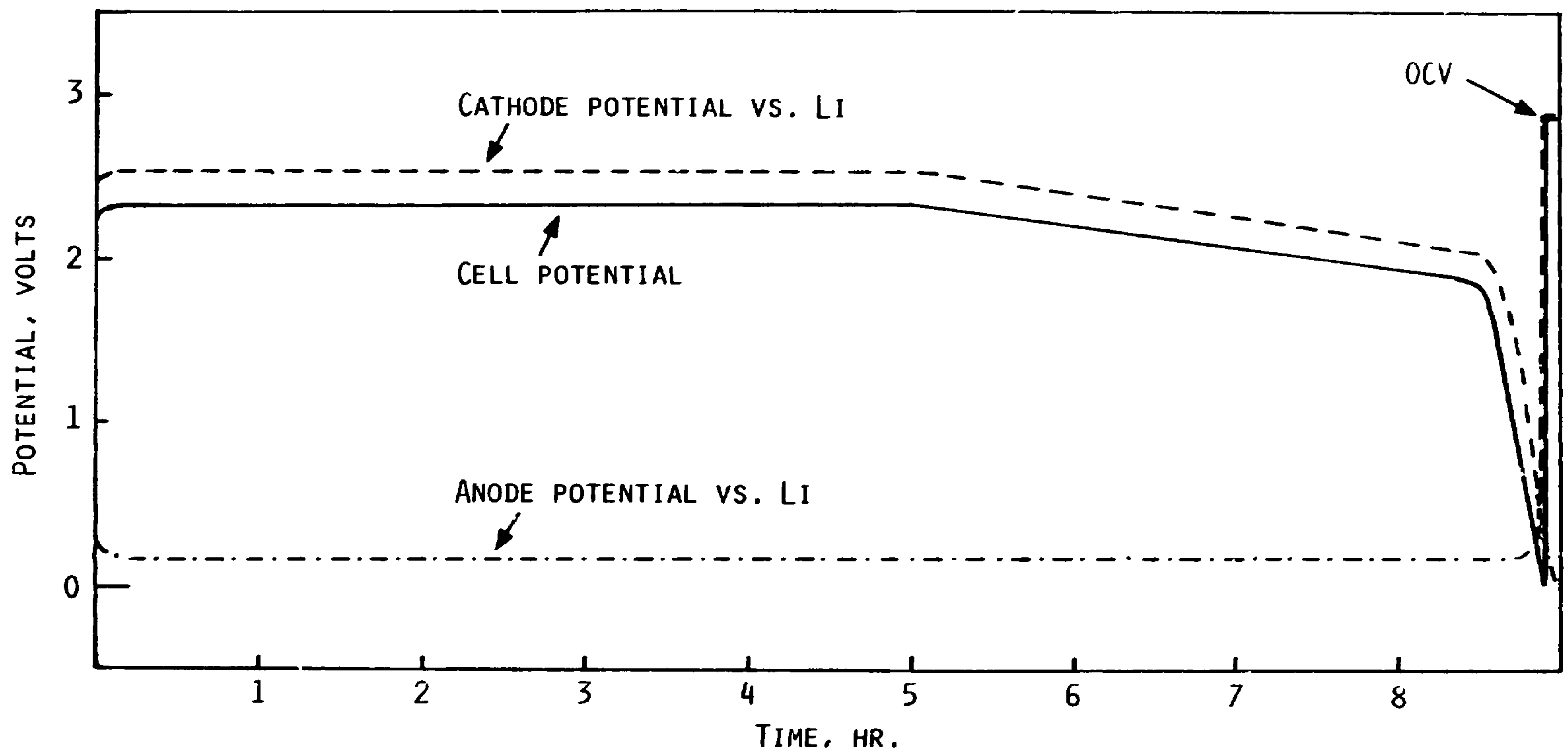

CURRENT, 300 mA

FIGURE 4. DISCHARGE CURVE FOR CELL E-16 AT -25°C

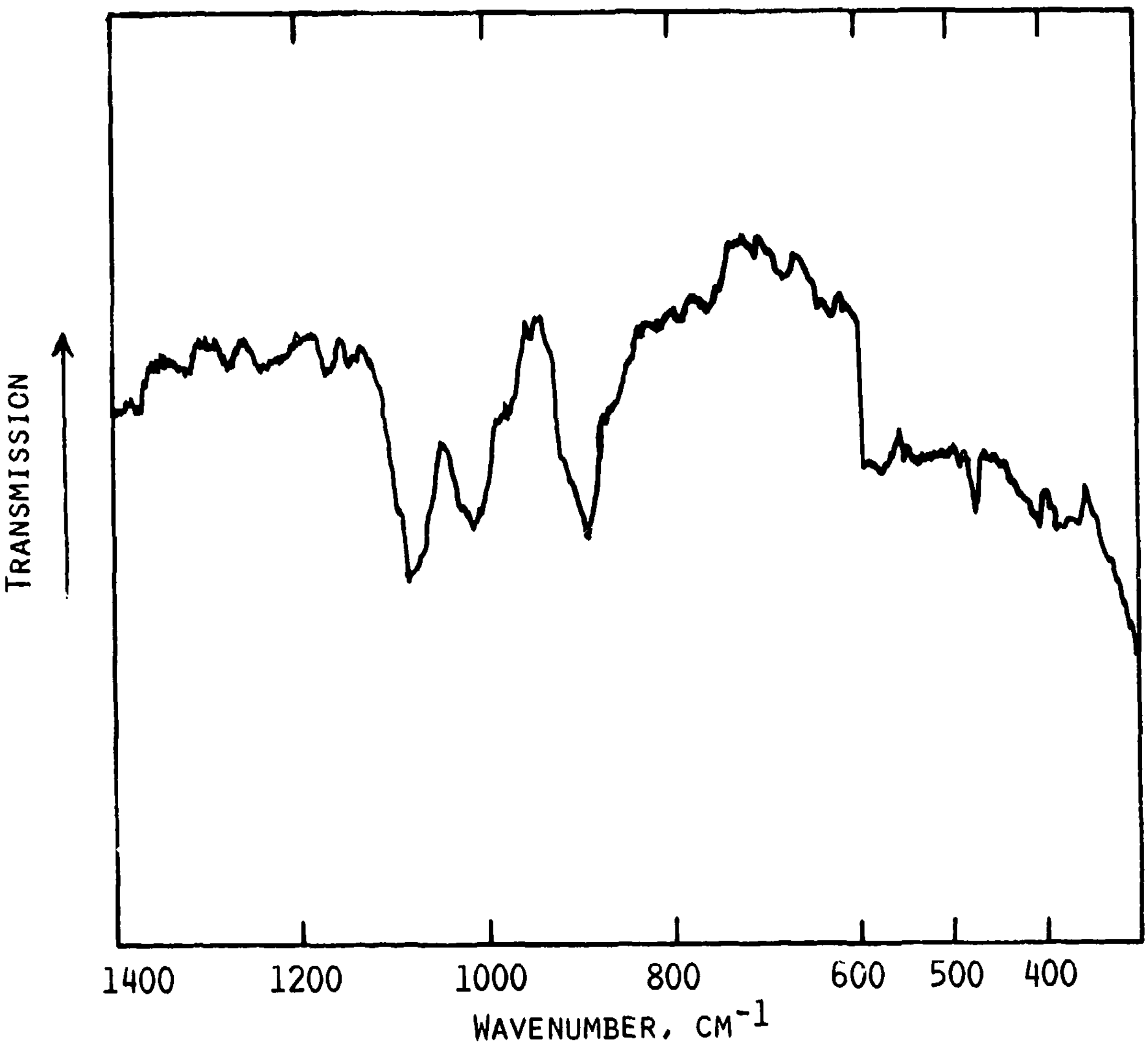

FIGURE 5. INFRARED SPECTRUM OF THE CATHODE FROM CELL E-16, DISCHARGED AT -25°C

CHAPTER 4

ERMAL DECOMPOSITION OF CATHODES FROM DISCHARGED Li/SO_2 CELLS

Because of its potential relevance to the safety related chemistry of the cell, the thermal decomposition of cathodes from discharged cells was investigated qualitatively by mass and IR spectral analysis, and semi-quantitatively by collecting and determining the total amount of volatile materials produced. The cathodes used in these analyses had been dried by prolonged pumping in vacuum, thus, removing practically all of the adhering CH_3CN and SO_2. The discharged cathode samples comprised, in addition to the carbon mix on the Al grid, $Li_2S_2O_4$ and a small amount of LiBr.

MASS SPECTRAL ANALYSIS

A small cathode sample from a cell discharged to 0.0V was inserted, by direct injection, into the probe of a mass spectrometer while the probe was heated to ~ 250°C. The mass spectrum obtained for the volatile decomposition products is given in Figure 6. The peak intensities are normalized to mass 64. The molecular ion peak at mass 256 and the related fragmentation peaks at mass units separated by 32 are consistent with the formation of S_8 as a decomposition product. The most intense peak after mass 64 is that at mass 48, which appears to correspond to SO^+, a fragmentation product of SO_2. The intensity of the peak at mass 48 when compared against a standard SO_2 mass spectrum shows good correlation and indicates a large amount of SO_2. It is reasonable to assume that both SO_2 and S_8 are decomposition products of $Li_2S_2O_4$. This is reinforced by the data discussed below.

QUANTITATIVE DETERMINATION OF VOLATILES AND INFRARED SPECTRAL CHARACTERIZATION

An experiment was designed to further characterize and to quantitatively determine the volatile products resulting from the thermal decomposition of $Li_2S_2O_4$ in a carbon cathode.

A C-size Li/SO_2 cell was discharged at 150 mA at room temperature to a cut-off of 2.0V. The cell capacity was 2.73 A-hr which corresponds to 24.2 mmoles of $Li_2S_2O_4$ per gram of the carbon cathode.

The carbon containing $Li_2S_2O_4$ was carefully separated from the Al grid. It was dried in vacuum, ground up, and divided into two portions. Identical experiments were run with each portion.

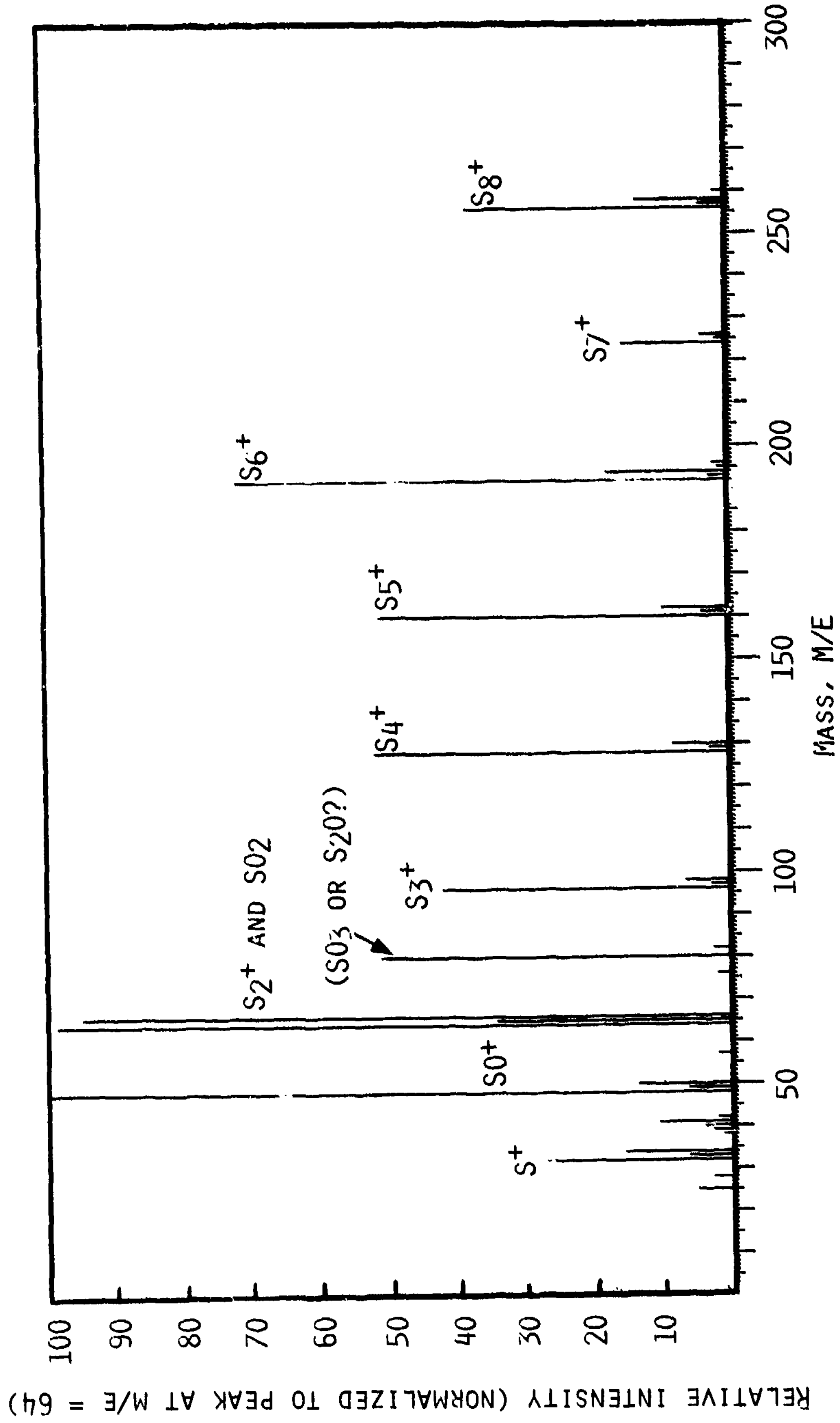

FIGURE 6. MASS SPECTRUM OF THE VOLATILE DECOMPOSITION PRODUCTS FROM A CATHODE DISCHARGED TO 0.0V

The experimental set up consisted of a flask, containing the sample, which was attached to a vacuum manifold, provided with a mercury manometer. An empty collection flask was also present in another part of the vacuum manifold in order to be able to collect the volatiles under vacuum by low temperature distillation.

The temperature of the flask was measured with an Omega Digital thermometer using an iron-constantan thermocouple junction placed on its outside wall. The flask was slowly heated at a rate of ~ 1°C/min.

Figures 7 and 8 depict the decomposition profiles for the two samples as measured by the increase in pressure of the volatile products versus temperature. The behavior of the two samples are practically identical. Significant decomposition of the cathode begins at ~ 170°C and it is complete by ~ 200°C.

The infrared spectrum of the volatiles collected is given in Figure 9. Practically all of the gas is SO_2. However, small amounts of CS_2 (1520 and 1540 cm^{-1}; doublet) COS (2040 and 2060 cm^{-1}; doublet) and CO_2 (2300 cm^{-1} - common to both SO_2 and CO_2 - and 3640 and 3720 cm^{-1}) are also present.* We had identified these carbon-based gases in the volatile products from cells vented during forced overdischarge (3-5). Indeed, thermal decomposition experiments carried out with cathodes from forced overdischarged cells indicated significant quantities of CO_2, CS_2 and COS, in addition to SO_2 (see later, Section 6.1).

The quantitative data given in Table 4 indicate that ~ 1 mole of SO_2 is produced by the decomposition of three moles of $Li_2S_2O_4$. Sulfur as a decomposition product was confirmed by separating it and identifying by its melting point.

TABLE 4. SUMMARY OF THERMAL DECOMPOSITION EXPERIMENTS

Sample	Total Weight (g)	Weight $Li_2S_2O_4$ (g)	Weight of Gas Collected† (g)	Mole Ratio of $Li_2S_2O_4/SO_2$
1	3.85	2.98	0.45	3.01
2	5.45	4.25	0.61	3.12

†Practically all of the gas is SO_2; see text.

The infrared spectrum of the residue left after the decomposition is given in Figure 10. The strong peak at 950 cm^{-1} seems to indicate the presence of Li_2SO_3.

The thermal decomposition of $Li_2S_2O_4$ apparently occurs as shown in equation 2. However, we do not rule out additional, as yet unidentified, decomposition products.

$$3Li_2S_2O_4 \xrightarrow[175-200^{\circ}C]{\Delta} SO_2 + xS + yLi_2SO_3 \qquad [2]$$

*Because the mass spectrum was normalized to mass 64 which combines the peak intensities of S_2 and SO_2, the mass peaks of CS_2, COS and CO_2 were attenuated so much that they did not show up in the mass spectrum.

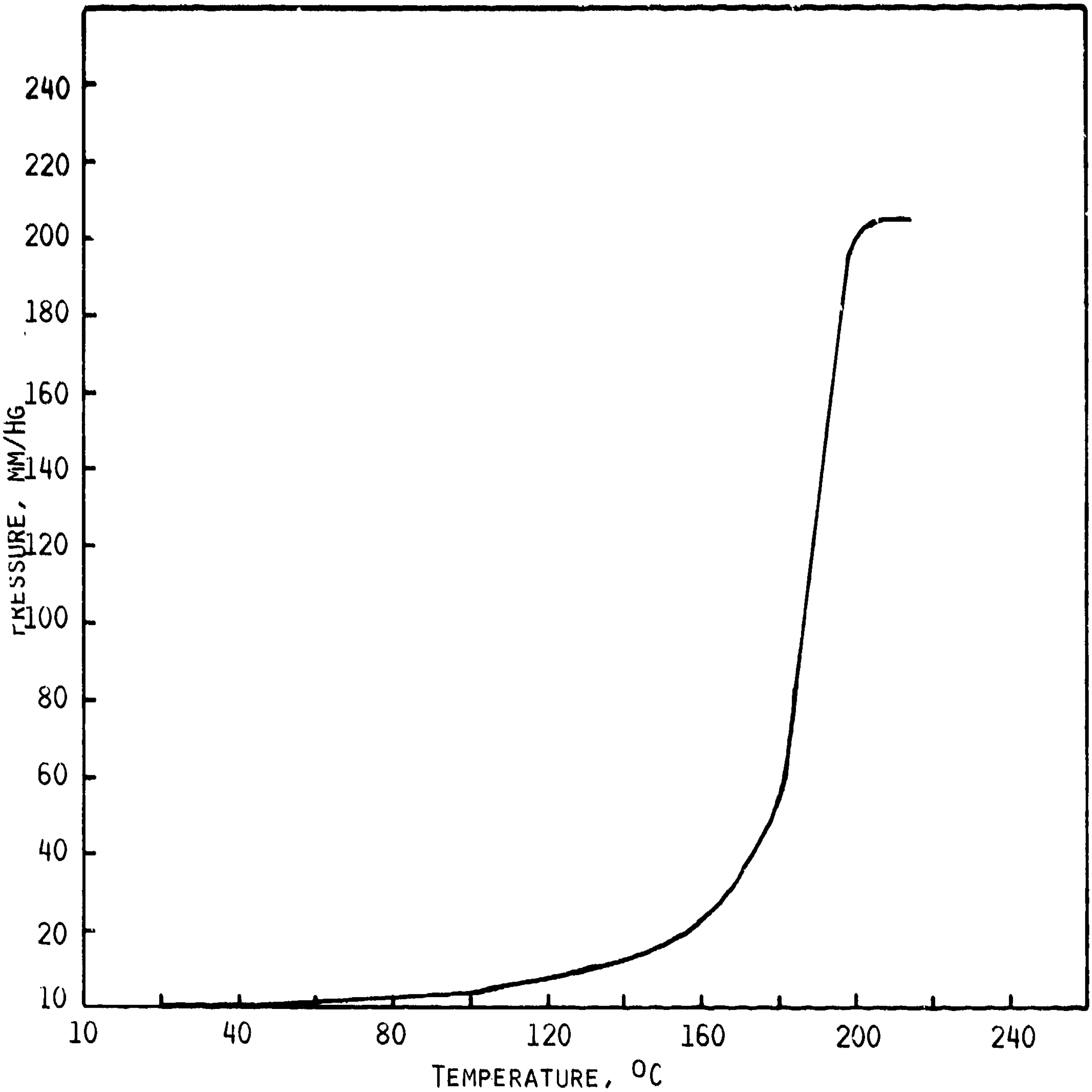

FIGURE 7. RATE OF FORMATION OF GAS PRODUCTS DURING THERMAL DECOMPOSITION OF A DISCHARGED CATHODE. SAMPLE 1

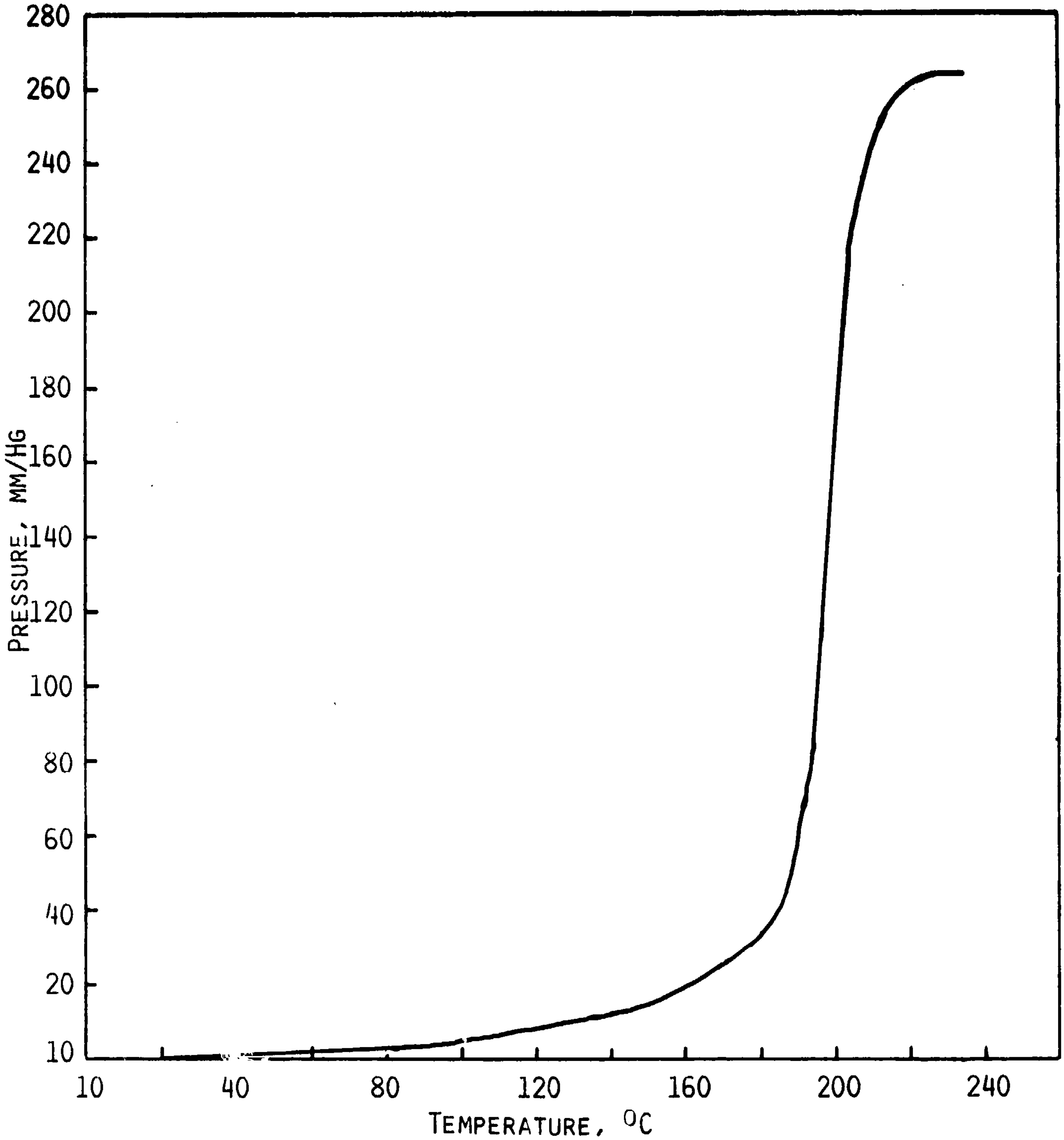

FIGURE 8. RATE OF FORMATION OF GAS PRODUCTS DURING THERMAL DECOMPOSITION OF A DISCHARGED CATHODE. SAMPLE 2

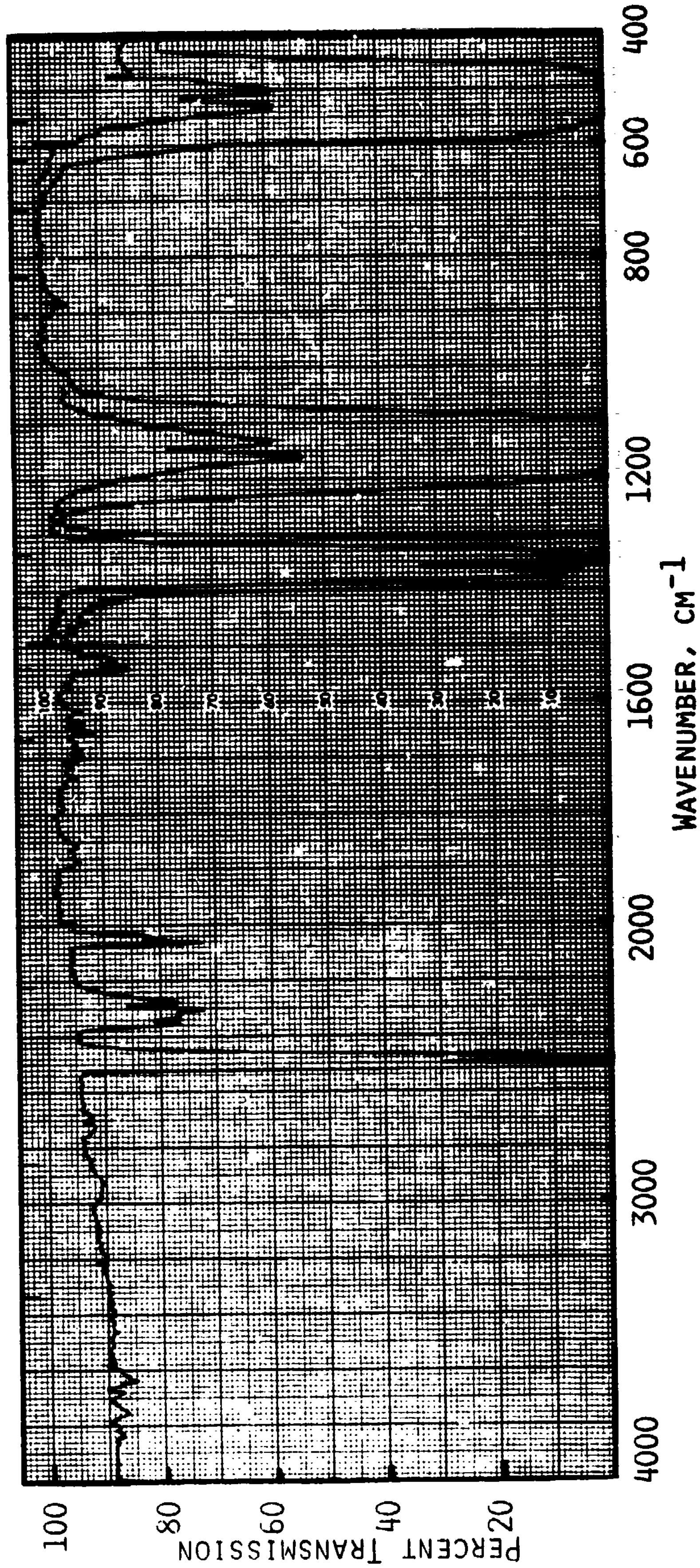

FIGURE 9. VAPOR PHASE IR SPECTRUM OF THE GASES OBTAINED FROM THE THERMAL DECOMPOSITION OF A DISCHARGED CATHODE

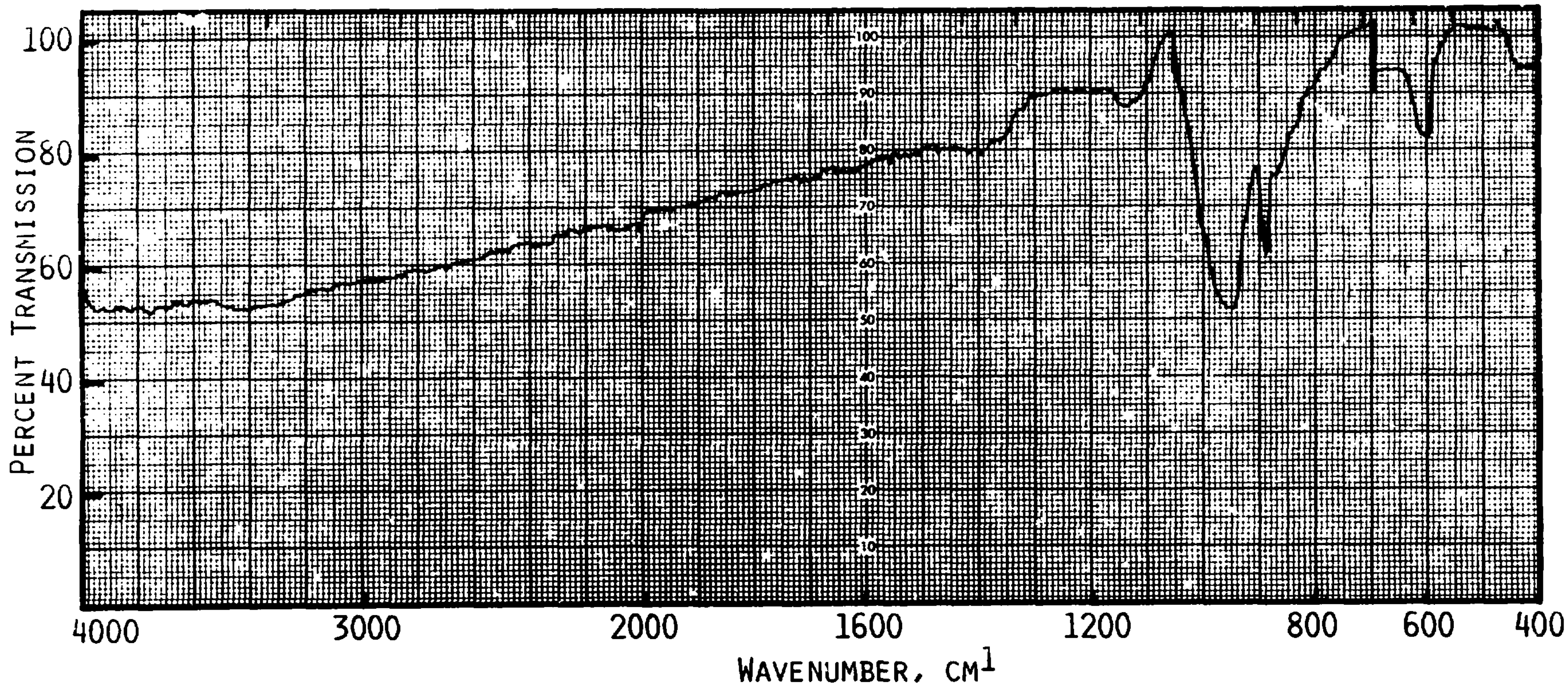

FIGURE 16. INFRARED SPECTRUM OF THE RESIDUE LEFT AFTER THE DECOMPOSITION OF A DISCHARGED CATHODE

The significance of the above observations in relation to the safety of the cell is obvious. Once the temperature in the cell rises to ~ 180°C, pressure build-up would be caused also by the SO_2 and other gases, associated with the thermal decomposition of $Li_2S_2O_4$. The CO_2, COS and CS_2 appear to come from the direct reaction of SO_2 and/or S with the carbon in the cathode. These reactions will be discussed in greater detail later. (See Section 6 .)

CHAPTER 5

FORCED OVERDISCHARGE BEHAVIOR AND CHEMISTRY OF Li/SO_2 CELLS

The major objectives of the forced overdischarge studies were to reproducibly characterize the hazards we had experienced in commercial cells (3,4) and to identify the mechanism of the forced overdischarge related explosion hazards. It was also the goal to confirm in our own well-specified cells the chemistry that was characterized in commercial cells and to further explore the chemistry under well-specified overdischarge conditions. The use of cells incorporating reference electrodes makes it possible to study the chemistry and behavior of cells under well-defined overdischarge conditions.

FORCED OVERDISCHARGE AT HIGH RATES AT ROOM TEMPERATURE

The room temperature forced overdischarge hazards in commercial cells were all observed at relatively high currents, i.e., ~ 0.8 to 1.0 ampere discharge and overdischarge in a C-cell (3). Therefore, in the present study we stressed tests at high currents. In the construction of the cells used in this study, we attempted to reproduce, as much as possible, the major features of the Type-Z commercial cells which had shown venting/explosion hazards during high current forced overdischarge.

Phenomenology of Forced Overdischarge

The various cells tested are listed in Table 4. Pertinent results are summarized in Table 5. The cells exhibited little consistency with respect to hazardous behavior during forced overdischarge. Only two cells among the nine listed in Tables 5 and 6 vented. Another cell had its cathode tab burned-off; it didn't vent. Despite the irreproducibility of the high current forced overdischarge behavior at room temperature, the phenomenology discussed below is useful in gaining an understanding of the problem.

Cells Which Did Not Vent or Explode on Forced Overdischarge. The discharge and overdischarge curves given in Figures 11-15 for Cells E-2, E-3, E-4, E-11 and E-12 respectively, illustrate the general behavior of the cells tested at high currents. The end-of-life of all these cells were caused by carbon cathode limitation. Carbon utilization is fairly high - about 1-1.3 Ah/g of carbon - even at the 1 ampere discharge which corresponds to ~ 8 mA/cm^2.

The overdischarge of Cell E-2 is characterized initially by a relatively small negative cell voltage of -0.8V. The latter is nearly the same as that of the carbon electrode. After about an hour of overdischarge at 800 mA, the cell went

TABLE 5. CONSTRUCTION PARAMETERS OF CELLS TESTED AT HIGH CURRENTS AT ROOM TEMPERATURE

	Anode		Cathode		Electrolyte			Test Current	
Cell No.	Area (cm^2)	Capacity (Ah)	Area (cm^2)	g (Carbon)	SO_2 (g) (Ahr)	CH_3CN (g)	LiBr (g)	Discharge (Amp)	Overdischg. (Amp)
E-2	185	7.0	125	2.1	9.2 (3.85)	3.94	1.25	0.8	0.8
E-3	185	7.0	125	2.0	9.0 (3.80)	3.85	1.22	1.0	1.0
E-4	185	7.0	125	2.1	8.9 (3.70)	3.80	1.20	1.0	1.0
E-5	185	7.0	125	2.1	[illegible] (3.6)	3.81	1.21	1.0	1.0
E-10	135	5.4	125	2.0	9.3 (3.9)	5.2	1.26	1.0	1.0
E-11	135	5.4	125	2.2	9.3 (3.9)	5.1	1.26	1.0	1.0
E-12	135	5.4	125	2.2	9.3 (3.9)	5.2	1.26	1.0	1.0
E-13	135	5.4	125	2.1	9.5 (3.95)	5.3	1.28	1.0	1.0
E-14	135	5.4	125	2.0	9.5 (3.95)	5.3	1.28	1.0	1.0

TABLE 6. TEST RESULTS FOR THE CELLS LISTED IN TABLE 5

Cell No.	Discharge Current (Amp)	Capacity to 2.0V (Ahr)	Capacity to 0.0V (Ahr)	Carbon Utilization (Ahr/g)	Forced Overdischarge Current (Amp)	Extent of overdischarge (Hr)	Comments
E-2	0.8	2.24	2.48	1.18	0.8	21	Cathode tab apparently had burned off after ~1 hr of O.D.
E-3	1	2.55	2.75	1.33	1	13.5	Did not vent.
E-4	1	2.20	2.50	1.18	1	16.5	Did not vent.
E-5	1	2.50	2.67	1.26	1	6.3	
E-10	1	2.18	2.50	1.18	1	3.4	Vented.
E-11	1	1.90	2.10	0.95	1	19	Did not vent, but evidence for internal burning.
E-12	1	1.70	2.10	0.95	1	20	Did not vent.
E-13	1	1.72	1.90	0.95	1	0.5	Vented
E-14	1	1.90	2.2	1.12	1	1.25	Cell intentionally terminated for chem. analysis.

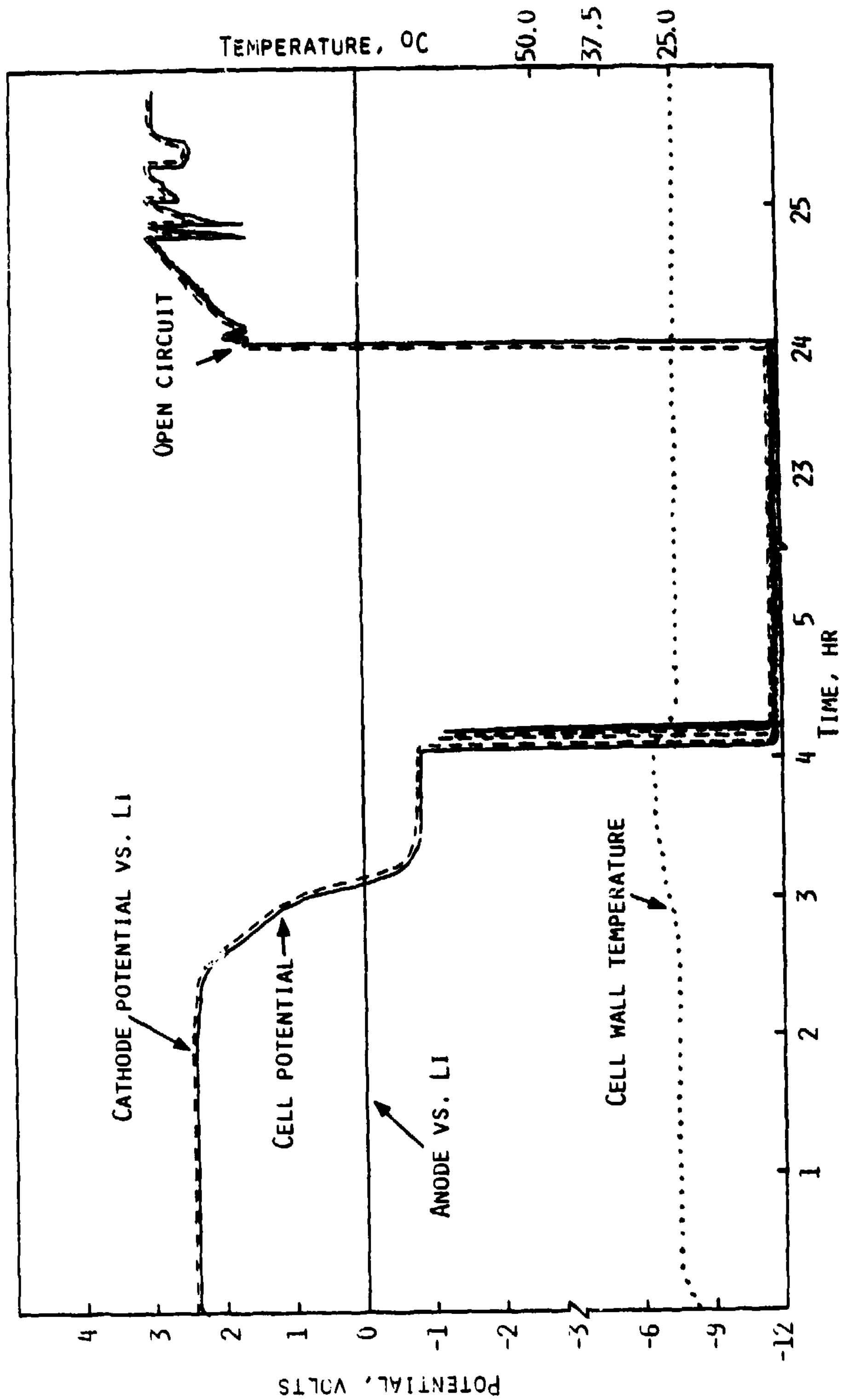

CURRENT, 800 mA; CURRENT DENSITY, 6.4 mA/cm^2

FIGURE 11. DISCHARGE AND OVERDISCHARGE DATA FOR CELL E-2

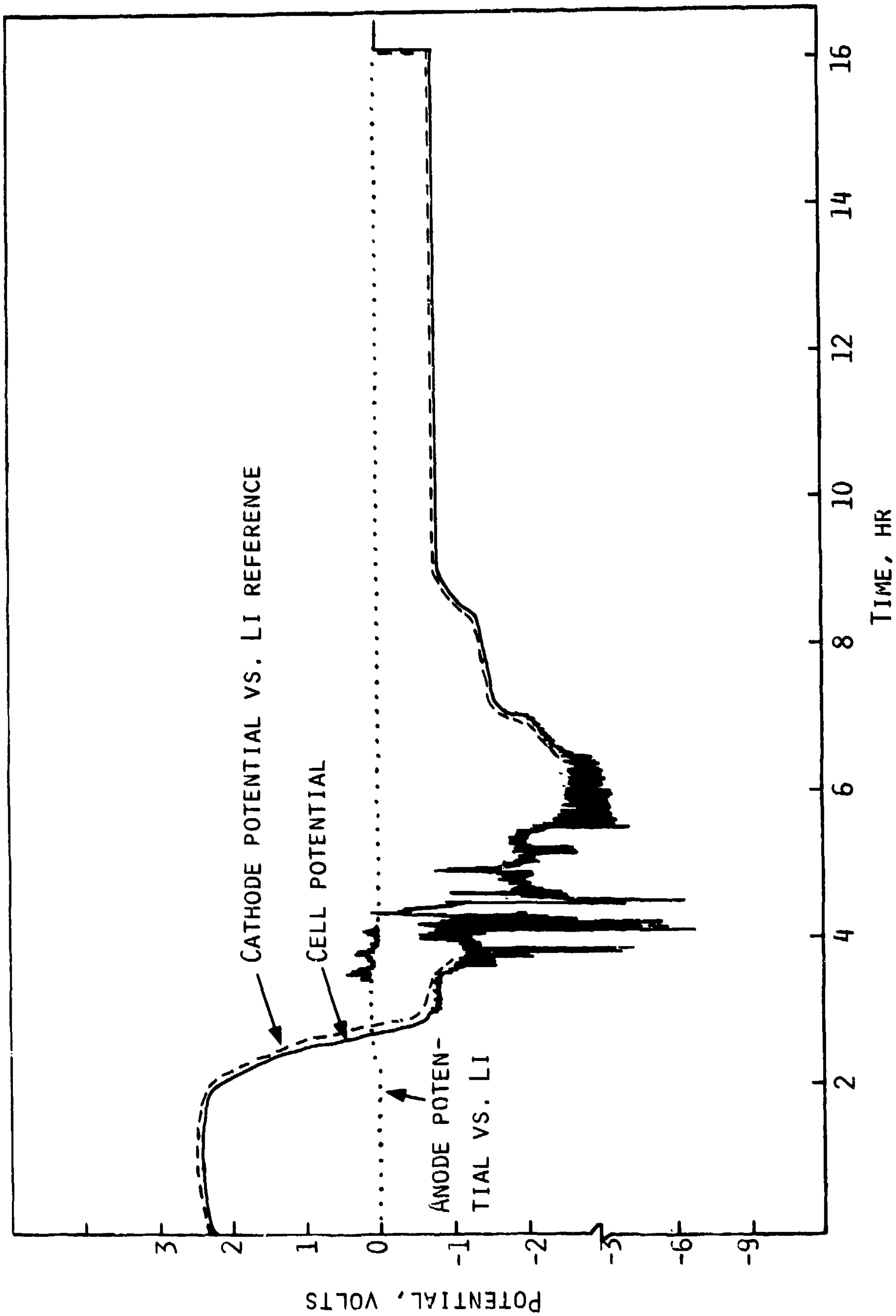

CURRENT, 1A; CURRENT DENSITY; 8 mA/cm^2

FIGURE 12. DISCHARGE AND OVERDISCHARGE DATA FOR CELL E-3

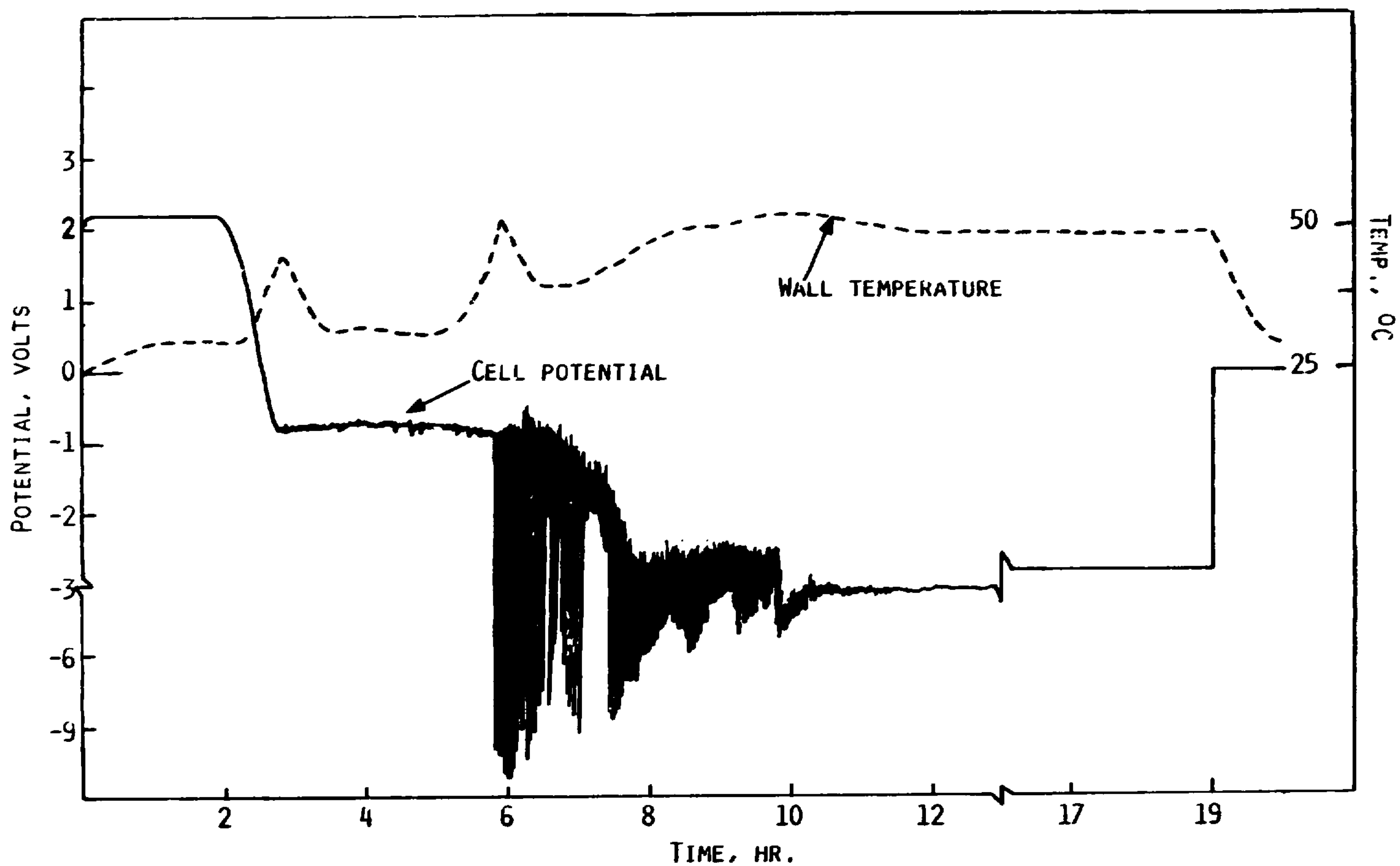

CURRENT, 1A

FIGURE 13A. DISCHARGE AND OVERDISCHARGE DATA FOR CELL E-4 (SEE NEXT FIGURE ALSO.)

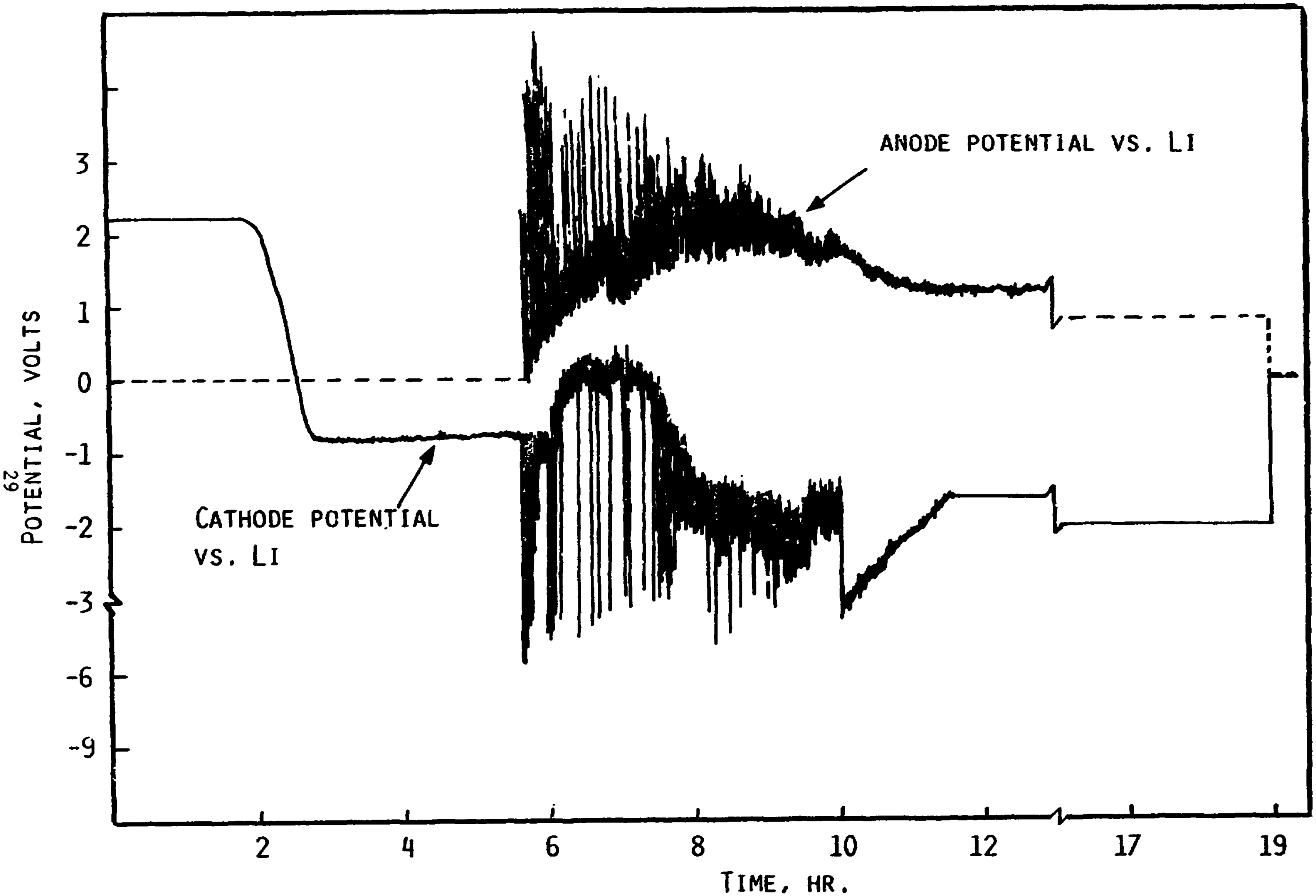

CURRENT, 1A (CONTINUED FROM FIG. 13A)

FIGURE 13B. DISCHARGE AND OVERDISCHARGE DATA FOR CELL E-4

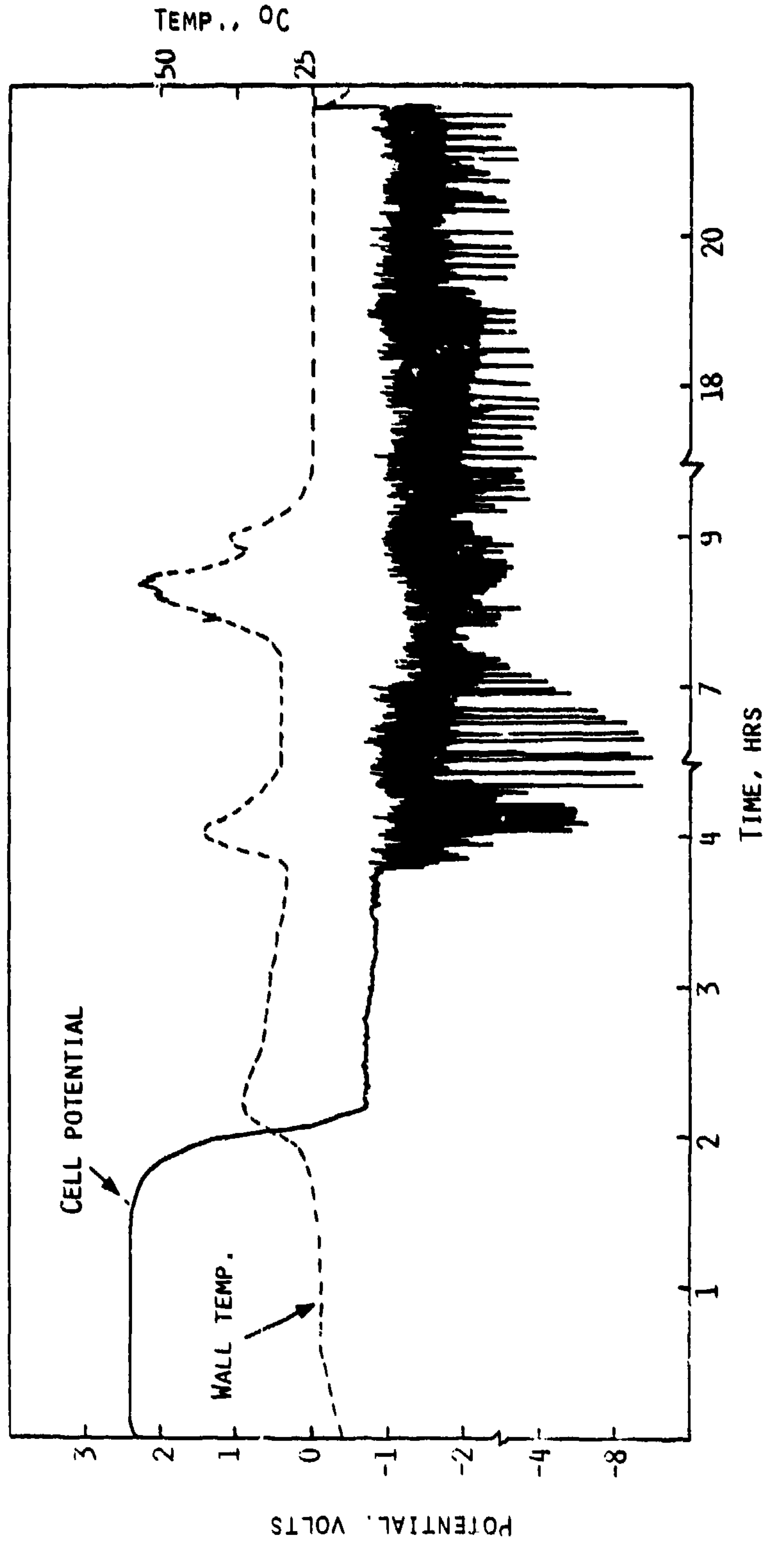

CURRENT, 1A

FIGURE 14A. DISCHARGE AND OVERDISCHARGE DATA FOR CELL E-11 (SEE NEXT FIGURE ALSO.)

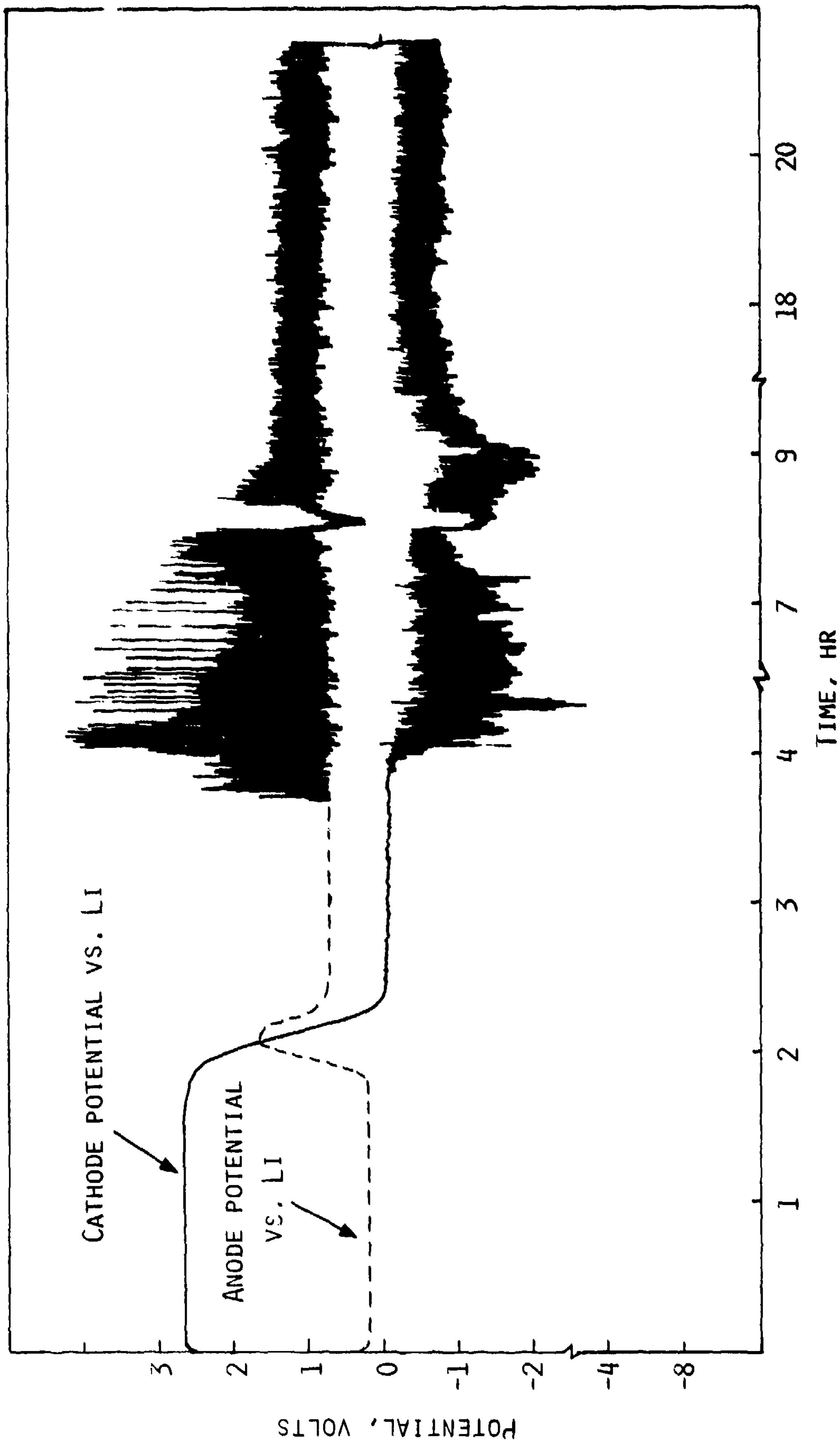

FIGURE 14B. DISCHARGE AND OVERDISCHARGE DATA FOR CELL E-11 (SEE FIG. 14A ALSO.)

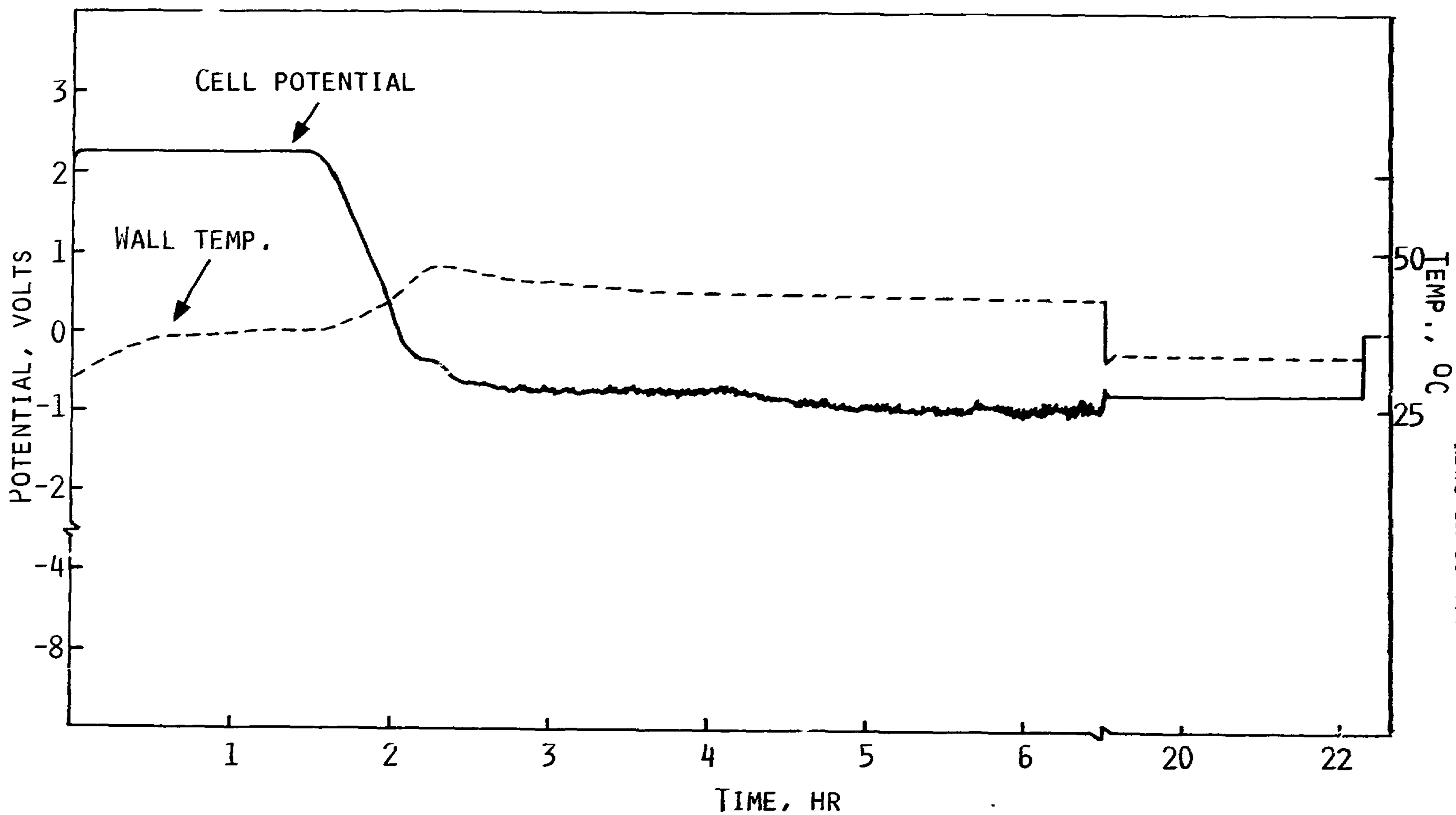

CURRENT, 1A

FIGURE 15A. DISCHARGE AND OVERDISCHARGE DATA FOR CELL E-12 (SEE NEXT FIGURE ALSO.)

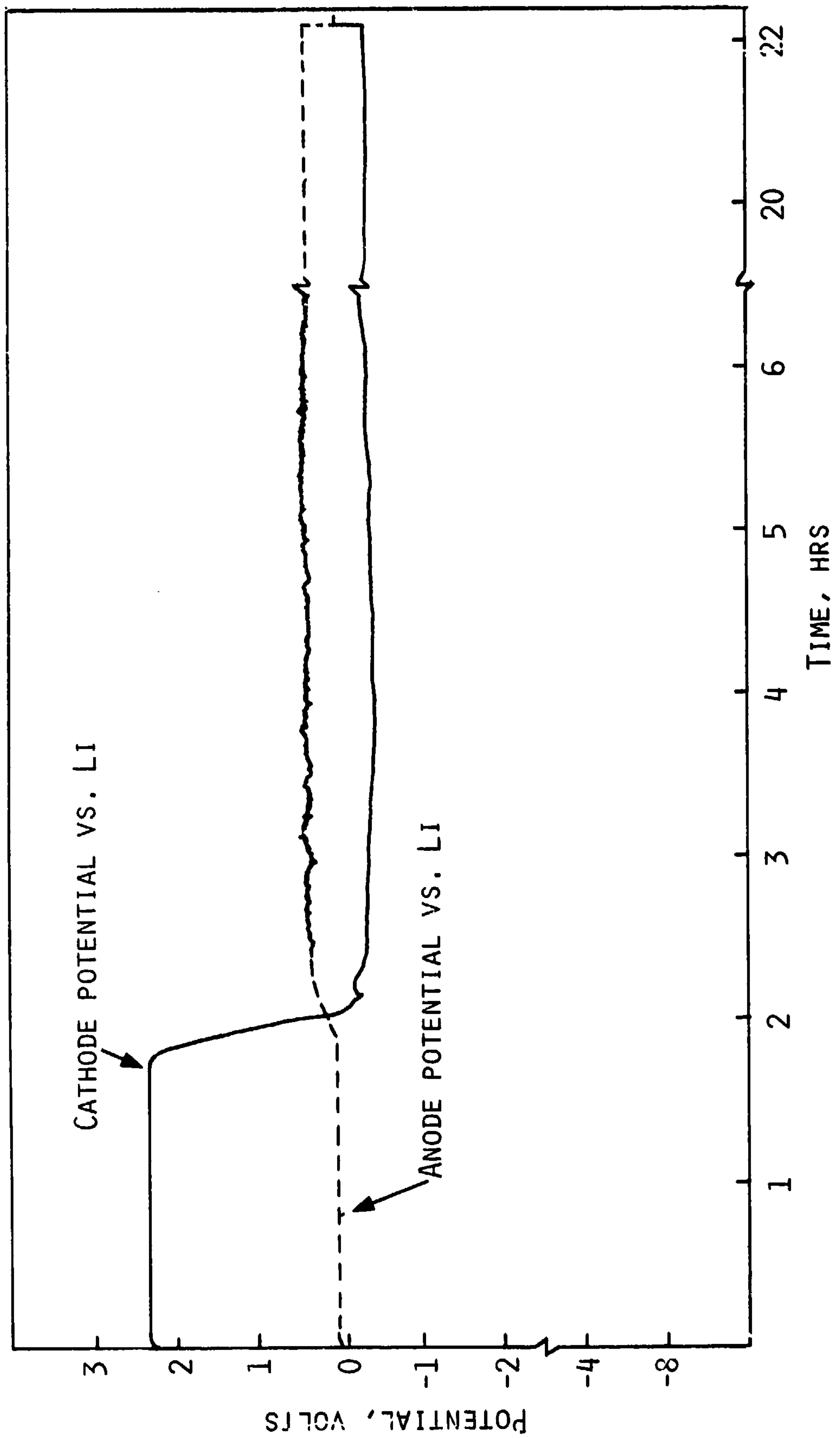

FIGURE 15B. DISCHARGE AND OVERDISCHARGE DATA FOR CELL E-12 (SEE FIG. 5 ALSO.)

into a deep reversal. An examination of the individual electrode potentials shows that the deep reversal is accompanied by a sharp drop in the cathode potential; there is no change in the potential of the anode. A post-test examination of the cell indicated that the cathode tab had burned off. This behavior is reminiscent of the behavior of the Type-Z commercial cells we reported earlier (3). The wall temperature of Cell E-2 shows a small rise (~ 5°C) towards the end of discharge and remains at the higher level until the deep reversal. There is no sharp temperature rise accompanying the deep reversal, which is in agreement with the fact that the cell neither vented nor exploded.

Cell E-3 was overdischarged for ~ 13 hours. The combined apparent charge utilized in the discharge and overdischarge corresponds to ~ 2.5 times the Li capacity. The cell did not show any hazardous behavior. The cell shows an initial fluctuating overdischarge voltage behavior for ~ 4 hours, and then, smooth, and relatively small, negative voltages. All the changes in the cell voltage during overdischarge reflect those of the cathode.

The overdischarge of Cell E-4 initially proceeds at ~ -0.8V which reflects the potential of the cathode. The reversal continues with this potential profile until almost the end of the 6th hour of cell operation when the cell potentials begin to show large fluctuations. An examination of the individual electrode potentials, given in Figure 13B, indicates fluctuations in both the anode and cathode voltages. When the anode potential polarizes to positive values, the cathode potential shows a corresponding negative polarization. It appears that the large voltage fluctuations during overdischarge result from an oscillating resistive path that has been formed in the cell.

The overdischarge behavior of Cell E-11 until the end of the 4th hour of operation is practically identical to that of E-4. During that period, overdischarge is characterized by a small negative cell voltage of ~ -0.75V and a cathode voltage of ~ -0.10V. Note that when the cell potentials begin to show the oscillations, the cell temperature increases and peaks to ~ 43°C. The overdischarge continues with substantial voltage fluctuations and a second temperature rise is seen beginning with about the 8th hour operation. The cell voltage fluctuations reflect the fluctuations in the voltage of both the anode and the cathode. The cell did not vent even after 19 hours of overdischarge. However, post-test examination revealed that at one place in the cathode, by the lower edge where lithium had plated, there was some burning of the separator in a length of about 1/3 inch. It is probable that there have been small localized "venting-reactions" in this cell, probably at those instances when we observe temperature rises. An infrared spectrum of the gases collected after deliberately opening the cell showed CH_4 and very small quantities of CO_2, CS_2 and COS. The presence of the latter compounds indicates that, indeed, there were localized venting reactions in this cell (3,4) (see Chapter 6 also).

The forced overdischarge of Cell E-12 exhibits a different behavior than many of the cells discussed so far. The data for this cell are given in Figures 15A-15B. The overdischarge at 1A which begins with a small negative cell voltage of -0.70V continues in that manner for about 20 hours. The cell neither vented, nor did it show any temperature increase during the entire overdischarge. When Cell E-12 was disassembled after the test, plated Li was found on the cathode. There was some discoloration of the separator also. A vapor phase IR spectrum did not show any of the gases that would be formed as a result of a "venting-reaction". It appears that the only manner in which the cell could have sustained such a long

overdischarge without any significant cell polarization is via a "short-circuit" following plating of Li onto the cathode.

Cells Which Vented on Forced Overdischarge. Only two among the nine cells listed in Table 5 vented during the high current forced overdischarge at room temperature. Unlike the forced overdischarge explosion/venting hazard at low temperatures (see later), the hazard at room temperature is less reproducible. Even cells with seemingly identical behavior do not always show an explosion/venting. The two cells which vented are E-10 and E-13.

The discharge and overdischarge data for Cell E-10 are shown in Figure 16. The discharge current of 1A corresponds to a current density of 8 mA/cm^2. The cell discharge is clearly limited by the carbon electrode. The capacity to 0.0 volt is 2.35 A-hr which corresponds to a carbon utilization of 1.18 A-hr/gram. The forced overdischarge is characterized by a rather small negative cell voltage of $\sim$ -0.50V. The cathode voltage is even smaller, remaining at $\sim$ -0.10V. There are small fluctuations in cell voltages which reflect those of the anode. The cell vented at about the 5.5th hour of operation. There were small oscillations in cell voltages just prior to the venting and they appear to reflect fluctuations in anode potentials. The venting is accompanied by a large negative polarization of the cell voltage which reflects the polarization of the cathode. It is also accompanied by a sudden rise in cell wall temperature. In addition to the temperature, a major indicator for cell venting is the gaseous products. An IR spectrum indicated that the gases consisted of CO_2, COS, CS_2, CH_4 and probably H_2S, C_2H_2, and C_2H_4, in addition to CH_3CN and SO_2. The quantities of C_2H_2 and C_2H_4 are relatively small in comparison to those identified previously in commercial cells. The difference seems to be a measure of the severity of the venting reaction. Post-test examination revealed that the "venting-reactions" were localized at the outer wrap of the cell package, and more specifically at the cathode. Portions of the cathode appeared burned. It seems that the reactions were initiated at the cathode. The latter finding is in agreement with the large negative polarization of the cathode accompanying the temperature rise. The explosion reaction was not very intense which seems to explain the relatively small quantities of C_2H_2 and C_2H_4 produced.

As indicated by the data in Figures 17A and 17B, the end-of-life of Cell E-13 also was caused by limitations at the carbon electrode. Its forced overdischarge proceeds with a relatively small negative cathode voltage. The cell potentials begin to show fluctuations after about 20 minutes into the overdischarge. Initially the fluctuations are caused by the cathode. However, just prior to venting, which occurred at about 1/2 hour into overdischarge, the anode also shows some voltage oscillations. This cell vented much sooner than Cell E-10, probably because of an overall higher temperature profile in the cell. Although the cathode discharge potentials remain at the normal values expected for this current, the cell voltages are lower than those found in the other cells listed in Table 5. This appears to be due to the anode which shows a much larger than normal polarization even from the beginning, probably because of a poor anode-to-can contact. As a result, there has been a larger resistive heating of the cell throughout discharge and overdischarge. A post-test examination revealed that the core of the jelly-rolled electrode package had burned off with the various parts of the package having been fused together. It appeared that the initiation of venting/explosion occurred at the core of the cell package. The damage to the cell was much more extensive than in Cell E-10. An infrared spectrum of the vented gases, given in Figure 18, is characterized by absorptions due to CO_2, COS, CS_2, CH_4, C_2H_2 and

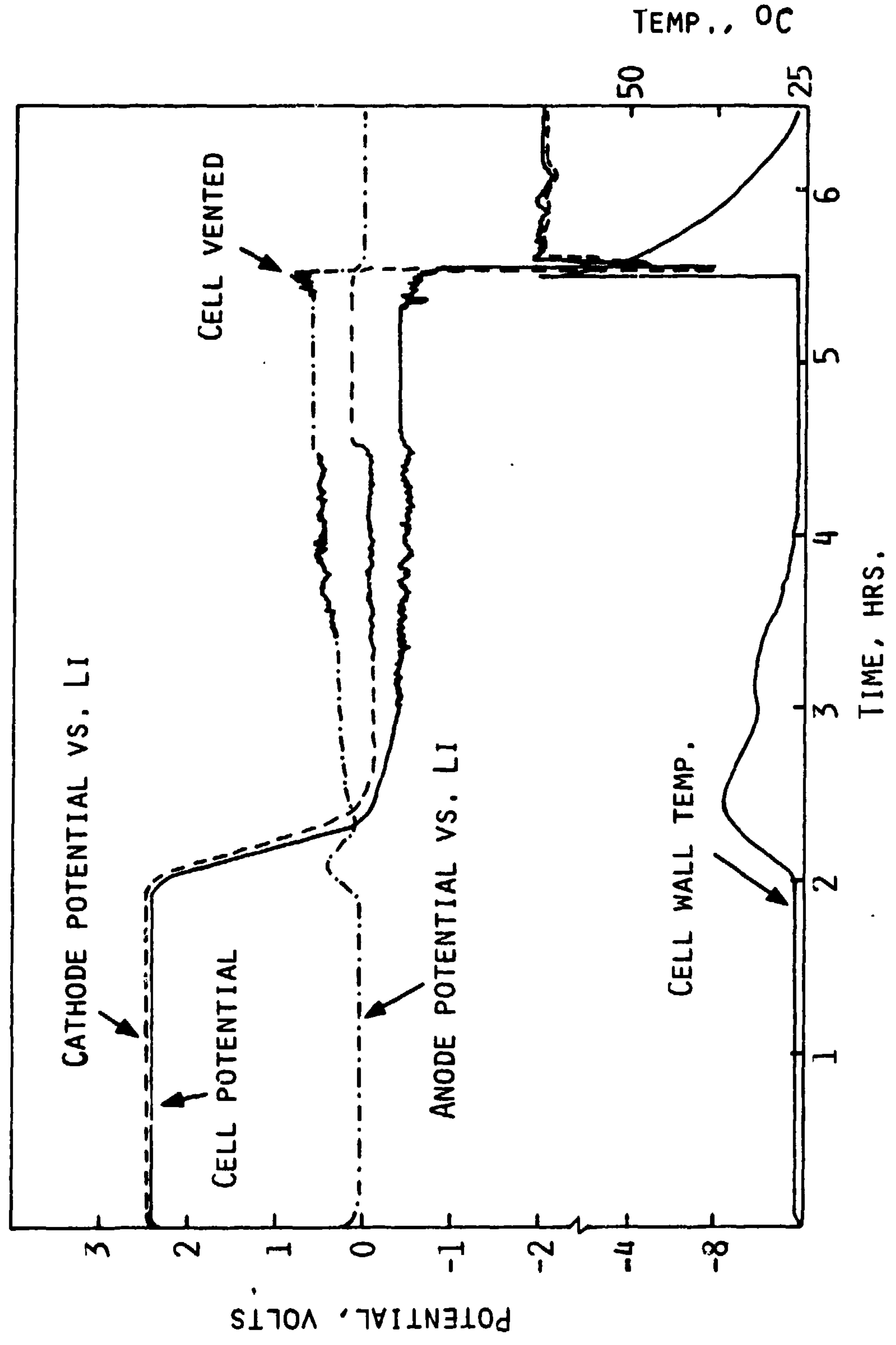

CURRENT, 1A

FIGURE 16. DISCHARGE AND OVERDISCHARGE DATA FOR CELL E-10

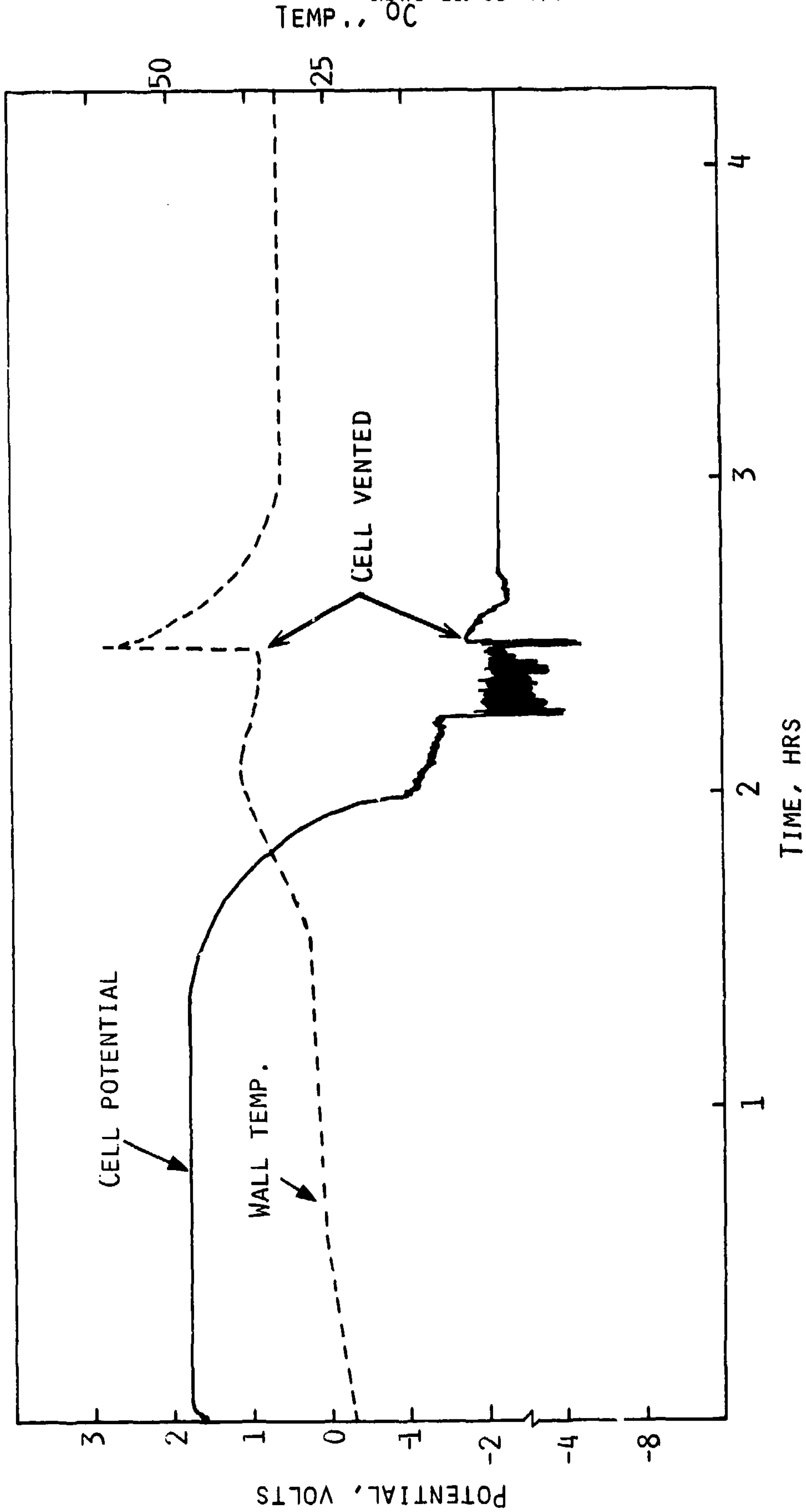

CURRENT, 1A

FIGURE 17A. DISCHARGE AND OVERDISCHARGE DATA FOR CELL E-13 (SEE NEXT FIGURE ALSO.)

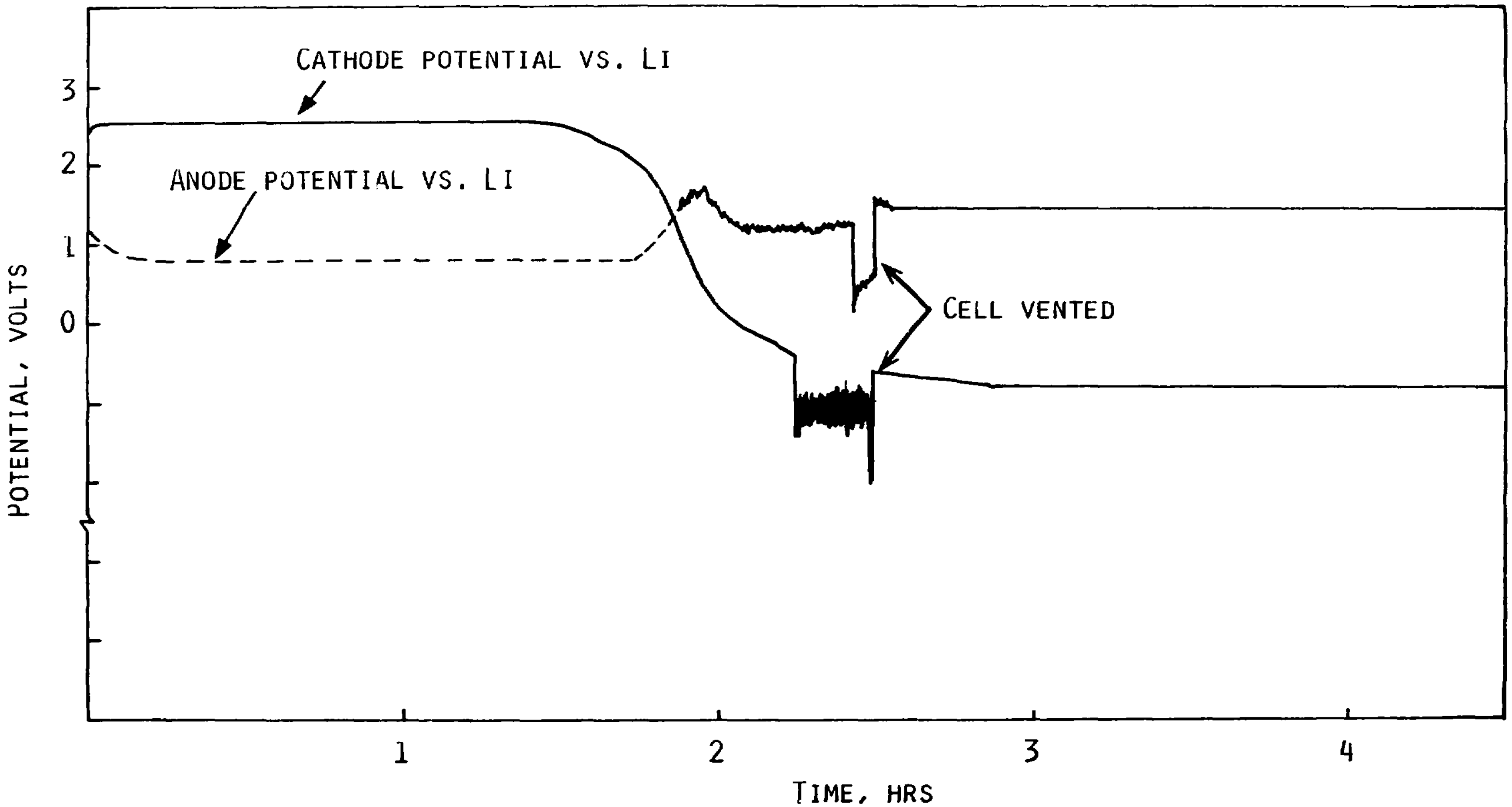

CURRENT, 1A

FIGURE 17B. DISCHARGE AND OVERDISCHARGE DATA FOR CELL E-13 (SEE FIG. 17A ALSO.)

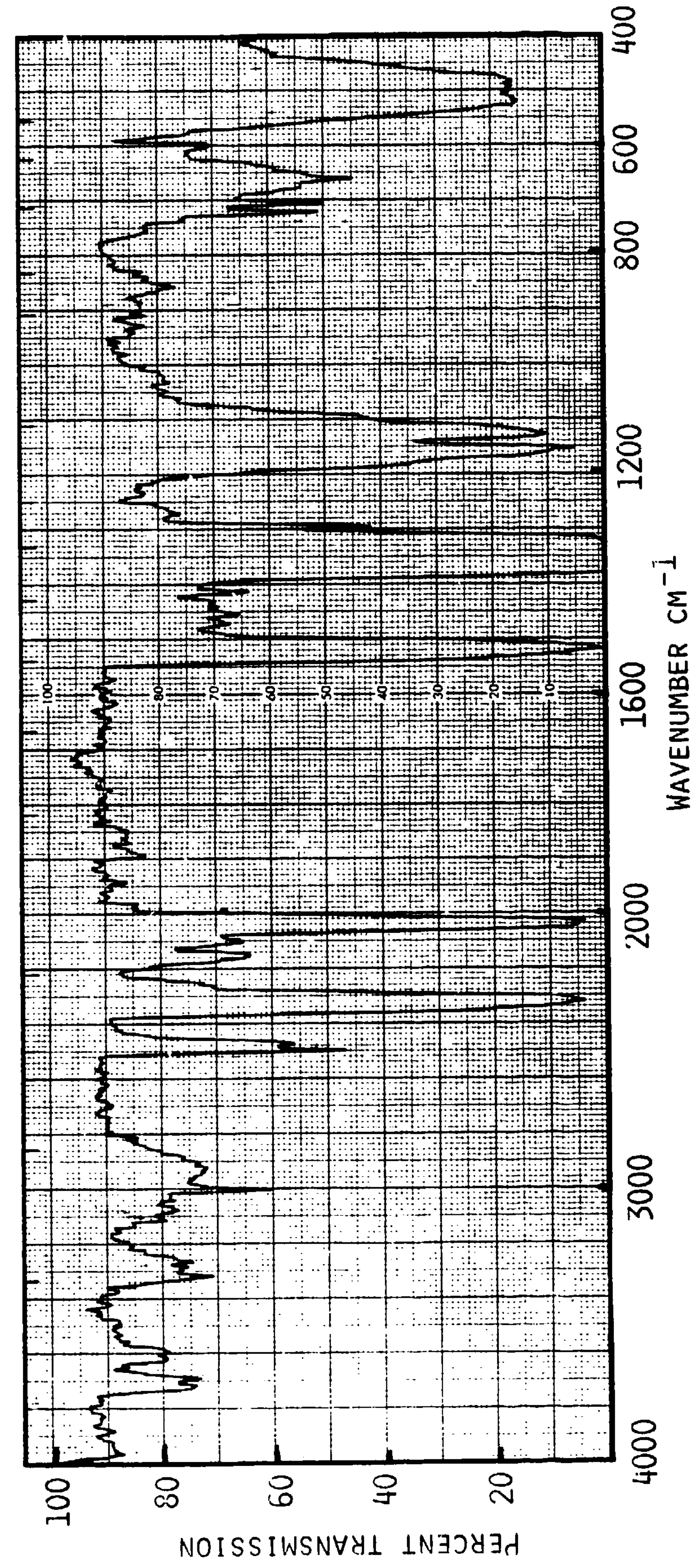

FIGURE 18. INFRARED SPECTRUM OF GASES VENTED FROM CELL E-13

C_2H_4, in addition to CH_3CN and SO_2. It should be noted that some of the SO_2 in the vented gases comes also from the decomposition of $Li_2S_2O_4$.

A comparison of the behavior of E-10 and E-13 seems to indicate that the timing of a venting reaction during forced overdischarge depends to a great extent on the cell's temperature profiles. It appears that, if the conditions in the cell do not permit the temperature to rise to a critical value, there may not be a venting or an explosion. It seems that the most probable time a venting can occur is when the cell shows voltage oscillations after deposition of Li at a relatively low overpotential. It appears that the voltage oscillations are the major cause of excessive cell heating. Indeed, the oscillations are the one common feature of all cells which vent/explode during forced overdischarge, either at room temperature or at low temperatures

Chemical Analysis

It is apparent that the chemical reactions which take place in the first stages of an overdischarge contributes significantly to the venting/explosion which ensues.

In the previous program, we carried out chemical analysis of cells, mostly forced overdischarged at low currents (3,5). In such cells, we identified CH_4 in the gas phase, and di- and tri-acetonitriles on the anode, along with LiCN, $Li_2S_2O_4$ and Li_2SO_3. We proposed the following mechanism to explain the formation of these products.

$$CH_3CN + 2Li \rightarrow CH_3Li + LiCN \qquad [3]$$

$$CH_3^- + CH_3CN \rightarrow CH_4 + {}^-CH_2CN \qquad [4]$$

$$CH_3C{\equiv}N + {}^-CH_2CN \rightarrow CH_3-\underset{\underset{\bar{N}}{\|}}{C}-CH_2CN \qquad [5]$$

$$CH_3-\underset{\underset{\bar{N}}{\|}}{C}-CH_2CN + CH_3CN \rightarrow {}^-CH_2CN + CH_3-\underset{\underset{NH}{\|}}{C}-CH_2CN \qquad [6]$$

$$CH_3-\underset{\underset{NH}{\|}}{C}-\bar{C}H-CN \rightarrow CH_3-\underset{\underset{NH_2}{|}}{C}=CH-CN \qquad [7]$$

Di-acetonitrile, I

$$CH_3-\underset{\underset{NH_2}{|}}{C}=CH-CN + {}^-CH_2CN \rightarrow\rightarrow\rightarrow CH_3-\underset{\underset{NH_2}{|}}{C}=CH-\underset{\underset{NH_2}{|}}{C}=CH-CN \qquad [8]$$

Tri-acetonitrile, II

The tri-acetonitrile could exist in isomeric forms II or III. It is difficult to distinguish between the two by mass-spectral data. The following scheme illustrates the formation of III.

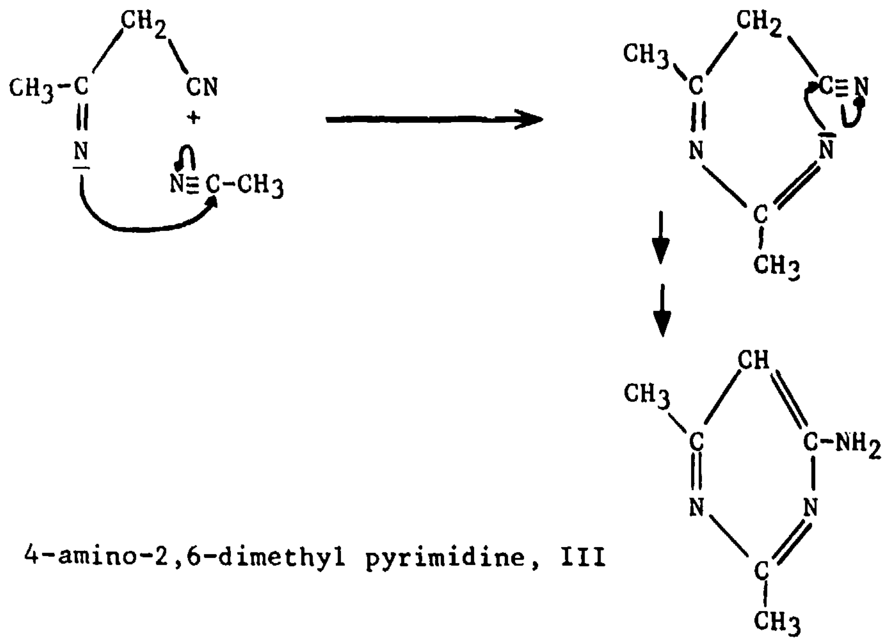

4-amino-2,6-dimethyl pyrimidine, III

The Li_2SO_3 on the anode of forced overdischarged cells probably comes from the reaction between SO_2 and organic Li compounds, e.g., $LiCH_2CN$. Supporting this, we have found that a reaction between n-C_4H_9Li and SO_2 results mainly in Li_2SO_3.

In C-cells that are discharged at low currents of 150-300 mA only small amounts of SO_2 are left when they go into reversal. This facilitates direct reaction between Li and CH_3CN. The situation is different in the cells tested at high currents. Nearly 40-50% of the SO_2 remains at the time the cell goes into reversal. Because of the larger amount of SO_2, a direct reaction between Li and CH_3CN would be sluggish.

We have analyzed Cell E-14 (Fig. 19) in order to gain further insight into the cell chemistry that proceeds a venting/explosion. The cell was discharged and overdischarged at 1A. After about 1.15 hr of overdischarge, it was opened and analyzed.

The anode had significantly less organic products than in extensively overdischarged cells. An IR spectrum revealed that the small amount of products consisted of a mixture of di- and tri-acetonitrile, LiCN, $Li_2S_2O_4$ and Li_2SO_3.

Our special interest was in characterizing the chemistry that had taken place at the carbon electrode since it appears to be at this electrode that the venting reactions are initiated.

An IR spectrum of the cathode showed only $Li_2S_2O_4$ suggesting that other sulfuroxy compounds are probably not formed during forced overdischarge. Quantitative analysis had revealed that an additional amount of $Li_2S_2O_4$ is formed during overdischarge, probably from direct reactions between plated Li and SO_2 (3).

The cathode contained a brittle grey deposit. When a small piece of this material was put into water there was an exothermic reaction. We X-rayed the grey deposit as well as a piece of the Al grid located at the tab connection. We obtained an IR spectrum of the cathode and also its mass spectrum.

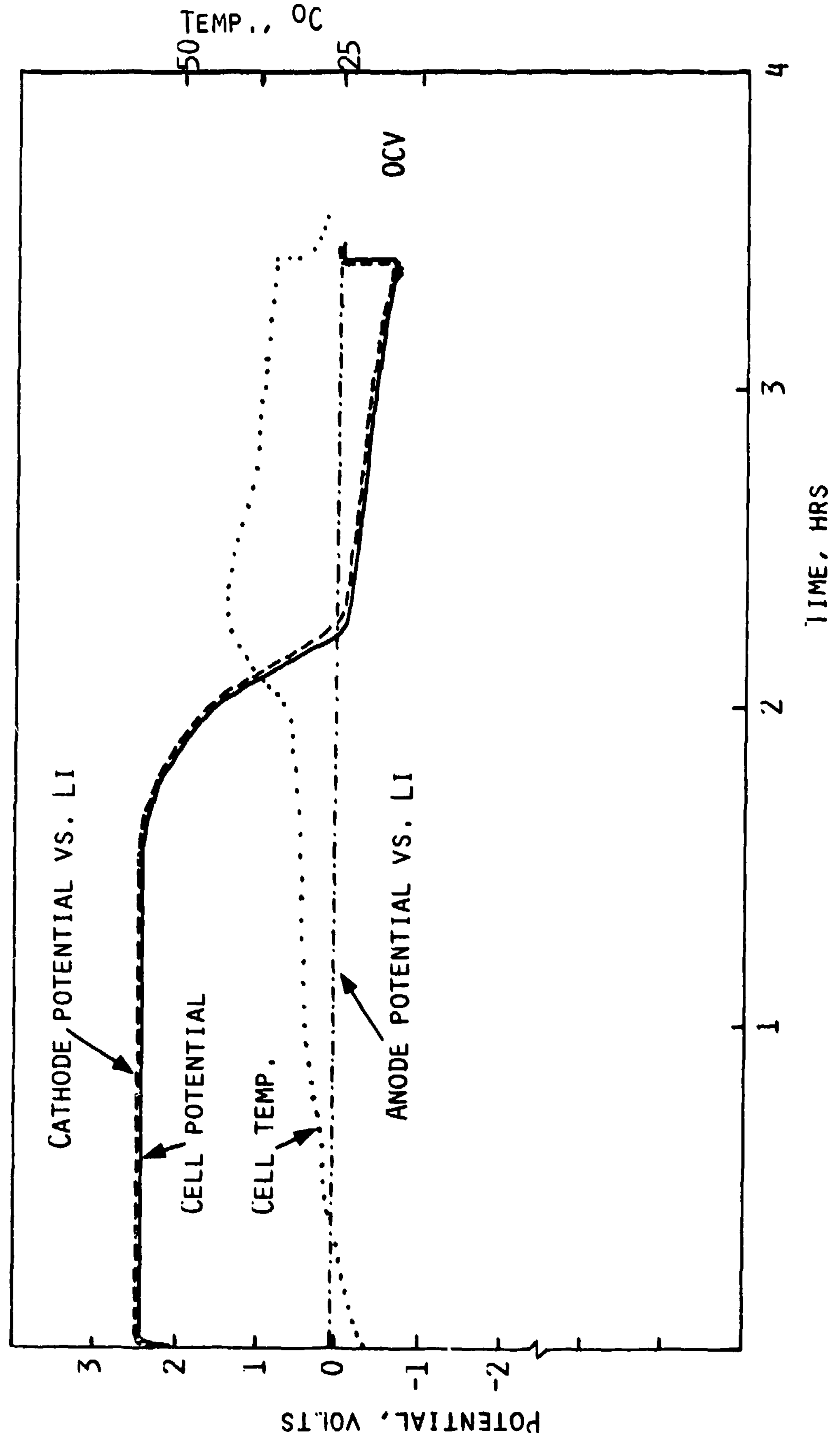

CURRENT, 1A

FIGURE 19. DISCHARGE AND OVERDISCHARGE DATA FOR CELL E-14

The X-ray data for the grey deposit are tabulated in Table 7, along with the literature X-ray patterns for $Li_2S_2O_4$, Li_2SO_4, LiBr, Li_2S, Li_2O, and Li. It is evident that the grey deposit mostly consists of Li and $Li_2S_2O_4$; that is, Li plated onto the $Li_2S_2O_4$ in the cathode. There are only a couple of lines that cannot be unequivocally identified, although they seem to match fairly well with Li_2S. There is also LiBr in the sample. We do not see any lithium sulfate.

An X-ray diffraction spectrum of the Al grid obtained from a location away from any carbon, is given in Figure 20. The spectrum can be identified with that of a mixture of LiH, Li and LiAl. It should be noted that LiH and LiF have nearly identical lines. Therefore, it is difficult to distinguish between them in the absence of any prior knowledge about the origin of the sample or without additional analytical information. However, since the tab sample is free of any carbon cathode, and hence any Teflon, it is possible to assign the lines unequivocally to LiH.

We have obtained a mass spectrum of the vacuum-dried cathode in order to see if even small quantities of the organic products (di- and tri-acetonitriles, and other compounds) had been formed at the cathode during forced overdischarge. The spectrum was obtained while heating the sample to 250°C. The mass spectrum, representing volatile or decomposition products, is shown in Figure 21. The major peaks in the spectrum are due to S_8, produced by the decomposition of $Li_2S_2O_4$ (see Fig. 6). In addition, we see weak fragmentation peaks characteristic of di- and tri-acetonitriles (3). The mass spectral data thus indicate that during forced overdischarge small quantities of the Li/CH_3CN reaction products are formed at the cathode also.

We have X-rayed the cathode from another cell, similar in performance to E-3, after an overdischarge for ~ 15 hrs. The analysis was performed on a small portion of the carbon, stripped away from the Al. The data, given in Table 8, show $Li_2S_2O_4$ and LiF and/or LiH.

The following reactions adequately explain the various products identified in the cathode.

$$Li^+ + e^- \rightarrow Li \qquad [9]$$

$$Li + Al \rightarrow LiAl \qquad [10]$$

$$CH_3CN + e^- \rightarrow CH_3\dot{\overline{CN}} \qquad [11]$$

$$Li + CH_3\dot{\overline{CN}} \rightarrow \overline{C}H_2CN + LiH \qquad [12]$$

$$2nLi + (CF_2)_n \rightarrow 2nLiF + nC \qquad [13]$$

The di- and tri-acetonitriles present on the cathode would result from $\overline{CH_2}CN$ and CH_3CN as discussed earlier in [3-8].

Discussion of High Rate Forced Overdischrge Studies at Room Temperature

The use of cells constructed with Li reference electrodes has enabled us to define conditions which lead to a venting/explosion during forced overdischarge at

TABLE 7. X-RAY DATA FOR THE GREY DEPOSIT FROM CELL E-14

Grey Deposit* from Cathode of Cell E-14		$Li_2S_2O_4$		Li_2SO_4		LiBr		Li_2S		Li	
d, Å	I/I_o	d, Å	I/I_o	d, Å	I/I_o	d, Å	I/I_o	d, Å	I/I_o	d, Å	I/I_o
4.38	50	4.37	80								
				4.05 }	100						
				4.03							
				4.00	100						
3.74	70	3.71	90	3.91	45						
				3.49	20						
3.35	10							3.31	100		
3.20	70	3.21	85			3.18	100				
2.99	30							2.85	33		
				2.79	10	2.75	80				
2.78	20										
2.67	90	2.67	100								
2.55	60	2.54	80								
2.50	100			2.48	20					2.48	100
				2.40	10						
2.30	5	2.25	15	2.30	10						
								2.02	72		
1.96	40					1.95	60				
1.77	20	1.78	5							1.76	30
1.67	10					1.66	45	1.70	66		
1.61	10					1.59	18				
								1.61	12		
1.45	10	1.47	5							1.43	40
		1.41	5			1.38	8	1.40	16		
								1.81	34		

*Debye Scherrer method; CuK_α radiation.

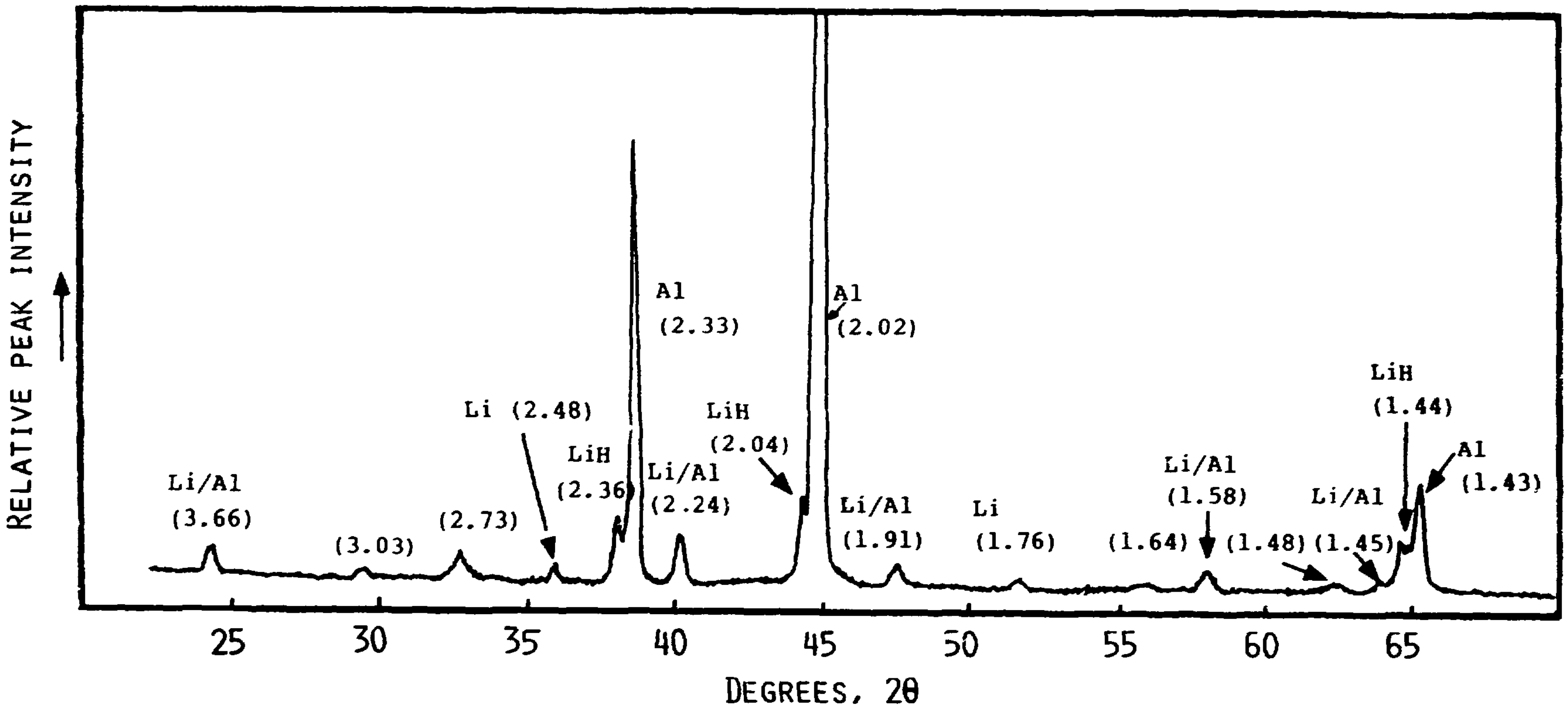

SOURCE: CuK_{α} RADIATION. THE NUMBERS IN PARENTHESES REPRESENT d VALUES.

FIGURE 20. X-RAY DIFFRACTION SPECTRUM OF THE Al TAB FROM CELL E-14

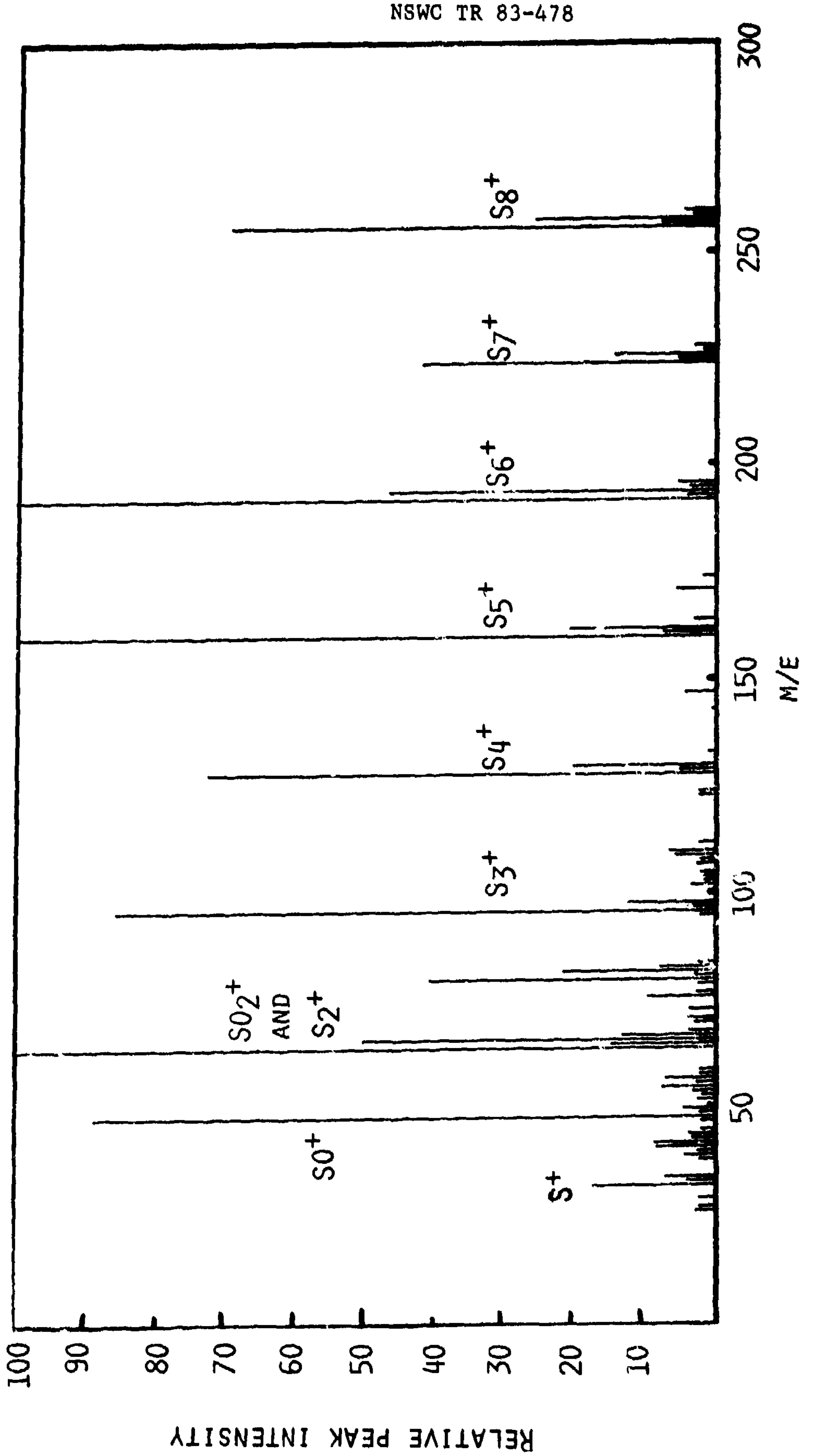

THE SPECTRUM WAS RECORDED WHILE HEATING THE SAMPLE TO 250°C (COMPARE WITH THE SPECTRUM IN FIGURE 6).

FIGURE 21. MASS SPECTRUM OF THE VOLATILE MATERIALS GIVEN OFF FROM THE CATHODE OF CELL E-14

TABLE 8. X-RAY DATA FOR A CATHODE OVERDISCHARGED AT 1A CURRENT

Overdischarge Cathode d (Å)	Overdischarge Cathode I/Io	$Li_2S_2O_4$**, (d Å)	LiF d (Å)	LiF I/Io
6.43	0.1			
4.95	0.2	5.09		
4.35	0.7	4.37		
3.70	0.9	3.73		
3.21	0.8	3.21		
2.95	0.6	2.96		
2.63	1.0	2.66		
2.54	0.8	2.54		
2.44	0.2	2.43		
2.32	0.1		2.32	95
2.25	0.4	2.25		
2.13	0.1			
2.08	0.1		2.01	100
1.93	0.5	1.92		
1.86	0.1			
1.79	0.3	1.80		
1.75	0.3	1.75		
1.71	0.3	1.71		
1.61	0.4	1.62		
1.57	0.4	1.57		
1.53	0.4	1.53		
1.47	0.4	1.47		
1.41	0.4		1.42	48
1.32	0.1	1.42		
1.29	0.1	1.30		
1.27	0.1	1.28		
1.19	0.1	1.19	1.22	10
1.16	0.1	1.17		
1.14	0.1	1.14	1.16	11

*Debye-Scherrer technique, CuK_{α} radiation.
**From Reference 3.

room temperature. The following events seem to occur.

- Plating of Li onto the carbon cathode. The plated Li seems to react further, gradually, forming LiH, Li-Al, LiF and $Li_2S_2O_4$. However, a significant quantity of the Li seems to accumulate on the cathode. It appears that the amount of SO_2 left in the cell is the critical factor which determines the extent of reaction of this Li on the cathode to form the above products.

- Thermal initiation of a violent reaction between the plated Li and other cell components (see later). Depending on the thermal conditions in the cell, a venting reaction may or may not occur, despite a favorable overdischarge chemistry.

The behavior of Cells E-10 and E-13 indicates that the most probable time a venting can occur is when the cell shows voltage oscillations after a relatively low overpotential deposition of Li onto the cathode. It appears that the voltage oscillations are responsible for the thermal initiation. Depending upon the location of the hot-spot and the thermal environments in the cell, and probably the amount of unreacted Li on the cathode, there may or may not be a "venting reaction". A careful examination of the temperature profile of E-4 (Fig. 13A) indicates that that cell could have vented; there was a temperature rise in Cell E-4, coinciding with the beginning of the voltage oscillations. It appears the cell escaped a "venting reaction" because of unfavorable conditions for an excessive heat build-up.

In our opinion, forced overdischarge related explosion hazards at room and low temperatures occur by practically the same mechanism. However, the hazard occurs more consistently at low temperatures because of substantially less passivation of the Li which is being plated onto the cathode. In both cases the hazard occurs after having plated a substantial quantity of Li into the cathode, suggesting possibilities of avoiding the hazard by careful balance of the cell components.

Further discussion of the mechanism of the forced overdischarge hazard is given later, following the presentation of the data for low temperature overdischarge.

FORCED OVERDISCHARGE AT LOW TEMPERATURES (-15 to -25°C)

In the prior NSWC program (3), we have shown that Li/SO_2 cells* vent/explode more consistently at low temperatures. In addition, we have found that at low temperatures, the hazard occurs even at low currents; for example, 150-300 mA in a C-cell. In this program the chemistry and phenomenology have been further studied utilizing cells constructed with reference electrodes. In addition, we have studied the overdischarge behavior of two types of commercial C-size cells in an attempt to find correlations among the extent of overdischarge, the mass of dendritic Li plated onto the cathode and the initiation of a venting/explosion.

*As mentioned earlier, the explosion hazard may be minimized or eliminated by carefully balancing the cell components, mainly Li, SO_2 and C. The objective in our work is to characterize the chemistry in cells which vent/explode during overdischarge.

Studies of Cells Having Reference Electrodes

The construction parameters of the cells studied are given in Table 9. The relevant results are presented in Table 10.

Phenomenology. The data for Cell E-20, discharged and overdischarged at 300 mA are given in Figures 22A and 22B. The data for E-21, discharged and overdischarged at 1A are given in Figures 23A and 23B. Although discharged at widely different currents, the two cells exhibited practically the same capacity. Both of the cells vented with flame. Interestingly enough, Cell E-20, discharged at 300 mA, vented much sooner than Cell E-21, discharged at 1 amp. Both of the cells had shown significant voltage fluctuations prior to venting. In Cell E-20, the voltage oscillations are associated with the cathode; in Cell E-21, they appear to be mostly associated with the anode.

Chemical Analysis. The vented gases from both E-20 and E-21 exhibited identical IR spectra. The spectrum from Cell E-20 is shown in Figure 24. The latter spectrum, except for peak intensities, is identical to that shown in Figure 18, obtained for the gases from Cell E-13, vented during forced overdischarge at room temperature. The principal components of the gases vented from Cells E-20 and E-21 are CS_2, CO_2, COS, CH_4, C_2H_2 and SO_2. A small amount of C_2H_4 also appears to be present, in addition to CH_3CN.

Cell E-23 was terminated after ~ 3 hrs of forced overdischarge at 300 mA, and chemical analysis was performed on the cell components. Gas-phase IR spectrum indicated that practically no CH_4 had been produced. Absence of CH_4 had been noted in commercial cells forced overdischarged for even longer periods at -25°C. This is in contrast to the chemistry at 25°C. There was a slight discoloration on one part of the anode. However, we found no evidence for any of the organic products usually found on the anodes of cells overdischarged at room temperature. It appears that the Li/CH_3CN reaction is significantly suppressed at -25°C, probably due to poor kinetics at the low temperature and the relatively higher amount of SO_2 present in the cell. The situation is somewhat similar to that in cells tested at high rates at room temperature. In both cases a significant amount of SO_2 remains in the cell at the time the cell goes into reversal.

The cathode had a grey deposit, presumably high surface area Li, which ignited when scratched with a spatula. Because of its high reactivity, it was not possible to obtain additional analytical data on the grey deposit. However, it appears that it simply is high surface Li with only minimal passivation. It is this property of the Li deposit on the cathode that seems to make the cells highly prone to a venting/explosion during forced overdischarge at -25°C, even at low currents.

Cell E-22 is an example of an anode-limited cell (Figs. 25A and 25B). At the beginning of cell reversal, the cathode potential is above 1V and stays at this value until the current is turned off. There are large polarizations of both the anode and the cathode when the current was subsequently turned on, apparently due to some kind of resistance build up in the cell during the open-circuit stand. At this stage, the observed cell voltage is that of the power supply, -12V, and very little current is passing through the cell. Post-test analysis indicated that the cathode had none of the grey reactive Li deposit. The anode showed no discoloration, and, indeed, there was no evidence of any reaction product at all. There was no CH_4 in the gas phase of this cell either. Some evidence for chemical changes

TABLE 9. CONSTRUCTION PARAMETERS OF CELLS TESTED AT $-25^{o}C$

Cell	Anode		Cathode		Electrolyte			Test Current	
No.	Area (cm^2)	Capacity (Ah)	Area (cm^2)	g (Carbon)	SO_2 (g) (Ahr)	CH_3CN (g)	LiBr (g)	Discharge (Amp)	Overdischg. (Amp)
E-20	185	7.53	125	2.1	4.07	3.92	1.24	0.3	0.3
E-21	185	7.53	125	2.1	4.01	3.87	1.22	1	1
E-22	185	5.02	175	3.4	3.95	3.81	1.21	0.3	0.3
E-23	185	7.34	125	2.1	4.21	4.06	1.28	0.3	0.3

TABLE 10. TEST RESULTS FOR THE CELLS LISTED IN TABLE 9*

Cell No.	Discharge Current (Amp)	Capacity to 2.0V (Ahr)	Capacity to 0.0V (Ahr)	Cathode Utilization (Ahr/g)	Forced Overdischarge Current (Amp)	Extent of overdischarge (Hr)	Comments
E-20	0.3	2.48	2.76	1.31	0.3	7.2	Cell vented.
E-21	1.0	1.50	2.8	1.32	1	17.2	Cell vented.
E-22	0.3	1.35	2.55	0.75	0.3	7	Cell terminated and analyzed.
E-23	0.3	2.43	2.56	1.22	0.3	3	Cell terminated for analysis.

*Discharge and overdischarge at $-25^{\circ}C$.

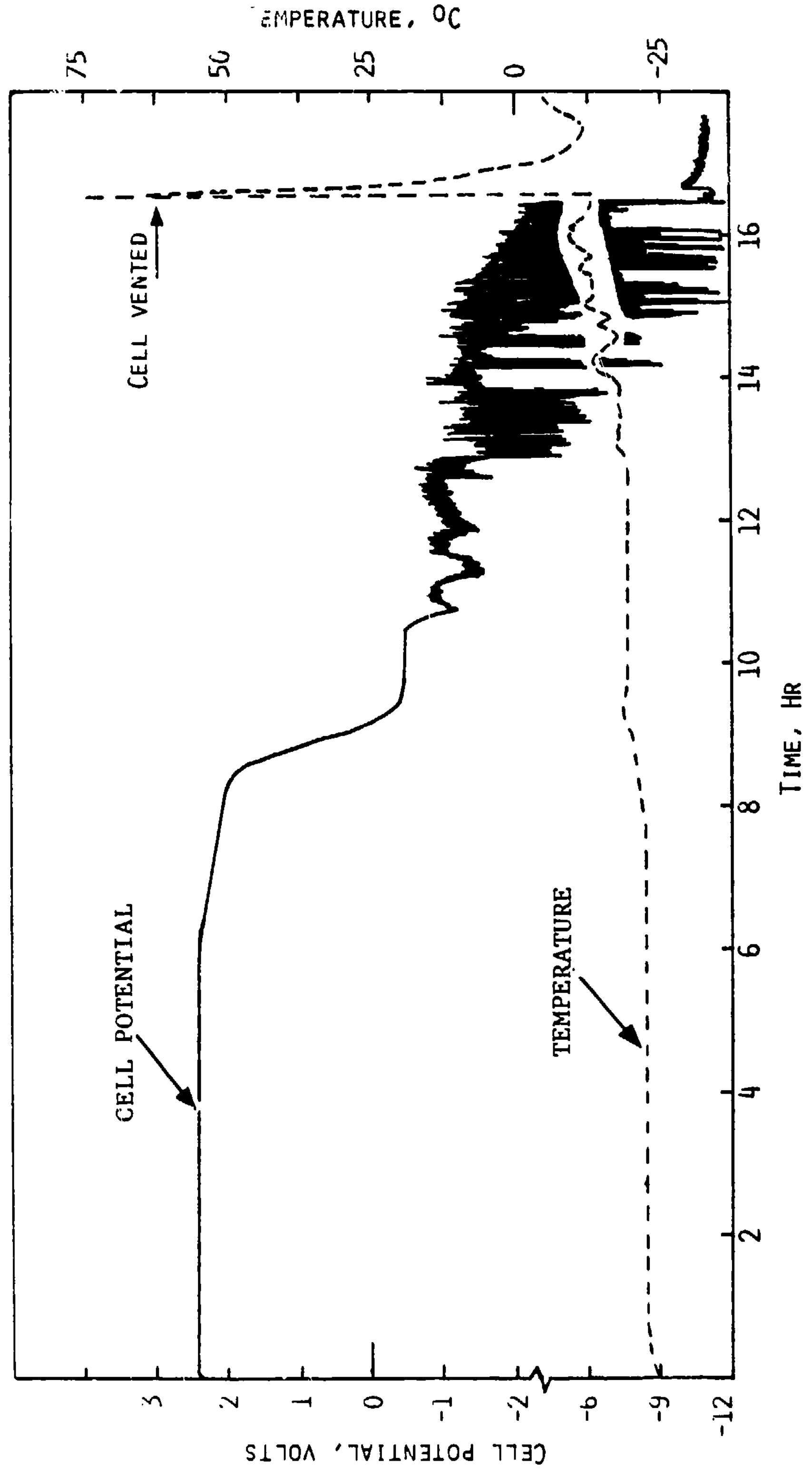

CURRENT, 300 mA

FIGURE 22A. DISCHARGE AND OVERDISCHARGE DATA FOR CELL E-20 AT -25°C (SEE NEXT FIGURE ALSO.)

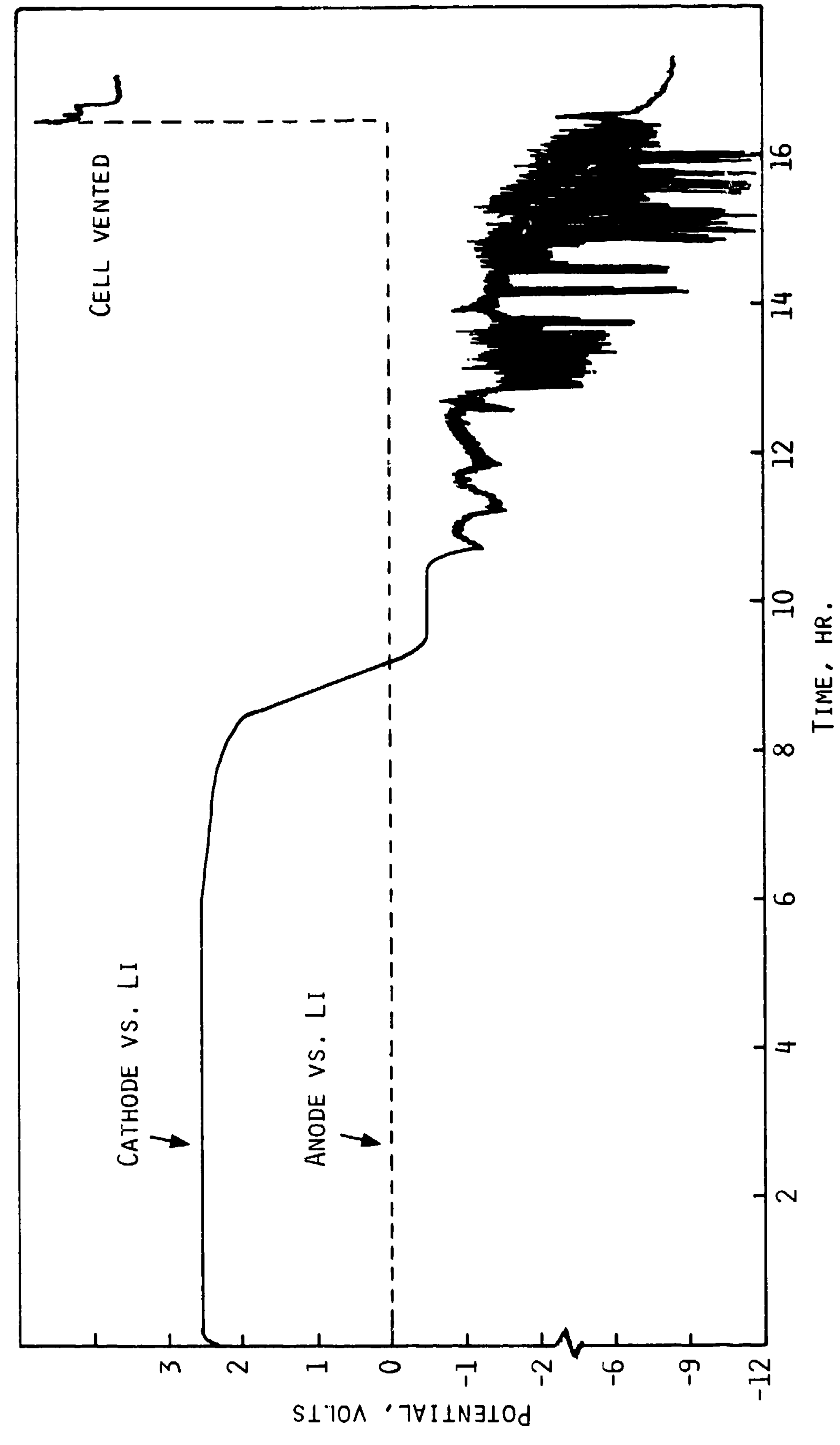

CURRENT , 300 mA.

FIGURE 22B. DISCHARGE AND OVERDISCHARGE DATA FOR CELL E-20 AT -25°C

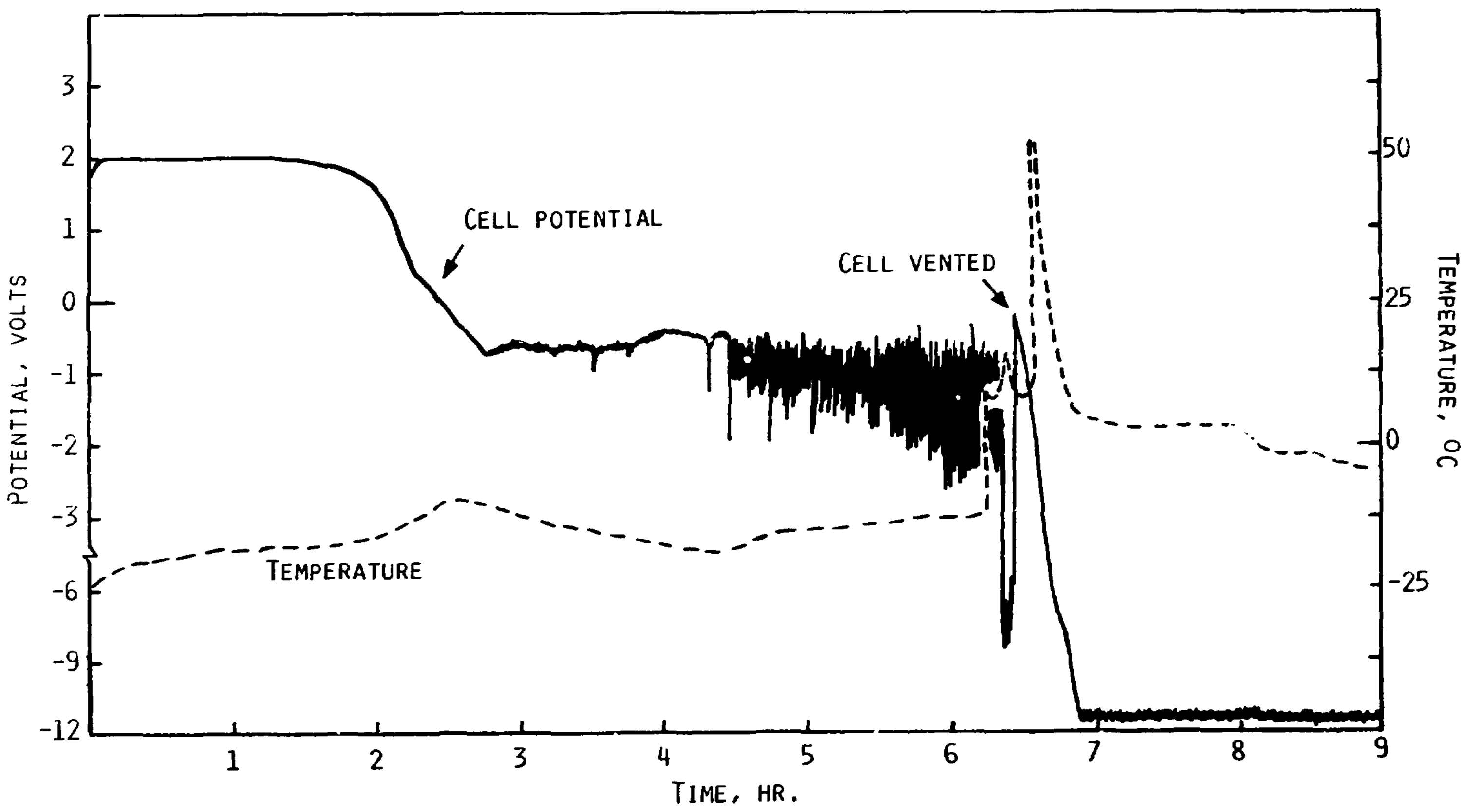

CURRENT, 1 AMPERE

FIGURE 23A. DISCHARGE AND FORCED OVERDISCHARGE DATA FOR CELL E-21 AT -25°C (SEE NEXT FIGURE ALSO.)

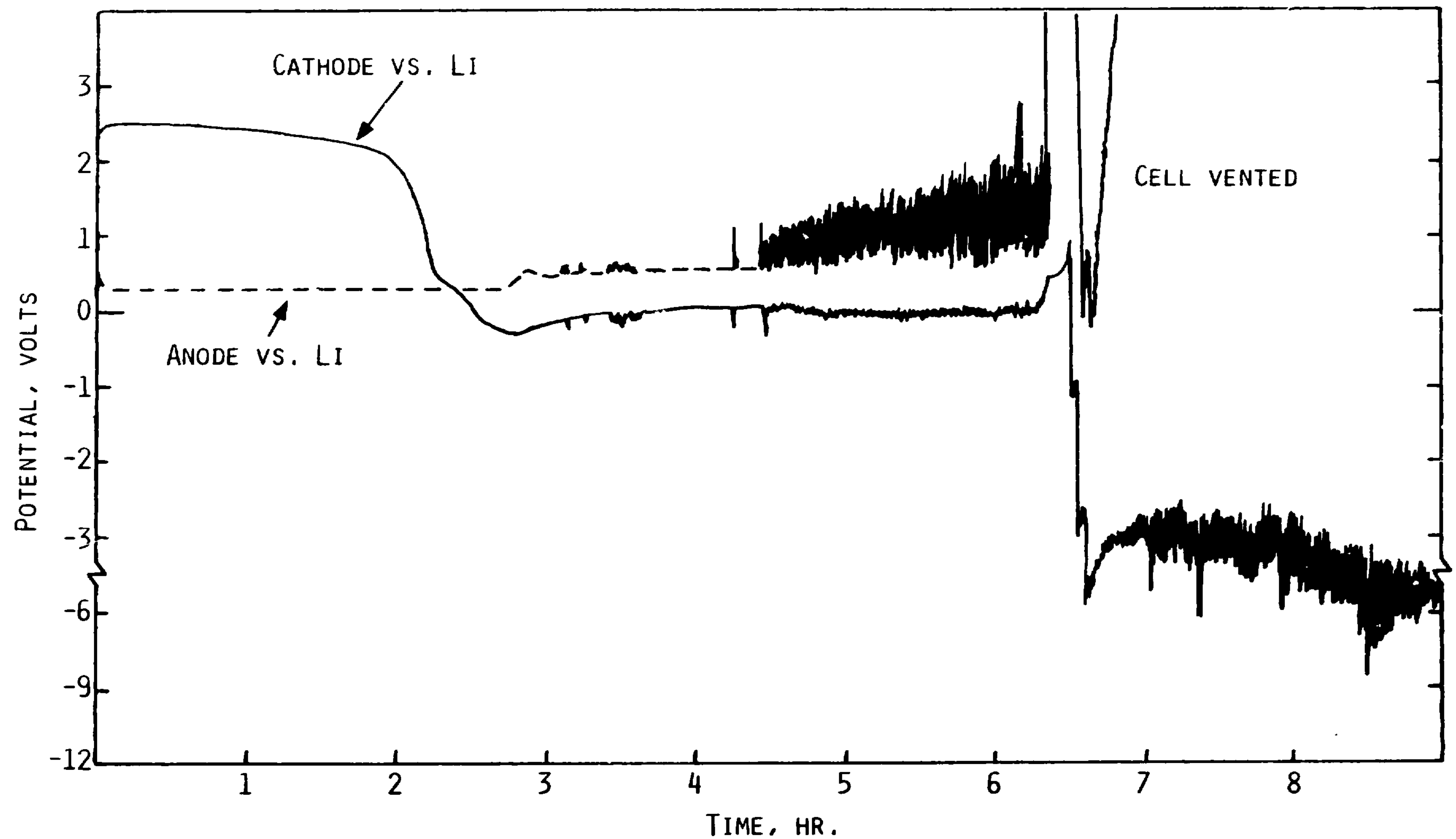

CURRENT, 1 AMP

FIGURE 23B. DISCHARGE AND OVERDISCHARGE DATA FOR CELL E-21 AT -25°C

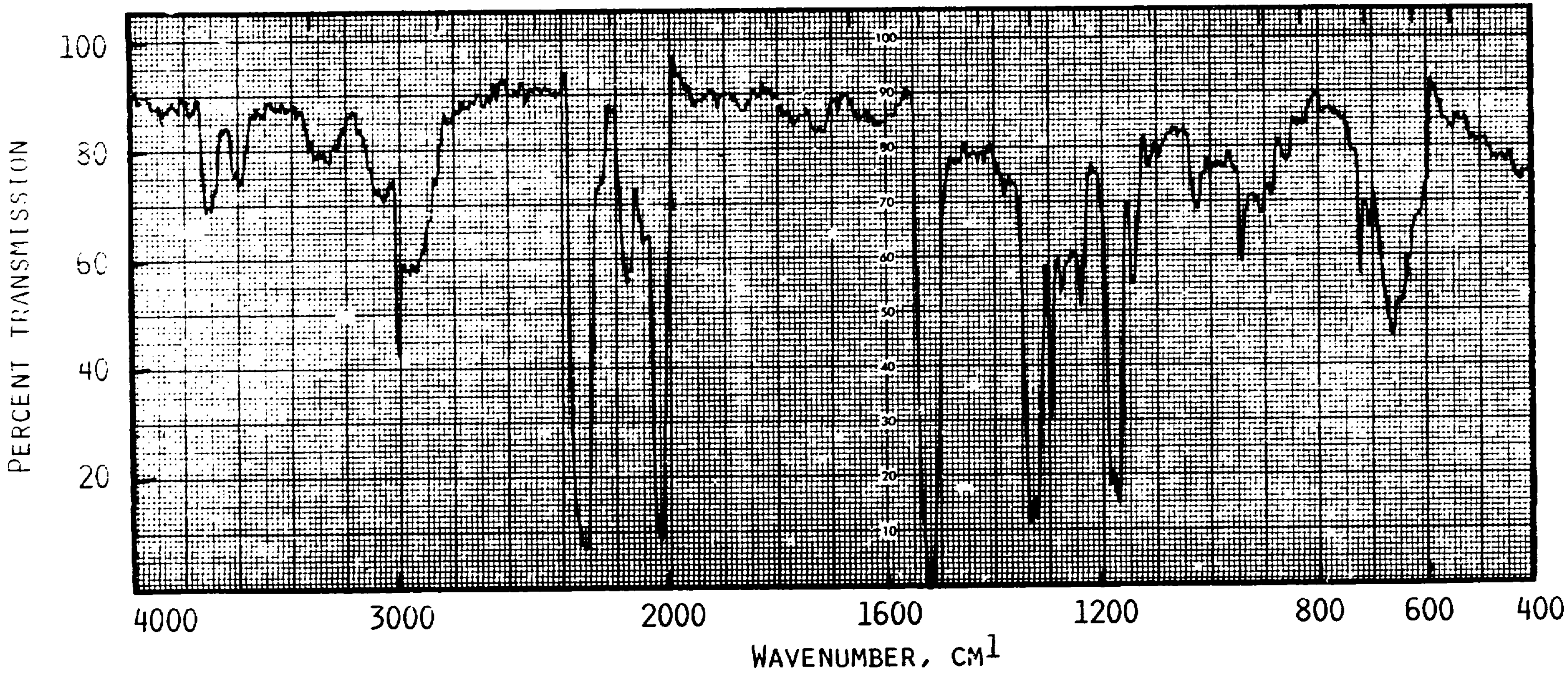

FIGURE 24. VAPOR PHASE IR SPECTRUM OF THE GASES VENTED FROM CELL E-20. AN IDENTICAL SPECTRUM WAS OBTAINED FOR THE GASES FROM E-21

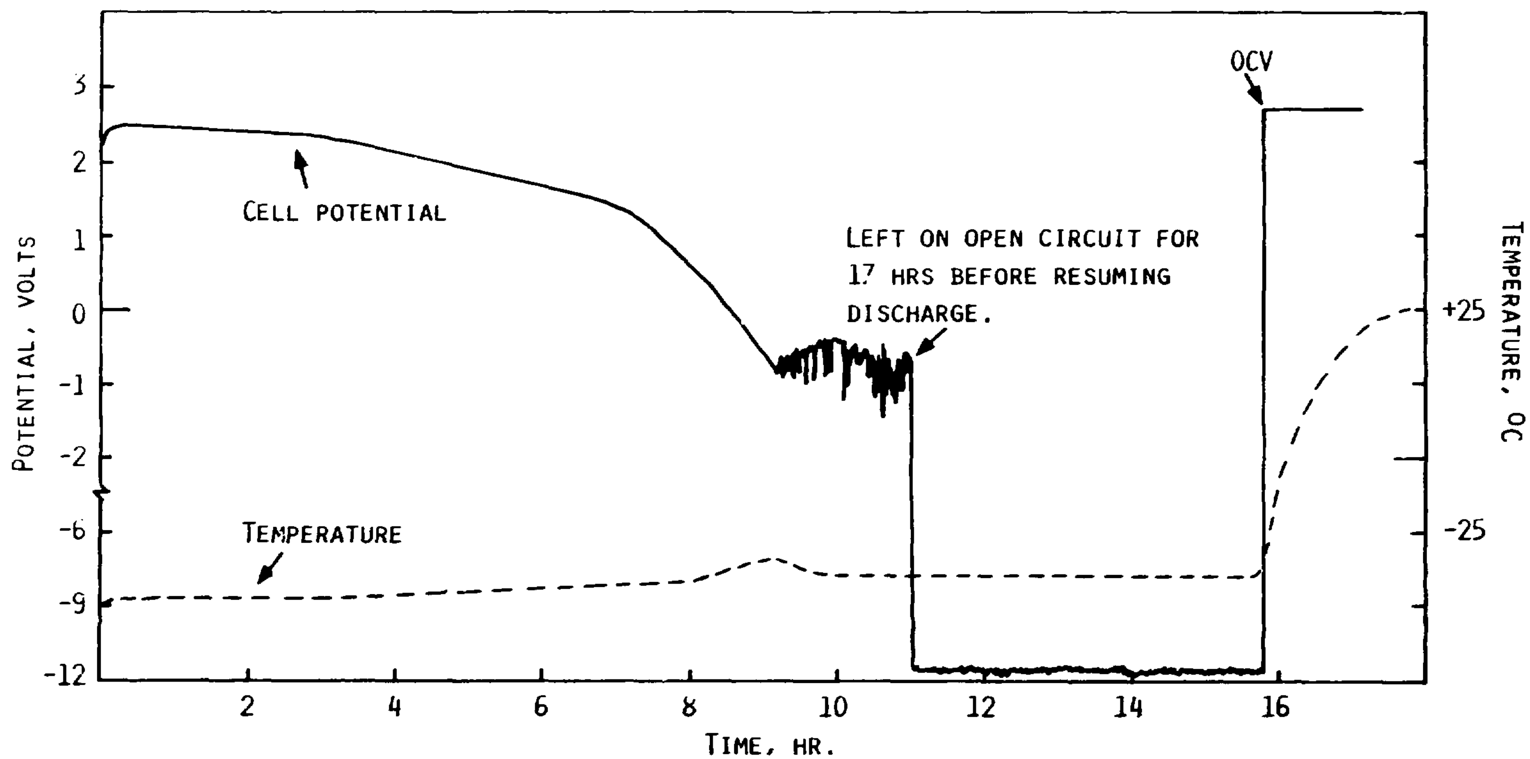

CURRENT, 300 mA

FIGURE 25A. DISCHARGE AND FORCED OVERDISCHARGE DATA OF CELL E-22 AT -25°C (SEE NEXT FIGURE ALSO.)

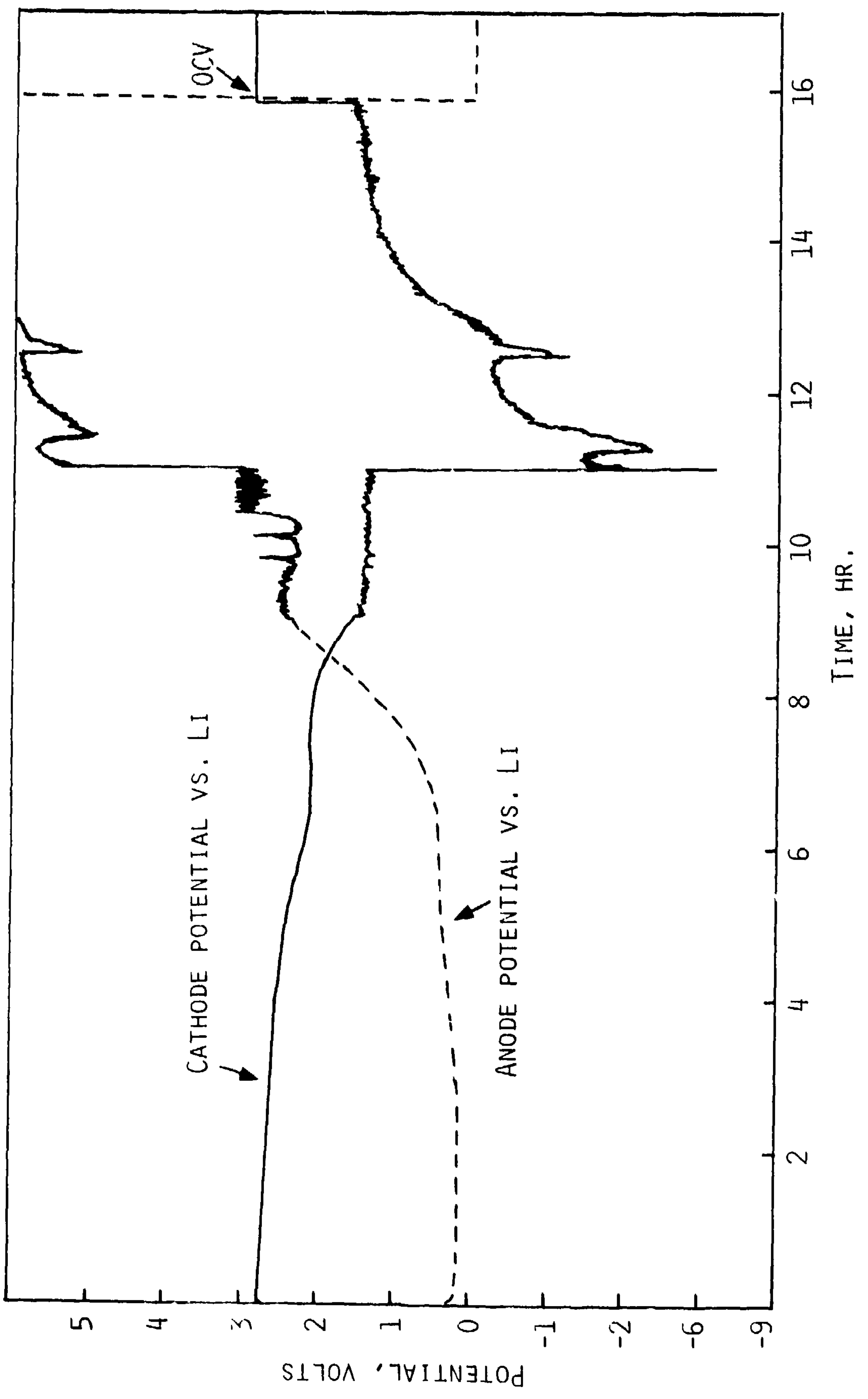

CURRENT, 300 mA

FIGURE 25B. DISCHARGE AND FORCED OVERDISCHARGE DATA OF CELL E-22

occurring during overdischarge comes from the discolored separator; it had an orange coloration. An IR spectrum of this discolored separator provided little information on the nature of the discoloration.

In summary, chemical analysis of cells forced overdischarged at -25°C indicates that under conditions leading to cell venting/explosion Li^+ is reduced and plated onto the cathode. This high surface area Li appears to undergo little passivation, rendering it highly reactive. In addition, very little CH_4 is produced during the course of the overdischarge so that practically all of the Li present in the cell at the time of reversal is available for exothermic "venting reaction", once the initiation of such a reaction has taken place.

CH_4 and the various other gaseous products identified in vented cells are apparently formed during the exothermic "venting reaction". The phenomenology of overdischarge prior to a venting indicates that the exothermic reaction is most probably initiated by the accompanying voltage oscillations.

Statistical Study of Forced Overdischarge at Low Temperatures

A major purpose of this study has been to elucidate the relationship between the extent of overdischarge and the occurrence of a venting/explosion hazard. Two types of commercial C-size cells were used. They are the same types of cell as we used in the previous NSWC program. The cells are designated Type-X and Type-Z, as we did previously. The specifications of these cells, obtained on the basis of our analysis, have been given in our previous report (3).

The experiments were carried out at -15°C. For a given cell the overdischarge and discharge currents have been the same. Type-Z cells have been tested at currents of 150, 300 and 450 mA, using five cells for each current. Type-X cells have been tested at currents of 300, 450 and 600 mA, using $\geq$ 2 cells for each current.

Relevant test results are given in Tables 11 and 12. Representative discharge data are given in Figures 26-30.

All of the Type-Z cells vented, virtually in all cases with flame. The Type-X cells were significantly more abuse resistant. They were subjected to higher currents also. Only two out of eight Type-X cells vented, one at 450 mA and the other at 600 mA. However, some of the Type-X cells which did not vent revealed, upon disassembly, signs of internal burning. It appears in most of the Type-X cells the conditions were not appropriate for a full-scale exothermic reaction. A major difference between Type-X and Type-Z cells is that in the latter there is substantially more Li present on the anode at the time of reversal.

The data in Table 11 for Type-Z cells indicate little correlation between the extent of overdischarge and the initiation of a violent reaction. The reproducibility of the event for each current is extremely poor.

A common feature for all cells which vented is the considerable voltage oscillations prior to venting. Preceding the oscillating voltage regime, there is a region of low negative voltages, apparently corresponding to low overvoltage plating of Li. In the oscillating voltage region it is difficult to estimate the

TABLE 11. -15°C TEST RESULTS FOR TYPE-Z CELLS

Cell No.	Test Current (mA)	Capacity to 0.0V (Ahr)	Li Remaining on the Anode at Time of Reversal (Ahr)	Extent of Overdischarge: Prior to Voltage Oscillation (Hr) (mA-hr)	Extent of Overdischarge: With Voltage Oscillation (Hr)	Comments
Z-50	150	1.92	4.88	10.7 (1610)	15	Vented with flame.
Z-51	150	2.12	4.68	8.0 (1200)	4	
Z-52	150	2.70	4.10	4.2 (630)	9	
Z-53	150	2.68	4.72	10.0 (1500)	8	
Z-54	150	2.10	4.70	12.0 (1800)	0.2	
Z-55	300	2.25	4.55	2.7 (825)	32	
Z-56	300	1.60	5.20	2.0 (600)	1	
Z-57	300	1.91	4.89	1.2 (375)	2	
Z-58	300	1.89	4.91	2.8 (855)	0.5	
Z-59	300	1.53	5.27	5.0 (1500)	0.2	
Z-60	450	1.72	5.08	4.2 (1900)	1	
Z-61	450	1.30	5.50	1.3 (585)	0.7	
Z-62	450	1.50	5.30	2.5 (1125)	14	
Z-63	450	1.63	5.17	3.0 (1350)	3	

TABLE 12. -15°C TEST RESULTS FOR TYPE-X CELLS

Cell No.	Test Current (mA)	Capacity to 0.0V (Ahr)	Li Remaining on the Anode at Time of Reversal (Ahr)	Extent of Overdischarge: Prior to Voltage Oscillation (Hr) (mA-hr)	Extent of Overdischarge: With Voltage Oscillation (Hr)	Comments
X-50	300	2.76	2.04	2.75 (825)	84	Did not vent, burning inside cell.*
X-51	300	2.67	2.13	2.75 (825)	36	Did not vent.
X-52	450	3.00	1.80	0.75 (340)	21	Did not vent, minor burning.
X-53	450	2.98	1.82	1.10 (495)	16	Vented.
X-54	450	3.08	1.72	0.55 (250)	88	Did not vent, some internal burning.
X-55	450	3.22	1.58	0.75 (340)	64	Did not vent, some internal burning.
X-56	600	2.88	1.94	0.70 (420)	21	Did not vent, internal burning.
X-57	600	2.94	1.86	0.63 (375)	3	Vented.

*Discovered during post-test examination.

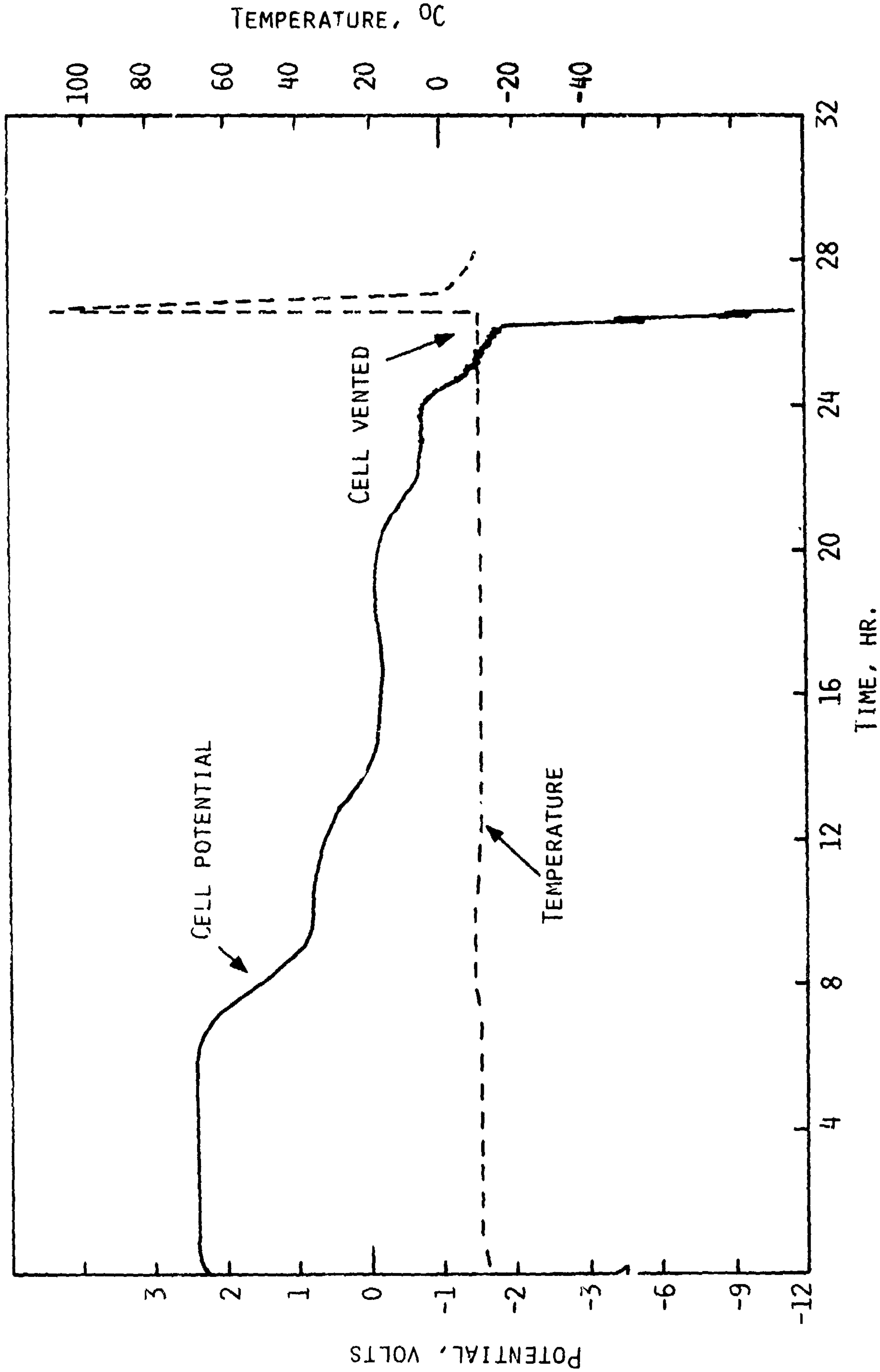

FIGURE 26. A TYPICAL TYPE Z CELL FORCED OVERDISCHARGED AT 150 mA AT -15°C

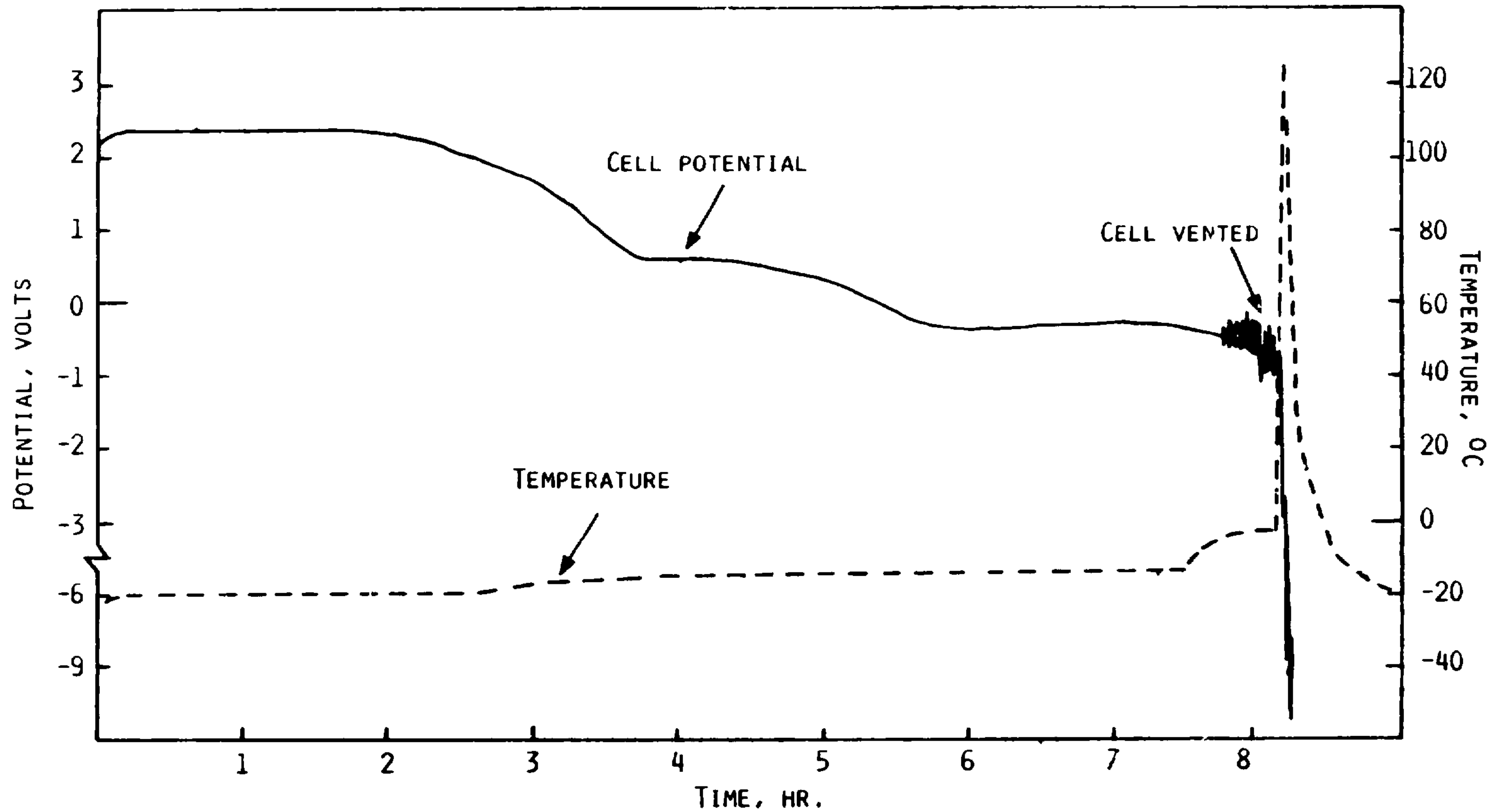

FIGURE 27. TYPICAL FORCED OVERDISCHARGE OF A TYPE Z CELL AT -15°C AT 300 mA

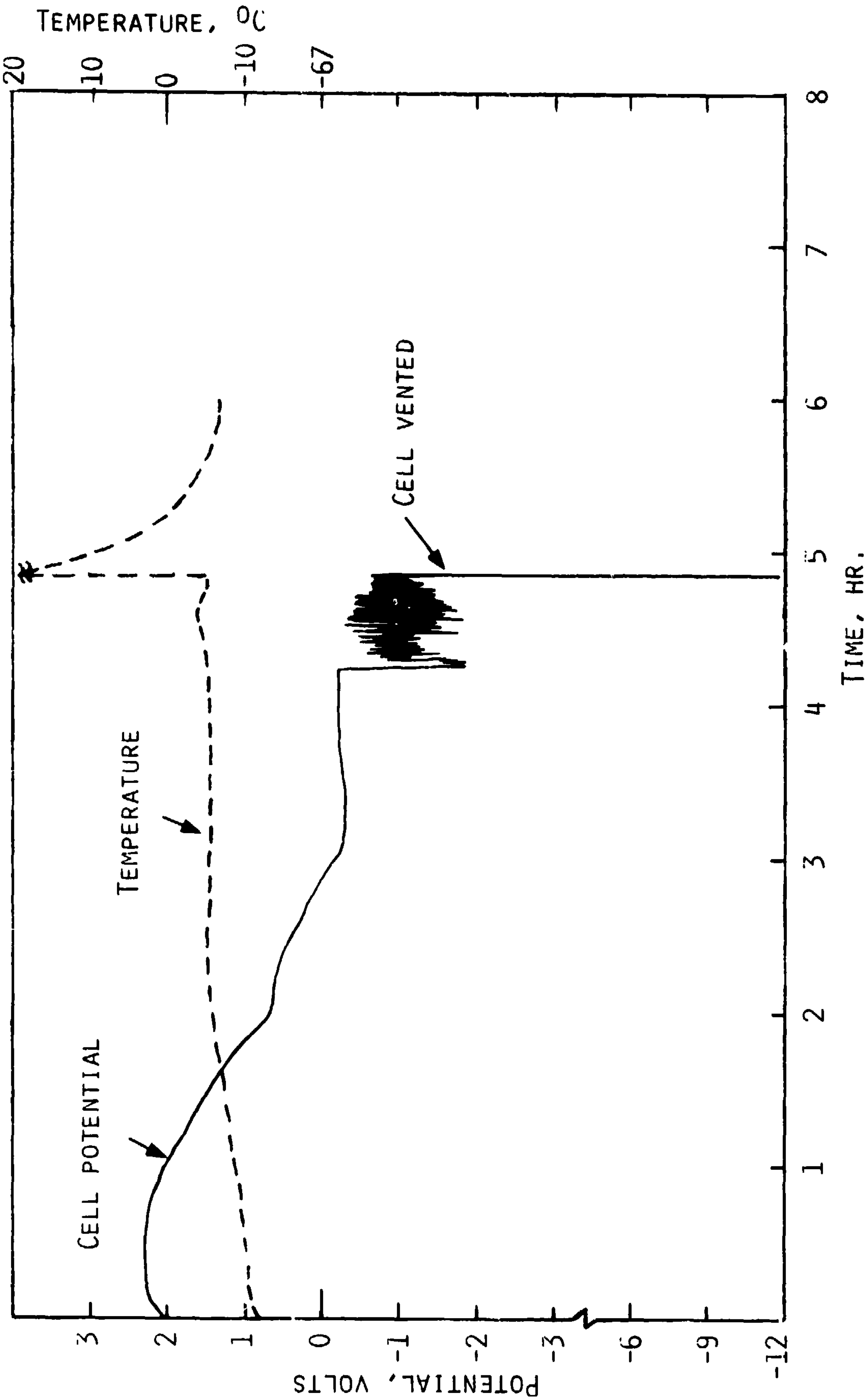

FIGURE 28. TYPICAL FORCED OVERDISCHARGE OF A TYPE Z CELL AT -15°C AT 450 mA

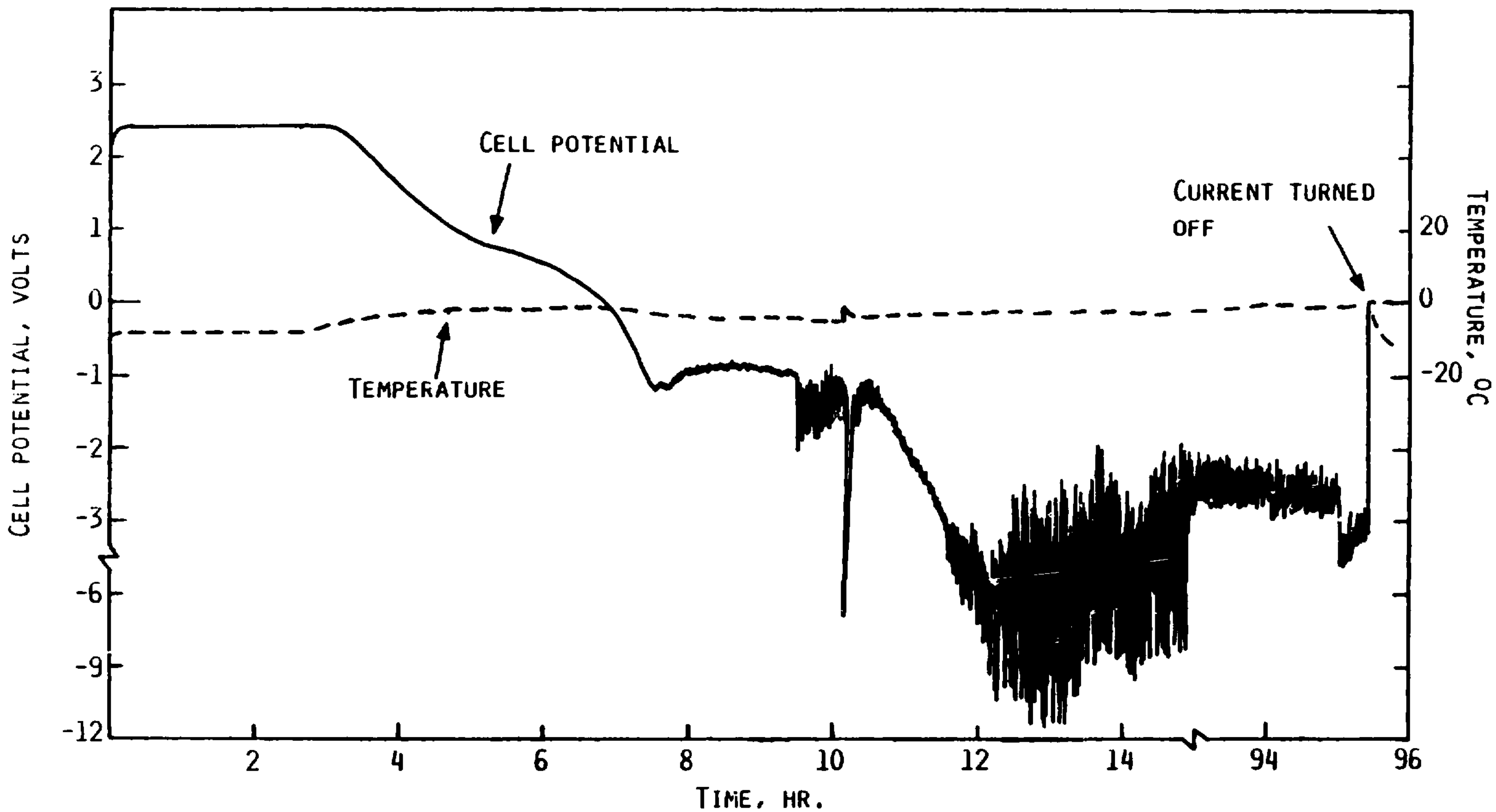

FIGURE 29. TYPICAL FORCED OVERDISCHARGE OF A TYPE X CELL AT -15°C AT 450 mA

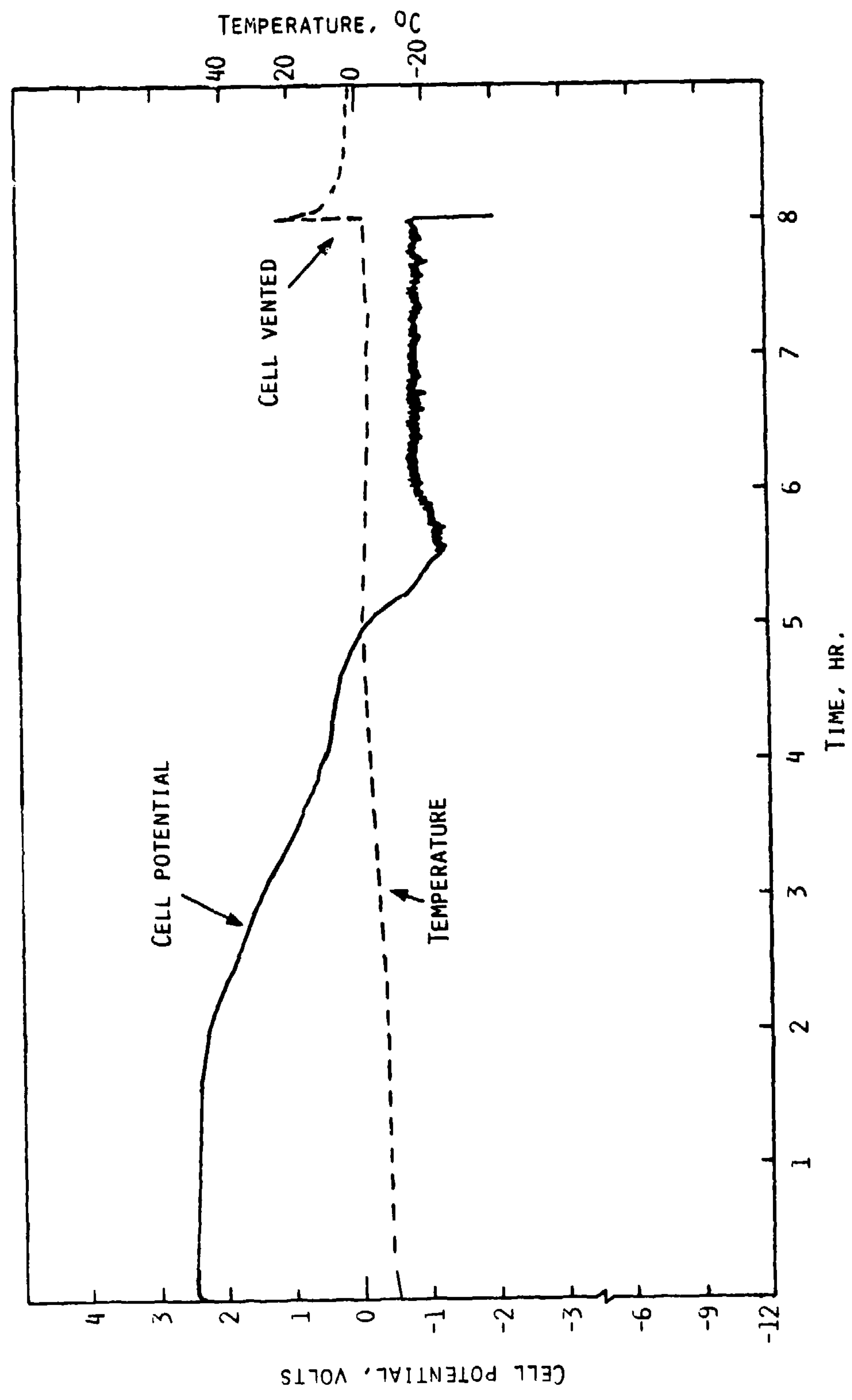

FIGURE 30. TYPICAL FORCED OVERDISCHARGE OF A TYPE X CELL AT -15°C AT 600 mA

amount of Li being plated onto the cathode since the current decreases substantially during deep reversals.

The scenario for the forced overdischarge related venting hazards, at low temperature, as discernible from the present data, appears to be the same as presented earlier. High surface area Li is plated onto the cathode. A runaway reaction involving this Li is initiated by resistive heating, brought about by the voltage oscillations. The lack of any significant correlation between current density and the extent of overdischarge as well as the irreproducibility of the event for each current strongly suggest that the reactive species are Li and other insoluble solids. Experiments performed to elucidate this aspect further are discussed in the next section.

CHAPTER 6

MECHANISM OF FORCED OVERDISCHARGE RELATED HAZARDS

Further insight into the mechanism of forced overdischarge-related hazards has been obtained from the results of experiments, designed and executed on the basis of products identified in the gas phase of vented cells. These experiments are discussed below.

THERMAL DECOMPOSITION OF CATHODES FROM FORCED OVERDISCHARGED CELLS

The experiments were carried out using carbon cathodes from cells that had been forced overdischarged at -15°C. The forced overdischarge had been terminated prior to venting. Visual examination of the cathodes had revealed plated Li on them. Most of the Al was physically separated from the carbon samples used in the decomposition study. The experiment was carried out in an identical manner as described in Chapter 4.

The experiments were performed with two cathode samples: One without the separator and the other mixed with pieces of a fresh polypropylene separator. The rate of decomposition was monitored by measuring the pressure of the gases produced.

The pressure versus temperature plots are given in Figures 31 and 32. The two curves are almost identical; however, they differ from the decomposition profiles of cathodes containing only $Li_2S_2O_4$, given in Section 4.0. The data in Figures 31 and 32 show a very sharp increase in pressure at ~ 180°C. The reaction is very sudden. At this stage the rate of sample heating increased substantially over the rate of external heating, indicating an exothermic reaction within the flask.

IR spectrum of the gases from the two samples are given in Figures 33 and 34. The two spectra, except for peak intensities, are identical. It appears the separator did not make a contribution to the decomposition reaction. The gases comprise SO_2, COS, CS_2 and CS_2. The major component is SO_2.

It appears that the same decomposition reaction as in the case of cathodes containing only $Li_2S_2O_4$ is taking place, but the process is apparently catalyzed by the presence of plated Li. It is possible that the plated Li which is in intimate contact with $Li_2S_2O_4$ is reacting with it when the Li melts at ~ 180°C. The heat from this reaction appears to accelerate the thermal decomposition of $Li_2S_2O_4$ as well as reactions between C and SO_2, and S.

An X-ray analysis was carried out on the residues of the decomposed cathodes. The data are given in Table 13. Because of the large amount of carbon in the

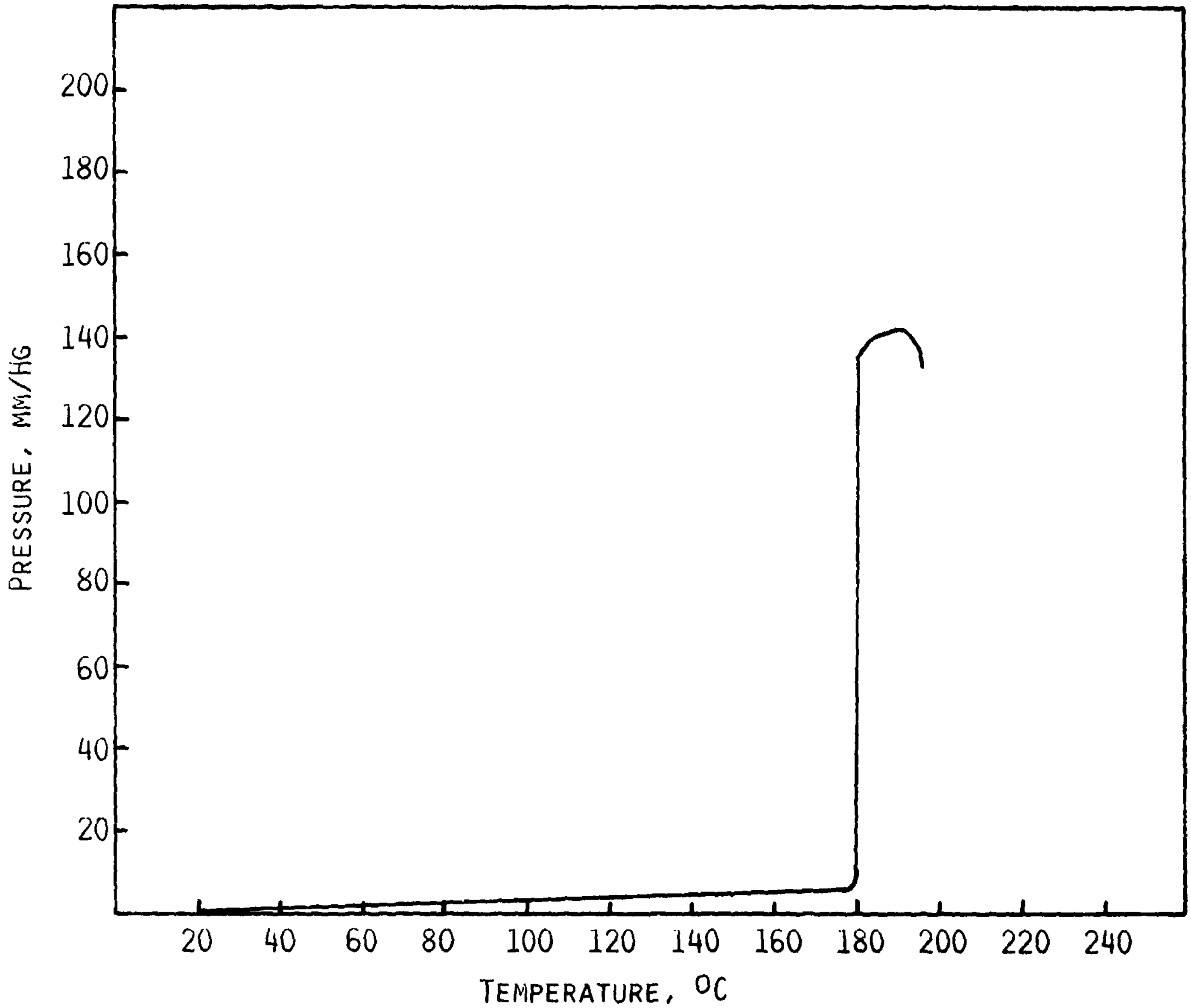

FIGURE 31. THERMAL DECOMPOSITION DATA FOR CATHODE FROM A FORCED OVERDISCHARGED CELL

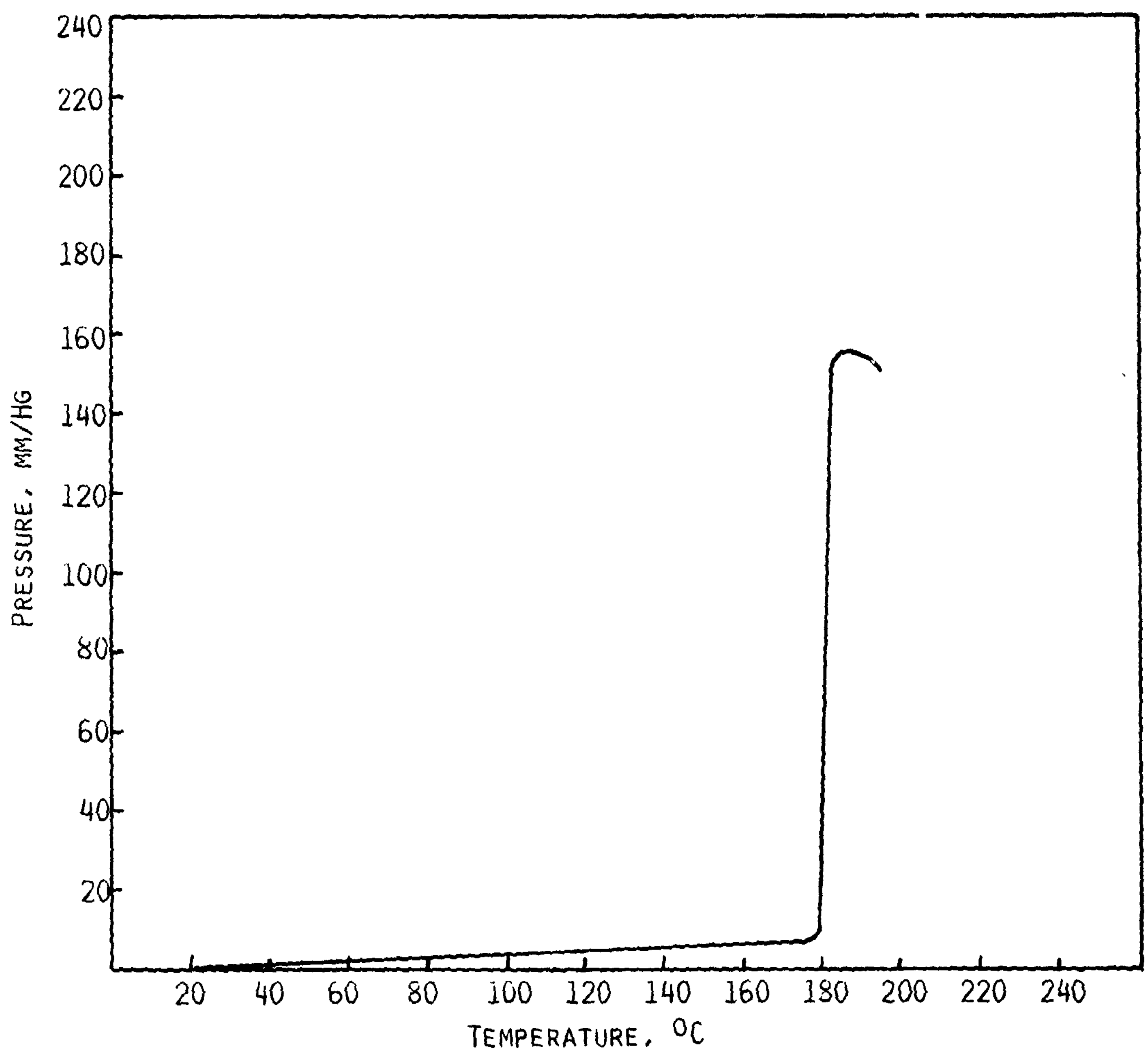

FIGURE 32. THERMAL COMPOSITION DATA FOR CATHODE FROM A FORCED OVERDISCHARGED CELL IN THE PRESENCE OF POLYPROPYLENE SEPARATOR

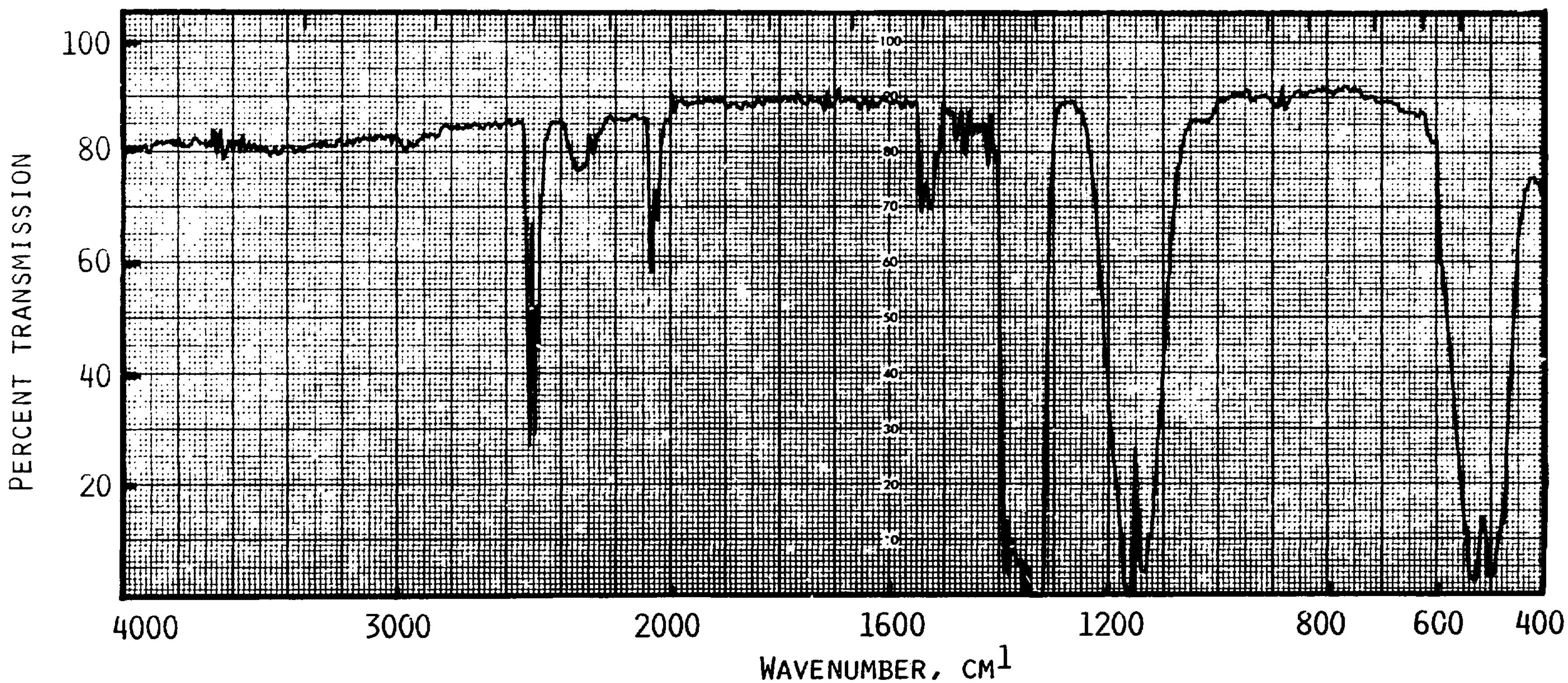

FIGURE 33. IR SPECTRUM OF GASES PRODUCED BY THERMAL DECOMPOSITION OF FORCED OVERDISCHARGED CATHODE

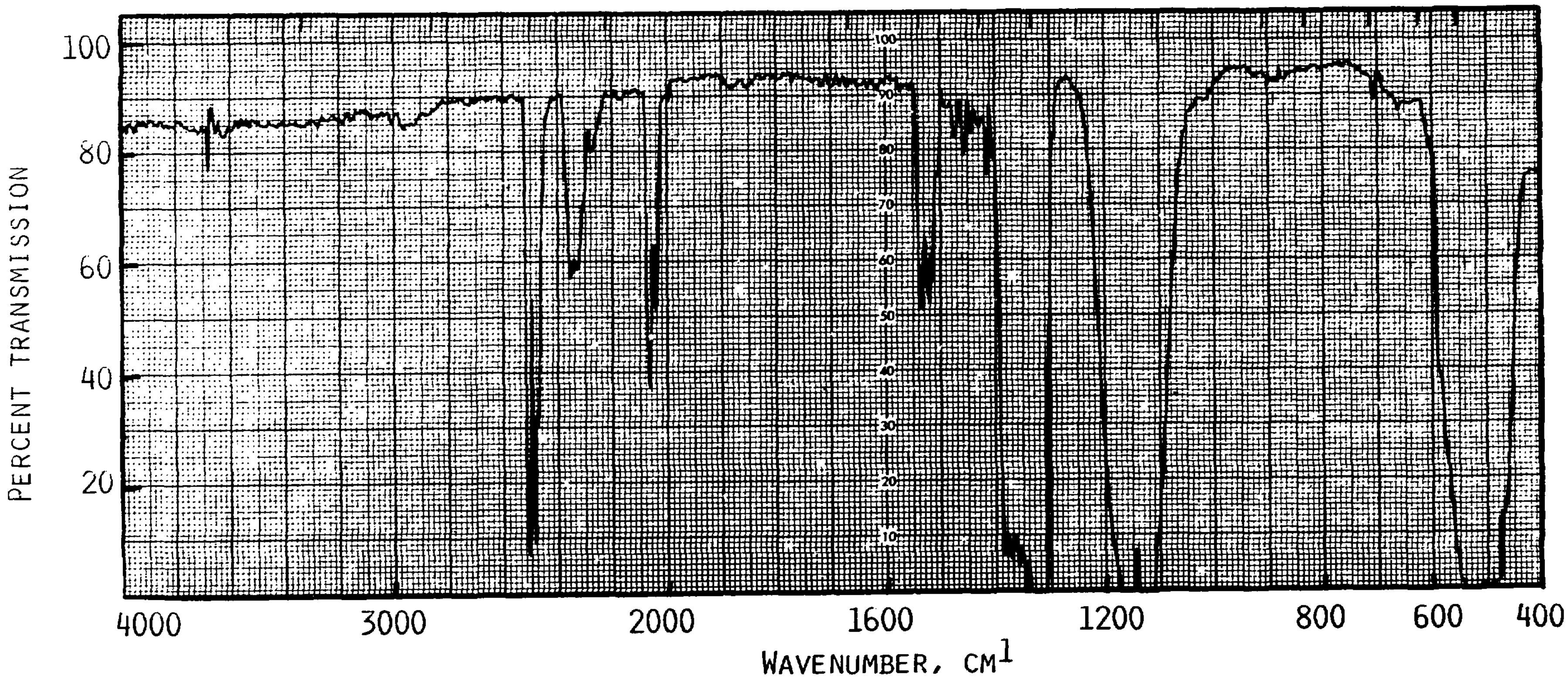

FIGURE 34. IR SPECTRUM OF GASES PRODUCED BY THERMAL DECOMPOSITION OF FORCED OVERDISCHARGED CATHODE IN THE PRESENCE OF POLYPROPYLENE SEPARATOR

TABLE 13. X-RAY DIFFRACTION PATTERN* OF RESIDUE FROM THERMALLY DECOMPOSED FORCED OVERDISCHARGED CATHODE

Sample		Li_2S		Li_2O		LiBr	
d, Å	I/I_o	d, Å	I/I_o	d, Å	I/I_o	d, Å	I/I_o
11.18	Diffuse ring						
7.08	Diffuse ring						
4.41	0.3						
4.11	0.9						
3.82	0.8						
3.42	0.1						
3.30	0.5	3.31	100				
3.14	1.0					3.18	100
2.95	0.1	2.85	33			2.75	80
2.65	0.4			2.66	100		
2.45	0.1			2.31	80		
2.12	0.3						
		2.02	72				

*Debye Scherrer method; CuK_{α} radiation.

sample, the diffraction pattern was not intense, and missed the lower d-values. Based on the available data, the solid products in the decomposed cathode appears to be Li_2O and Li_2S.

It appears that the following reactions take place when the overdischarged cathode containing Li and $Li_2S_2O_4$ is heated to ~ 180°C.

$$10Li + Li_2S_2O_4 \rightarrow 4Li_2O + 2Li_2S; \quad \Delta H^o = -400 \text{ Kcal} \qquad [14]$$

$$3Li_2S_2O_4 \rightarrow SO_2 + xS + yLi_2SO_3 \qquad [15]$$

$$2Li + S \rightarrow Li_2S \quad ; \Delta H^o = -100 \text{ Kcal} \qquad [16]$$

$$3C + 2SO_2 \rightarrow 2CO_2 + CS_2 \quad ; \Delta H^o = -13 \text{ Kcal} \qquad [17]$$

$$C + SO_2 \rightarrow CO_2 + S \quad ; \Delta H^o = -23 \text{ Kcal} \qquad [18]$$

$$C + SO_2 \rightarrow COS + CO \quad ; \Delta H^o = +15 \text{ Kcal} \qquad [19]$$

$$C + 2S \rightarrow CS_2 \quad ; \Delta H^o = +27 \text{ Kcal} \qquad [20]$$

It is interesting to note that the reactions involving C and S or SO_2 would occur preferably at higher temperatures. Reactions in equations [17-20] satisfactorily explain the formation of these same gases in "vented cells". This is confirmed by the results in the next section where we show that the same compounds, COS, CO_2 and CS_2, are formed in an exploded all-inorganic Li/SO_2 cell. The CH_4, C_2H_4 and C_2H_2 and probably H_2S, are additional gaseous products that are formed in cells which contain CH_3CN.

FORCED OVERDISCHARGE OF AN ALL-INORGANIC Li/SO_2 CELL AT -15°C

The major purpose of this experiment was to isolate the role of CH_3CN on the forced overdischarge-related explosion hazard and to identify those products which result from reactions involving CH_3CN. Thus, a cell was built without CH_3CN. Since LiBr in the absence of CH_3CN is insoluble in SO_2, we used $Li_2B_{10}Cl_{10}$ (0.25M) as the supporting electrolyte. Thus the cell had the configuration, $Li/Li_2B_{10}Cl_{10},SO_2/SO_2,C$.

The first experiment was carried out with a C-size cell at -25°C. The discharge curve is given in Figure 35. The test was begun at 1A but because of poor capacity, the current was turned down to 300 mA. Subsequently, part of the discharge and all of the overdischarge were carried out at 300 mA, Figure 37. The forced overdischarge proceeded with a rather smooth potential profile. The cell exploded violently at about the 9.75th hour of operation. It apeared from the intensity of the explosion and the cell potential profiles that the all-inorganic cell is more sensitive to overdischarge explosions than the organic analog. Since the explosion severely damaged the container in which the test was carried out, it was not possible to collect the vented gases for analysis.

The experiment was repeated using a much smaller cell of the same chemistry. The size of this cell was ~1/12 that of the C-cell. The discharge and overdis-

charge were performed at -15°C.* This cell exploded even before the cell had gone significantly into forced overdischarge. An IR spectrum of the gases was obtained and is shown in Figure 36. The vented gases comprise SO_2, COS, CS_2 and CO_2.

It is obvious that [illegible], CS_2 and CO_2 in exploded Li/SO_2 cells come from the reaction of carbon with SO_2 and/or S. The S comes from the decomposition of $Li_2S_2O_4$, while SO_2 is available both as originally added into the cell and from the decomposition of $Li_2S_2O_4$. It should be noted that the all-inorganic cell discussed here appeared to be particularly more sensitive to forced overdischarge related explosion hazards than Li/SO_2 cells containing CH_3CN.

SUMMARY OF THE MECHANISM OF FORCED OVERDISCHARGED SAFETY HAZARDS

Our experimental results suggest that practically the same mechanism is operating in both the room temperature and low temperature forced overdischarge explosion hazards of the Li/LiBr, CH_3CN/SO_2 cell. At low temperatures the explosive/venting reaction is more consistent even at low currents because the Li which plates onto the cathode remains active, devoid of passivation by reactions with CH_3CN or other cell components.

Apparent lack of significant reactions of the Li as it plates onto the cathode, and the apparent lack of a direct correlation between the extent of overdischarge and the onset of an explosive reaction suggest that the reactants, initially, are solids: Li and another solid(s). The latter probably is $Li_2S_2O_4$. This scenario is consistent with the products identified from the thermal decomposition of discharged and forced overdischarged cathodes.

The whole sequence of events appears to be initiated at the cathode by resistive heating or hot spots, apparently brought about by voltage oscillations during forced overdischarge.

Reactions involving carbon to produce the gaseous products, COS, CO_2 and CS_2 are an integral part of the mechanism of the explosion. Both S and SO_2 for those reactions are obtained by the decomposition of $Li_2S_2O_4$. The gases resulting from the Li/CH_3CN reaction, CH_4, C_2H_4, and C_2H_2 also contribute to the pressure build-up and venting.

*The explosion of the all-inorganic C-cell had damaged the Tenny Environmental Chamber. Therefore, a replacement chamber with a lower low temperature capability had to be used.

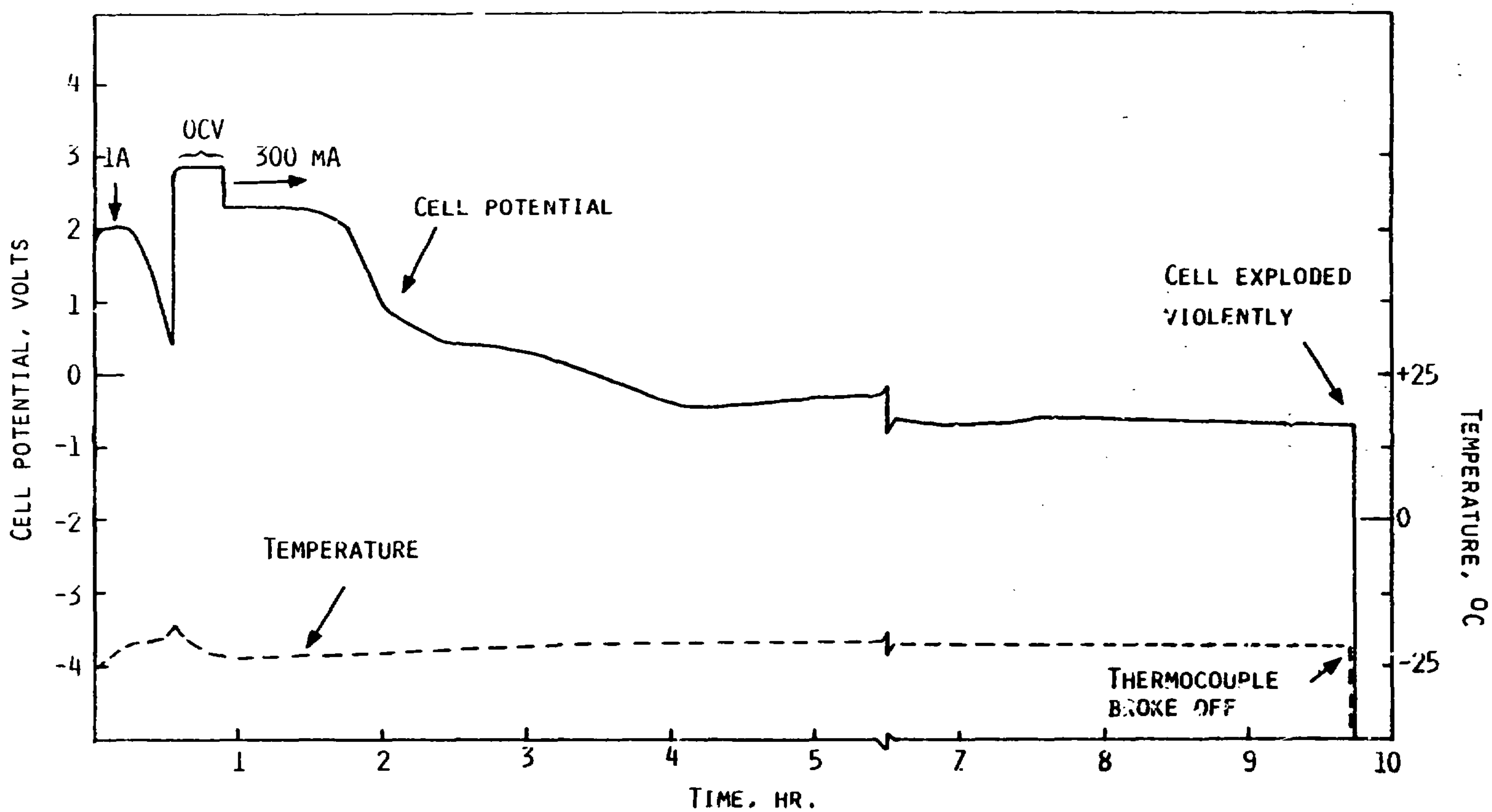

THE CURRENT INITIALLY WAS 1A, BUT WAS TURNED TO 300 mA FOR PART OF THE DISCHARGE AND ALL OF THE OVERDISCHARGE.

FIGURE 35. DISCHARGE AND FORCED OVERDISCHARGE OF AN ALL-INORGANIC C-SIZE CELL AT -25°C

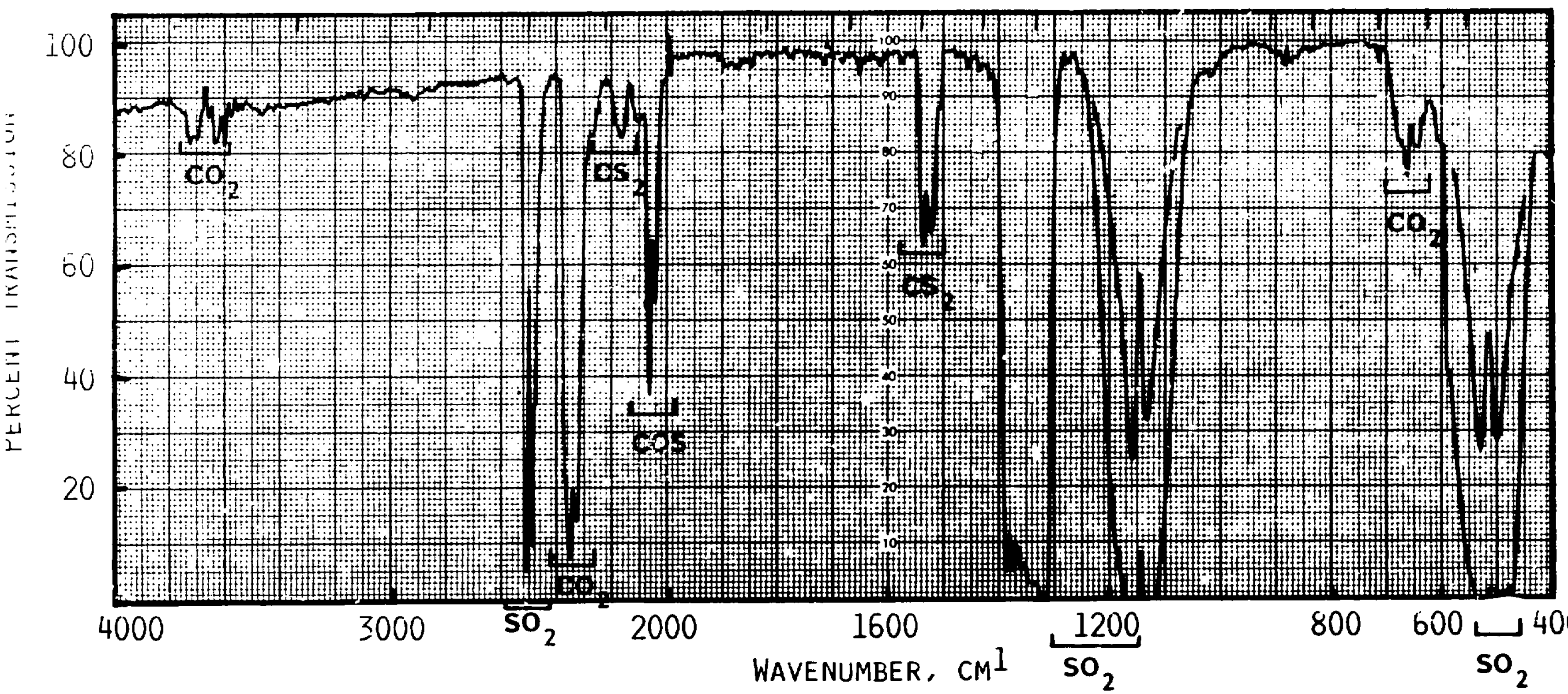

FIGURE 36. IR SPECTRUM OF THE GASES PRODUCED IN AN EXPLODED $Li/Li_2B_{10}Cl_{10}$, SO_2/C CELL **TESTED** AT -15°C

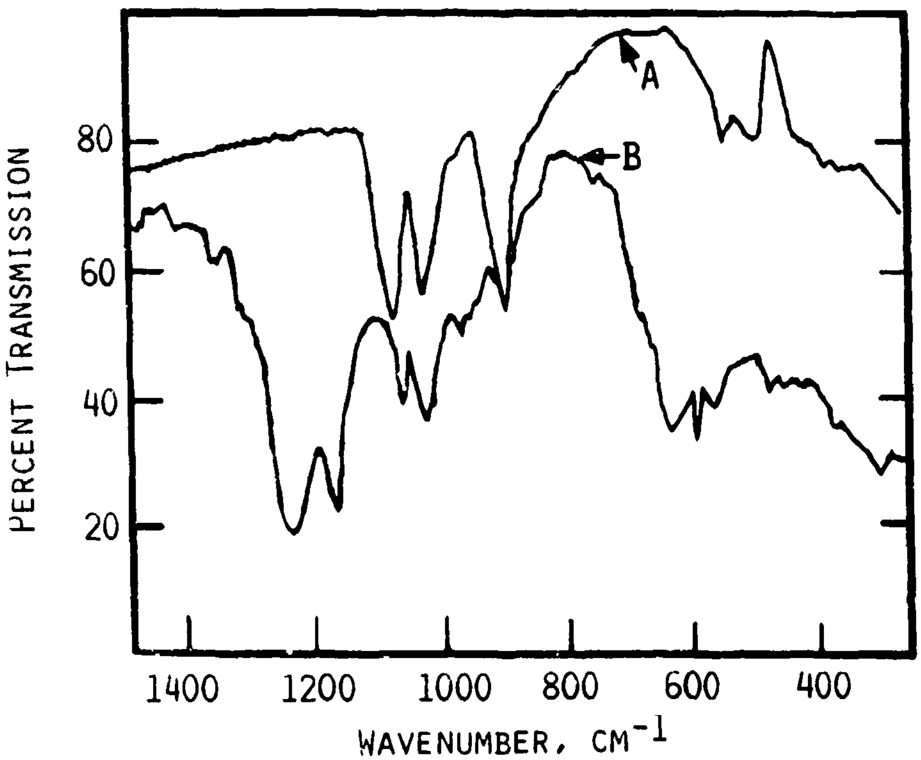

FIGURE 37. INFRARED SPECTRUM OF THE CATHODE (CURVE A) AND THE PRODUCT(S) FORMED ON THE LI ANODE (CURVE B) FROM A PARTIALLY DISCHARGED (~50% DOD) AND STORED (~1 YEAR AT 25°C) Li/SO_2 C-CELL

CHAPTER 7

ANALYSIS OF PARTIALLY DISCHARGED AND STORED CELLS

There is a great concern in the user community for the safety of partially discharged and stored Li/SO_2 cells. During the course of this contract, we have carried out a preliminary study of the chemistry in such cells. The results are presented below.

The Li/SO_2 cells were the Type-X and Type-Z commercial cells described in our previous report (3). The cells, having a rated capacity of ~ 3 A-hr, were discharged at a constant current of 100 mA to a depth of ~ 50% or 1.5 A-hr. The 100 mA current corresponds to current densities of 0.6 and 0.8 mA/cm^2 for the Type-X and Type-Z cells respectively. The cells were then stored at laboratory temperature for 11 months and two weeks prior to the analysis Several undischarged cells were similarly stored for comparative analysis. The stored cells were opened and analyzed for gaseous, liquid and solid products. Our technique which permits cell analysis without atmospheric contamination has been described elsewhere (3,5). Infrared (IR) spectrometry, ESCA, gas chromatography (GC) and mass spectrometry were the principal analytical tools (3,5). Qualitative identification of some of the sulfur-oxy compounds were also made using standard wet analytical procedures (8).

Vapor phase IR spectra and GC data revealed only SO_2 and CH_3CN in the gas phase. Our GC analysis conditions were suitable for detecting, among others, H_2 and CH_4. The IR spectrum of the cathode (Fig. 37) shows only the absorptions at 1085(s), 1020(s), 900(s), 550(m) and 500(m) cm^{-1} due to $Li_2S_2O_4$ (3).

Evidence for reaction products (several milligrams) on the anodes of partially discharged cells was obtained when their Li-anodes were compared with those of the undischarged cells, stored for the same period. The SEM micrographs in Figures 38 and 39 indicate that there are several components in the anode product The anodes of undischarged cells had so little material on them it could not be separated for analysis.

An IR spectrum (KBr pellet) of the product from the anode of a partially discharged cell is shown in Figure 37. The spectrum indicates that $Li_2S_2O_4$ is one of the components. This was confirmed by qualitative analysis with Naphthol Yellow-S (8). Of course, $Li_2S_2O_4$ is believed to be the protective film on Li. The spectrum showed practically no absorptions due to the organic compounds, β-aminocrotononitrile and 3,5-diamino-2,4-hexenenitrile which are products of the reaction between Li and CH_3CN (3,5).

A striking feature of the IR spectrum is the absorptions at 1240 (broad, s), 1170(s) and 570(m) cm A few inorganic sulfur-oxy compounds which give rise to IR absorptions in the 1200-1250 cm^{-1} region are the alkali metal thionates, $S_nO_6^{-2}$,

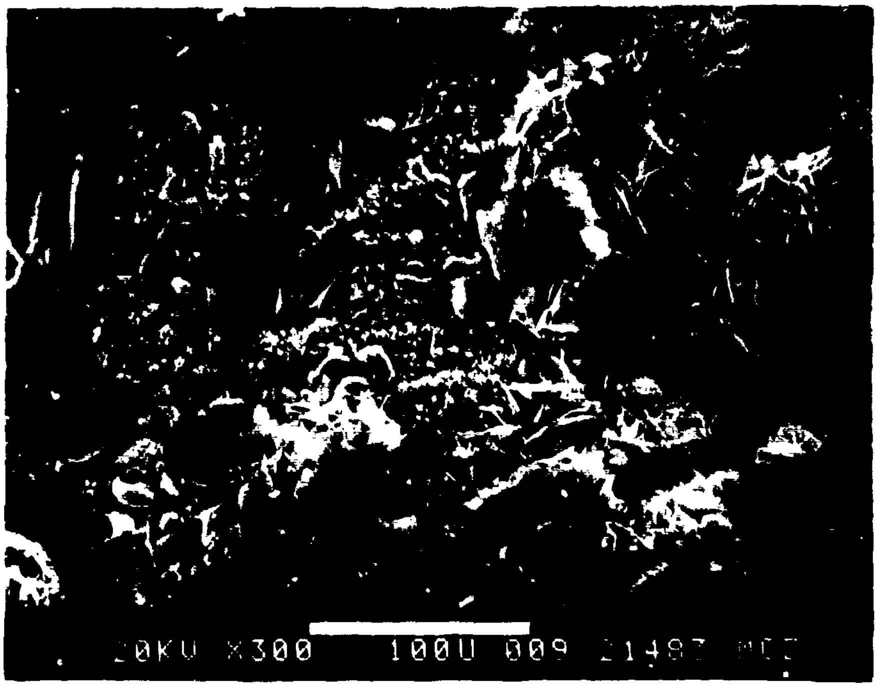

MAGNIFICATION 300X

FIGURE 38A. SEM PHOTOGRAPH OF THE ANODE SURFACE OF A 50% DISCHARGED AND 1 YEAR STORED TYPE-Z Li/SO_2 CELL

MAGNIFICATION 1000X

FIGURE 38B. SEM PHOTOGRAPH AT A HIGHER MAGNIFICATION OF A PORTION OF THE ANODE SURFACE OF THE CELL IN FIGURE 38A.

MAGNIFICATION 5000X

FIGURE 39. SEM PHOTOGRAPH OF THE ANODE SURFACE OF ANOTHER TYPE-Z CELL AFTER SIMILAR DISCHARGE AND STORAGE CONDITIONS AS THE CLLL IN FIGURE 38

n = 2-6 (10). The latter compounds also show absorptions around 1000-1050 cm^{-1} and 600 cm^{-1} (10). Alkali metal sulfates show characteristic absorptions at ~ 1100-1150 cm^{-1} (10). Thus, the IR absorptions strongly suggest that the anode film includes, in addition to $Li_2S_2O_4$, Li-thionate(s), and possibly Li_2SO_4. An ESCA spectrum of the sample had peaks due to three types of S with the S (2p) binding energies at 163.6, 166.8 and 168.3 eV. The peak at 166.8 eV is most probably due to the S in $Li_2S_2O_4$ (3). The peak at 163.6 V is in the range expected for "-S-" type sulfur and the broad peak at 168.3 eV is in the range expected for S^{V} or S^{VI} or both. The IR spectrum and ESCA data strongly support our contention that one of the components in the anode product is a thionate. Since none of these except $Li_2S_2O_4$ is found on the cathode, it seems that reactions involving Li are necessary for the formation of the anode products. We suggest the following reactions would satisfactorily account for the various observed products.

$$4Li + LiO\text{-}\overset{\overset{O}{\|}}{S}\text{-}\overset{\overset{O}{\|}}{S}\text{-}OLi \rightarrow 2Li_2O + \underset{I}{LiO\text{-}S\text{-}S\text{-}OLi} \qquad [21]$$

$$LiO\text{-}S\text{-}S\text{-}OLi + 2SO_2 \rightarrow \underset{\text{Li-tetrathionate, II}}{LiO\text{-}\overset{\overset{O}{\|}}{\underset{\underset{O}{\|}}{S}}\text{-}S\text{-}S\text{-}\overset{\overset{O}{\|}}{\underset{\underset{O}{\|}}{S}}\text{-}OLi} \qquad [22]$$

$$II \xrightarrow{\text{Reduction by Li}} \xrightarrow{SO_2 \text{ insertion}} Li_2S_nO_6,\ n>4 \qquad [23]$$

I is analogous to $H_2S_2O_2$, an intermediate proposed in the synthesis of thionic acids from sulfurous acid and H_2S (8). The proposed mechanism is also consistent with the synthesis of $K_2S_4O_6$ from S_2Cl_2 and sulfurous acid followed by neutralization with KOH (11). In the latter synthesis, the first step apparently involves the insertion of SO_2 into the S-OH bonds of HO-S-S-OH, formed first by hydrolysis of S_2Cl_2 (11).

Dithionate can be ruled out since it is formed under oxidizing conditions (10) and we do not find it on the cathode. It is possible to conceive of SO_4^{-2} formation via reactions of the type in equation [24]

$$LiO\text{-}\overset{\overset{O}{\|}}{\underset{\underset{O}{\|}}{S}}\text{-}S\text{-}S\text{-}\overset{\overset{O}{\|}}{\underset{\underset{O}{\|}}{S}}\text{-}OLi + 2Li_2O \rightarrow 2Li_2SO_4 + Li_2S_2 \qquad [24]$$

Such redistribution reactions are well known in solution chemistry but they are unusual in the solid state. It should be noted Li_2SO_4 was previously identified, from ESCA spectra, on the anodes of discharged cells (12), although the storage history of those cells after the discharge was not reported.

We note that polythionates have a tendency to decompose with heating to give off S which has been shown to sustain exothermic runaway reactions (9). Another implication of our findings is that given the opportunity, sulfur species ranging from S^{VI} to S^{-2} could be expected as reaction products in the Li/SO_2 cell.

The observed reduction of SO_2 mostly to $S_2O_4^{-2}$ in the normal discharge is simply because of the kinetic restrictions of the reaction. In this connection the recent report of Li_2S as a reaction product of Li and SO_2 is interesting (13).

The presence of larger amounts of reaction products on partially discharged as opposed to undischarged anodes may be attributed to the differences in the nature of the Li films in the two cases. Our evidence suggests that very small quantities of $S_nO_6^{-2}$ are also formed on the anodes of undischarged stored cells.

DISCUSSION

The results presented above correspond to only one storage condition. It is only logical to expect variations in both the type and extent of reactions occurring at the anode due to different discharge current densities, depth of discharge, electrolyte composition, and storage time and temperature. All these are expected to have significant effects on the safety of the cells. A study of such magnitude remains to be carried out. We consider such a study to be of immense importance in understanding and solving the safety problems of the Li/SO_2 cell system.

CHAPTER 8

CONCLUSIONS

We have established the normal discharge stoichiometry, $2Li + 2SO_2 \rightarrow Li_2S_2O_4$, for current densities up to 8 mA/cm^2 at room temperature, and for discharges at -25^oC.

We have found that the most favorable conditions for a forced overdischarge related venting/explosion are the following:

- An unbalanced cell with a large excess of Li.

- Forced overdischarge at high currents at room temperature; e.g., 7-10 mA/cm^2 in a C-cell.

- Forced overdischarge at both low and high currents at low temperatures; e.g., below -15^oC.

Our results suggest that practically the same mechanism is operating in both the room temperature and low temperature forced overdischarge related venting/explosions. The only apparent difference is that at low temperatures, the high surface area Li which becomes plated onto the carbon cathode remains highly active, i.e., less passivated, so that venting/explosions are rather easily initiated.

A very significant result has been our observation that very little or no CH_4 is produced during forced overdischarge at below -15^oC. It appears that the $Li-CH_3CN$ reaction is significantly suppressed at these low temperatures. It seems that, contrary to earlier belief, the $Li-CH_3CN$ reaction is only of secondary importance to the forced overdischarge related safety hazards - i.e., the related reaction products, CH_4, C_2H_4 and C_2H_2, contribute to the overall pressure increase in the cell. In our opinion, reactions most relevant to cell safety hazards are the $Li-Li_2S_2O_4$ reaction and the thermal decomposition of $Li_2S_2O_4$. Furthermore, direct reactions between C and SO_2, and C and S appear to be integral parts of the mechanism of explosions/venting.

Very little correlation has been found between the extent of forced overdischarge and the onset of a hazardous event. However, plating of a considerable amount of Li onto the cathode and oscillations in cell voltage precede a hazardous event. The voltage oscillations appear to produce the resistive heating (probably locally) required for initiating a runaway reaction.

Forced overdischarge related explosions/venting can be minimized by carefully balancing the initial ratio of Li, SO_2 and C. A Li-limited configuration with high rate cathode structure, ensuring a full or near full depletion of the Li,

appears to be the preferred design. Manufactured cells should be extensively and carefully tested to ensure compliance with design specifications. Further studies of the origin of the voltage oscillations and its role on safety hazards should be pursued.

A complete protection against any forced overdischarge hazards may be achieved by the use of additives which help deactivate (passivate) the high surface Li which becomes plated on the cathode. No useful additive is presently known.

We have identified reaction products composed of $Li_2S_4O_6$, $Li_2S_2O_4$ and possibly Li_2SO_4 on the anodes of partially discharged and ambient temperature stored Li/SO_2 cells. While $Li_2S_4O_6$ does not appear to be particularly more dangerous than $Li_2S_2O_4$, the formation of significant amounts of surface films can result in inhomogeneous current distribution, especially during high rate operations, leading potentially to the formation of hot-spots and thermal runaways. We believe further studies of the storage reactions at the anodes of partially discharged and stored cells are the key to solving the problems associated with such cells. In particular we recommend studies of the effects of discharge current density, depth-of-discharge, electrolyte composition, and storage time and temperature on the chemistry and behavior during storage of partially discharged cells.

REFERENCES

1. D. Linden and B. McDonald, J. Power Sources, Vol. 5, 1980, p. 35.

2. M. W. Rupich and K. M. Abraham, First Quarterly Report, NSWC Contract No. N60921-81-C-0084, May 1981.

3. K. M. Abraham, M. W. Rupich and L. Pitts, Final Report, NSWC Contract No. N60921-81-C-0084, April 1982.

4. K. M. Abraham, M. W. Rupich and L. Pitts, "Studies of the Safety of Li/SO_2 Cells," in Proceedings of the 30th Power Sources Symposium, Atlantic City, NJ, 1982.

5. M. W. Rupich, L. Pitts and K. M. Abraham, J. Electrochem. Soc., Vol. 129, 1982, p. 1857.

6. W. P. Kilroy and C. R. Anderson, paper presented at the International Meeting on Lithium Batteries, Rome, 1982, Extended Abstract No. 36.

7. W. L. Bowden et al., Spring Meeting of the Electrochemical Society Meeting, San Francisco, 1983, Abstract No. 11.

8. J. H. Karchmer, Editor, The Analytical Chemistry of Sulfur and Its Compounds, Part 1, Vol. 29, Wiley Interscience, NY, 1970.

9. A. N. Dey and R. W. Holmes, Safety Studies on Li/SO_2 Cells, ERADCOM, DELET-TR-77-0472-F, 1979.

10. Inorganic Sulfur Chemistry, G. Nickless, Editor, Elsevier Publishing Co., New York, 1968, p. 162.

11. W. A. Hart and C. F. Beumel, Jr. in Comprehensive Inorganic Chemistry, Vol. 1, J. C. Bailar, Jr., et al., Editors, Pergamon Press, NY, 1973.

12. C. R. Anderson and W. P. Kilroy, paper presented at the fall meeting of the Electrochemical Society, Detroit, MI, 1982, Extended Abstract No. 317.

13. K. W. Nebesny, R. Kaller, N. R. Armstrong and R. K. Quinn, J. Electrochem. Soc., Vol. 129, 1982, p. 2861.

DISTRIBUTION

	Copies
Defense Technical Information Ctr Cameron Station Alexandria, VA 22314	12
Defense Nuclear Agency Attn: Library Washington, DC 20301	2
Institute for Defense Analyses R&E Support Division 400 Army-Navy Drive Arlington, VA 22202	1
Naval Material Command Attn: Code 08T223 Washington, DC 20360	1
Office of Naval Research Attn: G. Neece (Code ONR 472)	2
J. Smith (Code ONR 472) 800 N. Quincy Street Arlington, VA 22217	1
Naval Research Laboratory 4555 Overlook Avenue, SW Chemistry Division Washington, DC 20360	1
Naval Post Graduate School Attn: Dr. Oscar Biblarz Monterey, CA 93940	1
Naval Air Systems Command Attn: Dr. H. Rosenwasser (Code NAVAIR 301C)	1
E. Nebus (Code NAVAIR 5332) Washington, DC 20361	1
Naval Electronics Systems Command Attn: A. H. Sobel (Code PME 124-31) Washington, DC 20360	1
Naval Sea Systems Command Attn: F. Romano (Code 63R3)	1
E. Daugherty (Code 06H3) Washington, DC 20362	1
Strategic Systems Project Office Attn: K. N. Boley (Code NSP 2721)	1
M. Meserole (Code NSP 2722) Department of the Navy Washington, DC 20360	1
Naval Air Development Center Attn: J. Segrest (Code 6012)	1
R. Schwartz (Code 30412) Warminster, PA 18974	1
Naval Civil Engineering Laboratory Dr. W. S. Haynes (Code L-52)	1
F. Rosell Port Hueneme, CA 93040	1
Naval Intelligence Support Center Attn: Dr. H. Ruskie (Code 362) Washington, DC 20390	1
Naval Ocean Systems Center Attn: Code 922	1
Dr. S. Spazk (Code 6343)	1
Dr. S. D. Yamamoto (Code 513) San Diego, CA 92152	1
US Development & Readiness Command Attn: J. W. Crellin (Code DRCDE-L) 5001 Eisenhower Avenue Alexandria, VA 22333	1

	Copies		Copies
US Army Electronics Command Attn: A. J. Legath (Code DRSEL-TL-P) E. Brooks (Code DRSEL-TL-PD) G. DiMasi Dr. W. K. Behl Fort Monmouth, NJ 07703	1 1 1 1	Department of Energy Attn: Dr. A. Landgrebe (Code MS E-463) Energy R&D Agency Division of Applied Technology Washington, DC 20545	1
Army Material & Mech. Res. Center Attn: J. J. DeMarco Watertown, MA 02172	1	Headquarters, Dept. of Transportation Attn: R. Potter (Code GEOE-3/61) U.S. Coast Guard, Ocean Engg. Division Washington, DC 20590	1
USA Mobility Equipment R&D Command Attn: J. Sullivan (Code DRXFB) Code DRME-EC Electrochemical Division Fort Belvoir, VA 22060	1 1	NASA Headquarters Attn: Dr. J. H. Ambrus (Code RTS-6) Washington, DC 20546	1
Edgewood Arsenal Attn: Library Aberdeen Proving Ground Aberdeen, MD 21010	1	NASA Goddard Space Flight Center Attn: (Code 711) T. Hennigan (Code 716.2) Greenbelt, MD 20771	1 1
Picatinny Arsenal Attn: M. Merriman (Code SARPA-FR-S-P) Dr. B. Werbel (Code SARPA-FR-E-L-C) A. E. Magistro (Code SARPA-ND-D-B) U.S. Army Dover, NJ 07801	1 1 1	NASA Lewis Research Center Attn: J. S. Fordyce (Code MS 309-1) H. J. Schwartz (Code MS 309-1) 21000 Brookpark Road Cleveland, OH 44135	1 1
		Naval Electronic Systems Command Attn: T. Sliwa (Code NAVELEX-01K) Washington, DC 20360	1
Harry Diamond Laboratory Attn: W. Kuper (Code DRDXO-RDD) J. T. Nelson (Code DRKDO-RDD) C. Campanguolo Department of Army Materiel Chief, Power Supply Branch 2800 Powder Mill Road Adelphi, MD 20783	 1 1 1	Naval Weapons Center Attn: Dr. A. Fletcher (Code 3852) China Lake, CA 93555	1
		Naval Weapons Support Center Attn: D. G. Miley (Code 305) Electrochemical Power Sources Div. Crane, IN 47522	1
Department of Energy Attn: L. J. Rogers (Code 2102) Division of Electric Energy Systems Washington, DC 20545	1	Naval Coastal Systems Center Attn: Library Panama City, FL 32407	1

	Copies
Naval Underwater Systems Center Attn: J. Moden (Code SB332) Newport, RI 02840	1
David W. Taylor Naval Ship R&D Ctr Attn: J. Woerner (Code 2724) H. R. Urbach (Code 2724) Annapolis Laboratory Annapolis, MD 21402	1 1
Scientific Advisor Attn: Code AX Commandant of the Marines Corps Washington, DC 20380	1
Air Force of Scientific Research Attn: R. A. Osteryoung Directorate of Chemical Science 1400 Wilson Boulevard Arlington, VA 22209	1
Frank J. Seiler Research Lab, AFSC Attn: Lt. Col. Lowell A. King (Code FJSRL/NC) USAF Academy, CO 80840	1
Air Force Materials Laboratory Attn: Major J. K. Erbacher Wright-Patterson AFB, OH 45433	1
Air Force Aero Propulsion Lab Attn: W. S. Bishop (Code AFAPL/POE-1) Dick Marsh (Code AFAPL/POE-1) Wright-Patterson AFB, OH 45433	1 1
Air Force Rocket Propulsion Lab Attn: Lt. D. Ferguson (Code MKPA) Edwards Air Force Base, CA 93523	1
Headquarters, Air Force Specia Communications Center Attn: Library USAFSS San Antonio, TX 78243	1
Office of Chief of R&D Department of the Army Attn: Dr. S. J. Magran Energy Conversion Branch Room 410, Highland Building Washington, DC 20315	1
US Army Research Office Attn: B. F. Spielvogel P. O. Box 12211 Research Triangle Park, NC 27709	1
NASA Scientific & Technical Information Facility Attn: Library P. O. Box 33 College Park, MD 20740	1
National Bureau of Standards Metallurgy Division Inorganic Materials Division Washington, DC 20234	2
Battelle Memorial Institute Defense Metals & Ceramics Information Center 505 King Avenue Columbus, OH 43201	1
Bell Laboratories Attn: Dr. J. J. Auborn 600 Mountain Avenue Murray Hill, NJ 07974	1
California Institute of Technology Attn: Library Jet Propulsion Laboratory 4800 Oak Grove Drive Pasadena, CA 91103	1
Argonne National Laboratory Attn: H. Shimotake 9700 South Cass Avenue Argonne, IL 60439	1

	Copies
John Hopkins Applied Physics Lab	
Attn: R. Rumpf	1
Howard County	
Johns Hopkins Road	
Laurel, MD 20707	
Oak Ridge National Laboratory	
Attn: K. Braunstein	1
Oak Ridge, TN 37830	
Sandia Laboratories	
Attn: R. D. Wehrle (Code 2522)	1
B. H. Van Domelan (Code 2523)	1
Albuquerque, NM 87115	
Catholic University	
Chemical Engineering Department	
Washington, DC 20064	1
University of Tennessee	
Attn: G. Mamantov	1
Department of Chemistry	
Knoxville, TN 37916	
University of Florida	
Attn: R. D. Walker	1
Department of Chemical Engineering	
Gainesville, FL 32611	
Applied Research Laboratory	
Attn: Library	1
Penn State University	
University Park, PA 16802	
Catalyst Research Corporation	
1421 Clarkview Road	
Baltimore, MD 21209	1
ESB Research Center	
Attn: Library	1
19 W. College Avenue	
Yardley, PA 19067	
Old Dominion University	
Attn: Dr. Robert Ake	1
Department of Chemical Science	
Norfolk, VA 23508	

	Copies
Eagle-Picher Industries, Inc.	
Attn: D. R. Cottingham	1
Rex Erisman	1
Electronics Division, Couples Dept.	
PO Box 47	
Joplin, MO 64801	
Eagle-Picher Industries, Inc.	
Attn: P. E. Grayson	1
Miami Research Laboratories	
200 Ninth Avenue, NE	
Miami, OK 74354	
EIC Laboratories, Inc.	
Attn: K. M. Abraham	20
111 Downey Street	
Norwood, MA 02062	
Electrochimica Corporation	
2485 Charleston Road	
Mountain View, CA 94040	1
Globe Union Inc.	
Attn: Dr. R. A. Rizzo	1
5757 N. Green Bay Avenue	
Milwaukee, WI 53201	
Foote Mineral Company	
Attn: H. R. Grady	1
Exton, PA 19341	
General Electric Company	
Attn: R. D. Walton	1
R. Szwarc	1
Neutron Devices Department	
P. O. Box 11508	
St. Petersburg, FL 33733	
Gould, Inc.	
Attn: S. S. Nielsen	1
40 Gould Center	
Rolling Meadows, IL 60008	
Honeywell, Inc.	
Attn: Library	1
E. Ebner	1
Defense Systems Division	
Power Sources Center	
104 Rock Road	
Horsham, PA 19044	

	Copies
Hughes Aircraft Company	
Attn: Library	1
Dr. L. H. Fentnor	1
Aerospace Groups	
Missile Systems Group	
Tucson Engineering Laboratory	
Tucson, AZ 85734	
SAFT AMERICA	
Attn: L. A. Stein	1
F. DeMarco	1
K. K. Press	1
200 Wight Avenue	
Cockeysville, MD 21030	
Lockheed Missiles & Space Co.	
Attn: Library	1
Lockheed Palo Alto Research Lab	
3251 Hanover Street	
Palo Alto, CA 94304	
Duracell International, Inc.	
Attn: G. F. Cruze	1
B. McDonald	1
D. Linden	1
Battery Division	
South Broadway	
Tarrytown, NY 10591	
Duracell International, Inc.	
Attn: Library	1
Dr. A. N. Dey	1
Dr. H. Taylor	1
Laboratory for Physical Science	
Burlington, MA 01803	
Power Conversion, Inc.	
70 MacQueston Parkway S	
Mount Vernon, NY 10550	1
Union Carbide Battery Products Div.	
Attn: R. A. Powers	1
P. O. Box 6116	
Cleveland, OH 44101	
Wilson Greatbatch Ltd.	
Attn: Library	1
1000 Wehrle Drive	
Clarence, NY 14030	

	Copies
Yardney Electric Corporation	
Attn: Library	1
A. Beachielli	1
82 Mechanic Street	
Pawcatuck, CT 02891	
Callery Chemical Company	
Attn: Library	1
Callery, PA 16024	
Kawecki Berylco Industries, Inc.	
Attn: J. E. Eorgan	1
R. C. Miller	1
Boyertown, PA 19512	
Rockwell International	
Attn: Dr. Samuel J. Yosim	1
Atomics International Division	
8900 DeSoto Avenue	
Canogo Park, CA 91304	
Union Carbide	
Attn: Library	1
Nuclepore Corporation	
7035 Commercial Circle	
Pleasanton, CA 94556	
Ventron Corporation	
Attn: L. R. Frazier	1
10 Congress Street	
Beverly, MA 01915	
Stanford University	
Attn: C. John Wen	1
Center for Materials Research	
Room 249, McCullough Building	
Stanford, CA 94305	
EDO Corporation	
Attn: E.P. DiGiannantonio	1
Government Products Division	
2001 Jefferson Davis Highway	
Arlington, VA 22202	
Perry International, Inc.	
Attn: R. A. Webster	1
117 South 17th Street	
Philadelphia, PA 19103	

	Copies
Ford Aerospace & Comm. Corp. Attn: M. L. McClanahan R. A. Harlow Metallurgical Processes Advanced Development-Aeronutronic Div. Ford Road Newport Beach, CA 92663	 1 1
University of Missouri, Rolla Attn: Dr. J. M. Marcello 210 Parker Hall Rolla, MO 65401	 1
RAI Research Corporation Attn: Dr. Carl Perini 225 Marcus Boulevard Hauppauge, NY 11787	 1
Ray-O-Vac Attn: R. Foster Udell 101 East Washington Avenue Madison, WI 53703	 1
Litton Data Systems Division Attn: Frank Halula (MS-64-61) 8000 Woodley Avenue Van Nuys, CA 91409	 1
Lawrence Berkeley Laboratory Attn: F. McLamore University of California Berkeley, CA 94720	 1
TRW Systems Attn: Ed Moon, Rm. 2251, Bldg. 0-1 One Space Park Redondo Beach, CA 90278	 1
Altus Corporation Attn: Dr. Adrian E. Zolla 1610 Crane Court San Jose, CA 95112	 1
U. S. Air Force Attn: CAPT A. S. Alanis BME/ENBE Norton AFB, CA 92409	 1
U. S. Air Force Norton Air Force Base Attn: Code AFISC/SES Norton AFB, CA 92409	 1

Internal Distribution	Copies
R33 C. E. Mueller	1
R33 S. D. James	20
E431	9
E432	3
E35	1